CRES
THE UNIVERSITY OF KANSAS • CENTER FOR RESEARCH INC
ENGINEERING SCIENCE DIVISION • LAWRENCE, KANSAS

A STUDY OF HIGH PERFORMANCE ANTENNA SYSTEMS FOR DEEP SPACE COMMUNICATION

L. L. Bailin
Project Manager

Grant Number NGR 17-004-013
Status Report
February 15, 1968 to November 15, 1968

CONTENTS

CONTENTS

I. INTRODUCTION

The objective of this program is to study the most recently defined parameters for a high data rate of communication system which can operate between an earth station and a vehicle in space over great distances. An effort will be made to describe and delineate the characteristics of radiating subsystems and their internal sub-divisions which can satisfy the requisite performance criteria for an S-band system. Considerations will be given to the advance technology concerned with the ground based antenna, and where pertinent, to the spacecraft antenna as well. An effort will be made to determine the feasible design approaches for the ground antennas and its component parts. Appropriate design criteria will be investigated analytically, and where possible a comparison will be made with empirically determined results in an effort to define areas of research and development which need long term attention. The data rates of long term interest are 10^6 to 10^7 bits/second for a Mars mission and 10^4 to 10^6 bits/second for a Jupiter mission.

The ground-based antennas are discussed in this program as components of a link designed to fulfill the specific function of providing uninterrrupted communication from a spacecraft to the earth at planetary distances. For obvious reasons, the most attention is given the down link aspects using a carrier frequency of 2.3 GHz, since a frequency in this region has advantages for an all-weather ground station and is presently in use in the NASA Deep Space Instrumentation Facility. It is assumed also that future mission plans will require information rates of the order of 10^4 to 10^7 bits/second with a given probability of error, 10^{-2} to 10^{-5}. These parameters imply a specific system performance in terms of bandwidth and signal -to-noise ratio. When the characteristics of the available transmitter and receiver are evaluated or assumed, the required performance characteristics of the overall radiating system are determined either directly or by implication. The overall radiating system is taken to include the combination of the spacecraft and the ground or relay station antenna equipment. Thus, for this study, certain gain and aperture requirements will be assumed nominal as parameters to satisfy a variety of space missions.

There are two general areas of concern that must be investigated relative to the ground-based receiving system which of necessity must be large

compared to wavelength to achieve the desired performance characteristics. The first involves questions about the received signal to noise level or the gain that must be provided to handle it. Consideration must be given to methods by which it may be enhanced, and the limitations that may be encountered during the various phases of a mission. The second areas embraces questions about the contributions made to the noise of the communications link, the manner in which these are introduced, and methods by which they may be minimized. These questions are, of course, interrelated, and the limitations encountered are intensely practical and economic, as well as theoretical. For this study, emphasis will be given to the first area and when necessary, results of other investigations into the questions involved in the second area will be used.

The requirement of a minimum signal to noise level forces the sum of the gains of the space and ground antennas to be of some value that can be specifically determined for a particular mission. It is important to be able to allocate the antenna gains at each end of the link according to reasonable expectations concerning the practical designs and performance characteristics that can be accomplished in the next ten to fifteen years. An optimum allocation of these gains is difficult although some progress has been made along these lines. For this study nominal values shall be used as parameters in an effort to establish quantitative relationships between pertinent dimensions and techniques. It has been shown that at 2.3 GHz, dimensions on the order of 600 to 1000 ft or more are probably realistic aperture sizes to consider for the high data rates and low error probabilities listed above. Using the plans of the communication link characteristics for the 1971 Voyager Mission at 1AU as a basis for comparison, the sum of the gains on future missions can be estimated to be about 110 db to achieve a data rate of 10^6 bits/second or a 20 db increase over the gains specified in the Voyager link for which a spacecraft transmitter of 50 watts has been postulated. If the spacecraft antenna is postulated to be capable of 30-40 db of gain using a transmitter with 50-100 watts of power, then the ground based receiving system must be studied for the following range of parameters:

Antenna Gain-- 60 to 80 db
Data Rate -- 10^4 to 10^7 bits/second
Error Probability -- 10^{-2} to 10^{-5}

Final results will be given for this entire range of parameters although

nominal values will be used to illustrate and expedite the discussion of various techniques during the intermediate phase of this program.

Because of the significance of the noise level in determining the overall gain requirement, many studies have been directed to a consideration of the noise that competes with the signal and is collected and introduced at the ground end of the down link. The convention of treating the noise as resulting from an equivalent antenna temperature has followed in this program. Since the noise level is highest when the antenna beam is directed at or near a noise source, attention is being paid to techniques which can be used to mitigate these deleterious effects in certain special mission circumstance.

The characteristics of high gain techniques, either electrical or mechanical, form essential parts of tradeoffs in system accuracy, reliability, and cost. Of course practical compromises must be made for certain aspects of a particular mission. These compromises will depend on the techniques available for directing or steering the receiving beam on the ground as compared with those for controlling the vehicle attitude. Three types of steering mechanisms are possible for spacecraft antenna systems: mechanical (as for large appendage antennas); electromechanical; and electronic or inertialess. Electronic techniques offer the greatest versatility with regard to communications between a vehicle in space and earth. These are two generic types: those that require external controls to phase the elements properly and those that are self-steering. The externally controlled systems, such as the conventional phased array, need an external sensor (IR, RF, or ground station) to point the beam, and a computer, a phasing network, and an attitude sensing device to point the beam appropriately. In the self-steering system, however, attitude information is presented to the antenna system by a pilot beam from a ground station, and electronic circuitry senses the phase of incoming pilot signals to position a beam in the direction of these pilot signals. Multiple beam systems may be accommodated by the use of diplexers and multiple electronic channels. Each of these spacecraft systems is being worked on by various research and development groups through the country and abroad. Appropriate results of these efforts will be used to achieve stated objectives of this program.

II. PROGRAM DESCRIPTION

As has been discussed in earlier reports on this program, there are basically two fundamental kinds of antenna systems that can be used in DSCS application. The first is a large mechanically steerable paraboloidal reflector or a number of smaller reflectors of this type which are connected and fed as an array and mechanically steered as individual radiators. The second is a phased array with stationary or fixed apertures composed of subapertures whose relative phasing controls the direction of the antenna beam. Thus, this program considers the various aspects and organizations of the following generic types of large ground based antenna systems:

A. A SINGLE LARGE APERTURE -- mechanically steerable.

A system of this type will be discussed in this study only to provide a basis for the comparison of performance characteristics with the other systems listed below.

B. AN ARRAY OF LARGE DISHES -- each of which is mechanically steerable.

The appropriate organization of a system of this type is considered herein.

C. A PHASED ARRAY OF SMALL CLOSELY SPACED ELEMENTS ORGANIZED INTO SUBAPERTURES -- electronically steerable.

Most of the effort in this program will be concerned with the various organizations, the feeding techniques, and the elements appropriate to this type of system.

D. A SELF-STEERING ARRAY -- rapidly switched multiple beams or adaptive systems.

Systems of this type can be used to mitigate the effects of high intensity noise sources and employed in conjunction with the type III systems to accomplish optimum mission performance. The feasibility of application of these techniques for a high data rate communication system is being investigated during the course of this program.

Consideration is being given to the capabilities and limitations of each of the above types during the course of this study and a report made in the above listed catagories.

During this report period, the activities performed were a result of a cooperative effort between the personnel of the Center for Research (CRES) at The University of Kansas, and the Electro Science Laboratory (ESL) at Ohio State University. Although some of the results described herein were obtained in one institution and some in the other, this report and subsequent reports will be written with the idea of integrating the results of various research efforts and techniques . Results of this investigation will be described in such a way as to implement the objectives of the program without regard to the actual source of the material, whether it be obtained by the above mentioned institutions or by reference to activites outside this specific program. It will be the purpose of this report to glean as much pertinent material as possible and to organize it into a form which permits a quantitative comparison of the various possible antenna systems. Commencing with this report, all the pertinent results obtained during the course of this study will be presented as they are obtained and repeated or updated in subsequent reports.

In an effort to expedite the activities of this program, it was decided by the program manager at CRES and the technical monitor at ERC/NASA that a slight reorganization of the duties and responsibilities of the various groups involved was necessary. As has already been indicated, the major portion of th the work in this program is being done as a cooperative effort between CRES and ESL. At the conclusion of the study phase, a final report will be made of the entire study and submitted to a group of expert consultants as described in the original proposal and modified below. This group will serve as an evaluation team and will assist with the interpretation of the various results obtained during the course of the program, including the details of the overall system problems and the individual problems associated with the antenna subsystems. The outcome of this study will be a series of recommendations to ERC concerning the pacing technology which needs long term research and development. Appropriate design approaches and performance criteria will be suggested, primarily as they pertain to the ground based antenna subsystems and the subsystems on the space vehicle in an effort to optimize the overall performance characteristics of the down link (toward the earth) portion of the communication channel.

This program has been active for the past fifteen months and has un-

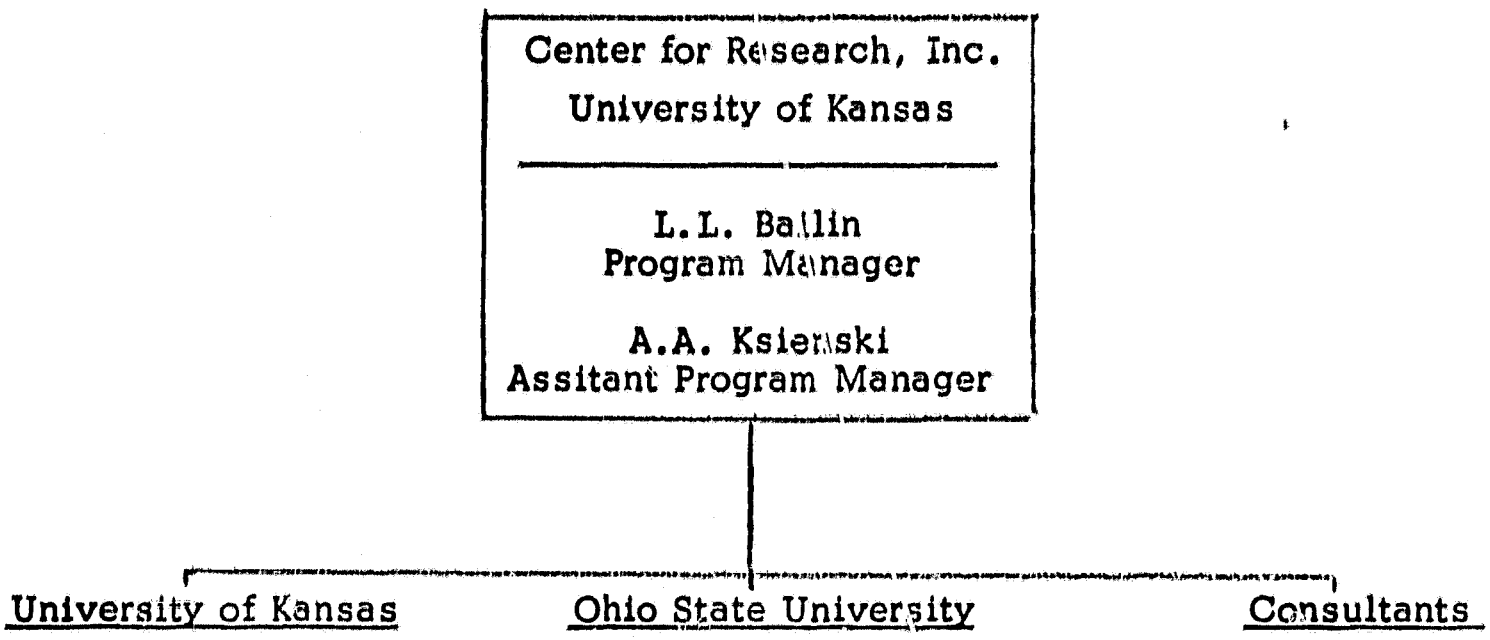

REVISED ORGANIZATION

covered a number of technical details that need further consideration and more recent fundamental data. Data are now becoming available that concern the performance characteristics and production costs of low loss transmission lines, radiating elements, and other subsystem components. Since these relationships are the primary factors which govern the establishment of criteria for a large scale antenna design, a proposal has been prepared and submitted asking that this program be extended until 15 September 1969. This extension of time will permit the research workers to obtain and utilize the additional and vital data, and to investigate some additional data processing techniques which offer some promise for improving the overall system capability during the period of high external noise levels. With the concurrence of the technical monitor and his staff at ERC/NASA a revised statement of work has been formulated as follows:

REVISED STATEMENT OF WORK

The Center for Research in Engineering Science at the University of Kansas proposes to extend its present study program with Electronic Research Center of NASA. This extension will continue and update four of the seven items listed in the original work statement to include considerations and estimates of the component costs involved in various array configurations. In addition, a fifth item is added which is pertinent to the processing techniques necessary to limit the external noise or interference in certain portions of deep space missions. A sixth item is included to provide a quantitative method for studying and optimizing the overall cost of the various types of ground antennas which appear to be most promising for a high data rate system. This program is to be accomplished as a cooperate effort between the personnel from Ohio State University and the University of Kansas. The extended program will include but not necessarily be limited to the following items as revised. The underlined portions of these tasks are revisions of those listed in the original proposal.

1. A continuing effort will be devoted to an intensive review and assessment of the research programs and techniques studies in progress or recently completed which may have influence on the objective of this program. This additional

study is to assist ERC/NASA in assuring that no significant matters or techniques on electronic beam shaping and steering have been slighted or overlooked.

2. A study will be made of various types and sizes of radiating elements and their associated control circuitry in an effort to evaluate their potential in a large ground based array with a very large number of elements. This investigation will be concerned primarily with low noise circuitry to provide the phase and amplitude control of the elements of the array. The circuit may include mechanical or ferrite phase shifters or the use of integrated semiconductor devices and heterodyning techniques. Consideration will be given to the state-of-the-art in techniques for phase controlling individual elements and groups of elements. An assessment will be made of their adequacy in providing control sufficient to satisfy the requirements of the system.

3. A study will be made of methods for arranging, grouping, exciting and interconnecting the requisite number of elements to provide the appropriate radiation characteristics from array antennas. Particular consideration will be given to the investigation of novel feeding and phasing techniques which would either significantly reduce array costs or increase their flexibility.

4. A study will be made of methods of achieving a capability to handle several satellites at planetary distance. The study also includes evaluation of the feasibility of providing rapidly switched multiple beams for communication with near earth orbital satellites.

5. A study will be made of the feasibility of switching from a self steering or adaptive array where the pattern is determined by the size of the subaperture to one where the steering is accomplished by externally controlling the phase between elements so that the pattern is determined by the entire radiating aperture. This switching is to be accomplished by an

appropriate signal processing scheme which is actuated by the externally generated noise or interference level. Such a scheme will produce a system capable of more efficient performance in the presence of high external noise and interference levels. For example, mission problems presented by the occultation of the sun and other high intensity noise sources will be minimized. The capability of switching to such an externally scanned accurately boresighted system must always be maintained.

6. The Electronic Reseach Center of NASA is currently developing the capability for simulation of communication systems. It is desired to expand this capability to include array antennas. The objectives of this study will be to provide the following:
   a) To identify and to describe by analytical means the pertinent parameters which should be considered in the analysis of array antennas such as element type and configuration gain, beam-scan angles, noise temperatures, data rate and line loss. Also included should be the associated computer parameters.
   b) The inputs to the analysis will be in the form of discrete point inputs. Data will be generated for array antennas relating weight and costs to the pertinent parameters which will have been established in a).

III. ACTIVITIES DURING THE PERIOD

During this report period several research and development organizations have been contacted in an effort to ascertain their latest findings on various subjects.

1. The first of these organizations is the Jet Propulsion Laboratory at Pasadena, California. Here the manager of the group in charge of developing an advanced antenna system (AAS), Mr. Gerald S. Levy, was contacted in order to discuss the progress on the latest improvements that are being made on the 210 ft. antenna which is used in the DSIF stations. The information gathered indicated the latest front end design using a maser will yield a noise temperature of about 18 K. This overall antenna system performance will permit a data rate of 16×10^3 bits/second in the reception from approximately 1 A.U. It was also pointed out that the staff at JPL is working on a revision of NASA Technical Report #32-848 which is entitled, "Large Antenna Apertures and Array for Deep Space Communications." An effort is being made to update the technical and economic data used in this report and to investigate the details involved in arraying four 210 ft. dish antennas.

2. A visit was made to the Texas Instrument Company in Richardson, Texas where Mr. Tom Hyltin, the manager of the microwave activity, was contacted regarding the MERA program. Here studies and experimentation have been conducted on an extremely compact integrated circuit version of a complete RF radar module which is both a transmitter and receiver. Drawings were obtained which indicate that there has been some very satisfactory progress towards the development of a module that can transmit and receive S-band signals and where the entire unit encompasses dimensions of $\frac{1}{4}$ inch by 1 inch and 2 inches. Thus, the possibilities for the applications of IC techniques for the individual circuit elements and their interconnections in a large array are increasing.

3. Contact was made with the Bendix Communication Division in Towson, Maryland with regard to the techniques and activities involved in the development of AN/FPS 85 antenna system which operates in the

V.H.F. range. Mr. William Rupp, Senior Engineer on this project, visited with people at CRES and presented a movie showing the general techniques and instrumentation used in the development of this large phased array radar. The basic configuration involves independent receiver and transmit arrays of 19,500 and 520 elements, respectively. Of course, this system operates at 440 MHz and consequently is not in the same frequency range as the proposed antenna system. However, many of the techniques and the problems associated with large number of elements and their subsystems will be comparable when the final S-band system configurations have been established. A cost effect study of several of the receiver techniques has become available which indicates the order of magnitude of some of the costs that are involved in the development of this rather unique UHF system. Semiconductor devices and solid state chip costs for the various modules have been estimated and some of the subsystem designs have been costed to perfection. Another interesting feature about this FPS-85 system is that the use of heterodyne steering techniques have been considered for this program. Thus, the cost effect study compares heterodyning with digital steering for possible application on this system.

4. Contact has been made with the personnel at the Hughes Aircraft Company in Culver City who are developing techniques for simulation of communications systems under ERC/NASA sponsorship. Mr. L.S. Stokes, one of the originators of the COPTRAN system, visited CRES and explained the use of computer programs to implement the trade-off studies necessary to optimize the various parameters involved in Space-Earth communications studies. It is one of the objectives of this program to identify and describe by analytical means the pertinent parameters which should be considered in the analysis of array antennas.

Since the design and development of large aperture antennas is always plagued by fundamental electrical limitations, it was decided to collect some previously obtained results of analysis, calculations, and measurement and publish them in a paper. A rough draft of a paper entitled "Some Fundamental Limitations of Large Aperture Antennas" by L.L. Bailin (University of Kansas) and S.D. Hamren (Hughes Aircraft Company) has been written, and is being

prepared for submission to the Transaction of IEEE Antennas and Propagation for publication at an early date. Although there are many factors which limit the performance of high gain antennas, it was the purpose of this paper to consider, in ways that are both fundamental and pragmatic, some of the effects which will influence the beam-width, the sidelobe level, the gain, and the bandwidth of large aperture antenna. In most instances, what was stated or derived applies to antennas in general although the effect of these factors become more significant as the aperture size becomes larger compared to the wavelength of the electromagnetic signal. Attention was focused primarily on array antennas which are becoming increasingly more popular as the appropriate technique for achieving certain precise radiation characteristics. Specifically, consideration was given to the effect of signal bandwidth (pulse length), the effect of array distortion, the transient response, and the various bandwidth characteristics of the pattern and antenna impedance. Although not all the items discussed in the paper are of great importance to a communication antenna, some of them are of primary concern to the successful design of any type of large aperture regardless of its ultimate application.

IV. TECHNICAL SUMMARY

The requirement of a constant information rate of the order of 10^6 bits per second with a given probability of error implies a specific system performance in terms of bandwidth and signal-to-noise ratio. In any communications link, the data rate system parameter, R_D, can be given as the product of the following three factors

$$R_D \alpha \quad P_T G_T(f) \quad \frac{\lambda^2}{4\pi R^2} \quad \frac{G_r(f)}{T_r(f)}$$

where the constant of proportionality directly involves such factors as data quality which is determined by the information coding method employed, and inversely the various loss factors in the transmission link. The bracketed terms list the design system and mission parameters as follows: the first bracket contains the transmitter parameters; the second bracket contains the transmission media or free space loss characteristics; the third factor involves the receiver parameters which are the primary concern in this study. Based on Shannon's work, the limiting value of the data rate in terms of signal-to-noise ratio and bandwidth is given by the expression

$$R_D \leq B \log_2 (1 + R_o/B)$$

where

$$R_o = \frac{S}{N} \qquad B = \text{information rate parameter}$$

The maximum data rate can be approached with negligible error by a proper choice of coding technique.[2, 3, 4] A simple and fairly efficient technique, for example, is coherent biphase coding. The characteristics of this code in terms of signal-to noise and bandwidth-to-data-rate ratios, and its relation to the Shannon limit are shown in Figure IV-1.

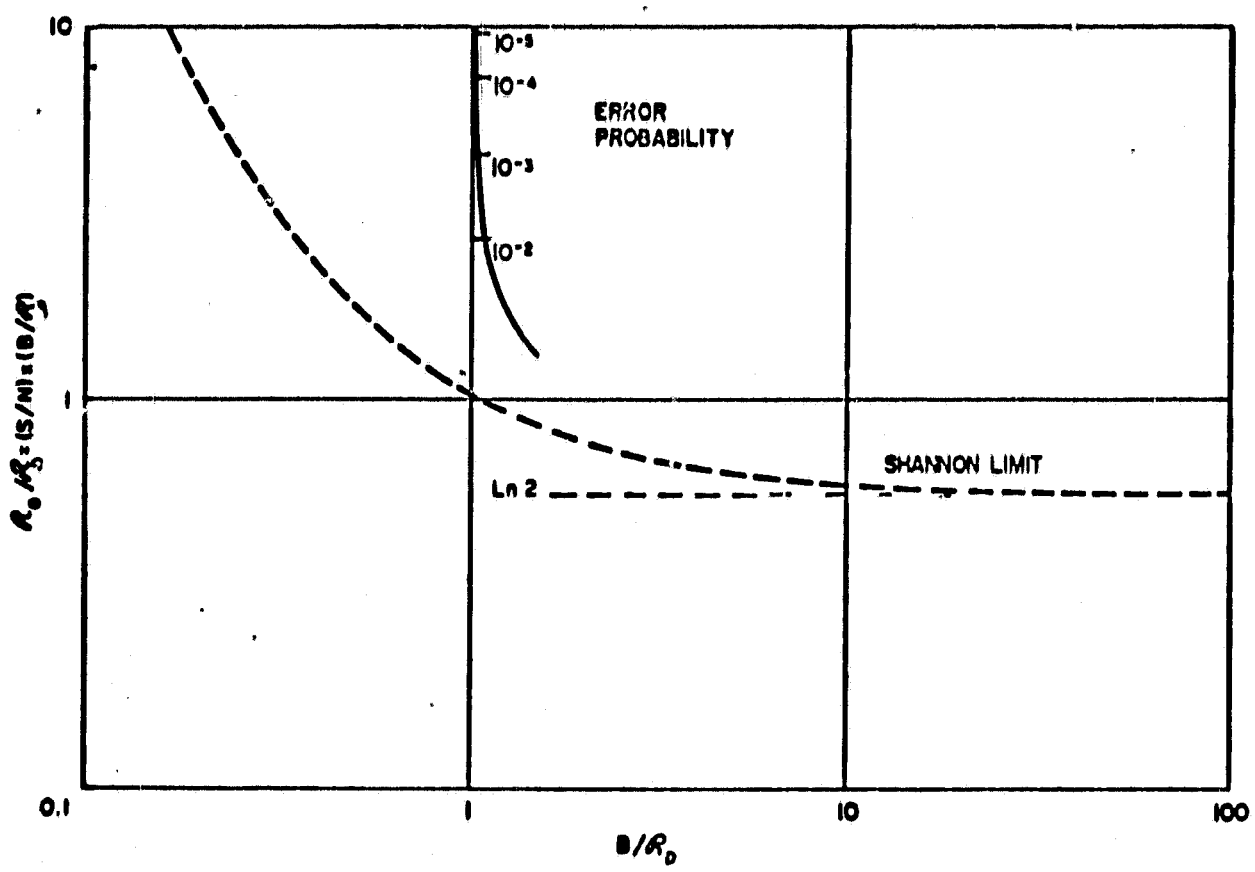

Figure IV-1 Efficiency of Biphase Coding

For small error probabilites, the figure indicated that the bandwidth required must be comparable with the data rate ($B/R_D \quad 1$). Thus an increase in SNR as measured by R_o/R_D is serving to reduce the error probability without appreciable effect on the bandwidth requirements. Tolerable error or probabilities range from 10^{-5} to 10^{-2} depending on the type of data.[5] Thus the practical limit for the product of signal-to-noise and bandwidth, even with a simple code, need not exceed the ideal limit by more than an order of magnitude to provide acceptable performance. The expression $R_o = (S/N)B = R_o = 10\ R_D$ will therefore be taken to represent a practical relationship between signal and bandwidth and the limiting noise level. (The actual relationship for a specific system design will depend on the particular coding scheme adopted as well as on error-rate requirements). Thus,

$$\frac{S}{N} = 10\frac{R_D}{B} \qquad 10 = 10 \text{ db}$$

correspond to the requisite error probabilities.

In view of the background material discussed above, it is possible to make some general assessments of the gain and associated aperture size required to provide nearly continuous communication between the ground and the spacecraft of future mission. It can be anticipated that a gain of 60 to 80 db will be needed for the ground antenna. The diameters of circular apertures corresponding to these gain values at 2.3 GHz are 200 and 2,000 feet, respectively. This is based on the supposition that the beam formed

is always perpendicular to the aperture during the steering processes and that an allowance is made for taper and other losses inherent to the antenna type. The 3-db beamwidths are on the order of 2.2×10^{-3} and 2.2×10^{-4} radians, respectively. In this section consideration is given to problems associated with satisfying the aperture and gain requirements with various types of ground based antenna systems. Each of the candidate types is discussed on the basis of its suitability to long range communication systems whether these antennas or their essential components have been developed, are in the experimental form, or are only in the conceptual or planning stages. Thus, each system is presented in terms of its capabilities and limitations even though some of the crucial component devices and techniques are still being developed. In some cases, the expected ultimate performance must be discussed in terms of a series of competing parameters whose final value is as yet unavailable.

In deep space communication systems requiring high data rates it is necessary to have a very large receiving antenna in order to achieve a SNR which will yield the error rates described above. Ultimately, as the distance or data rate increases, the required aperture may become too large to be constructed as a single antenna element as described in subsection A, and it is necessary to array several smaller apertures as described in subsection B and C. The upper limit on the subaperture size may be imposed by such factors as atmospherically induced wavefront distortion or unobtainable phase tolerances. An additional advantage of subdividing the large aperture into smaller subapertures is the possibility of arraying and processing them in a manner which will give improved performance over that of a single antenna. For example, the weighting factors on the subapertures as elements of the larger array might be adjusted to place a null or region of low sidelobes in the direction of an interfering source, thus reducing the effective array noise temperature. This process, however, requires sophisticated techniques and will be discussed in subsection D.

REFERENCES IV

1. R. C. Hansen and R. G. Stephenson,"Communications at Megamile Ranges,"Micro. Jour. 4, December 1961.

2. R. W. Sanders,"Communication Efficiency Comparison of Several Communication Systems,"Proc. IRE 48, April 1960.

3. A. J. Viterbi,"On Coded Phase-Coherent Communications,"IRE Trans. SET 7, March 1961.

4. R. C. Hansen and R G. Stephenson,"Communications at Megamile Ranges,"Micro. Jour. 5, January 1962.

5. L. S. Stokes and K. L. Brinkman,"Reference Data for Advanced Space Communication and Tracking Systems,"Report P66-135, Contract No. NAS 5-9637, Hughes Aircraft Company ASG, Culver City, California, 1966.

A. A SINGLE LARGE APERTURE

The steerable paraboloidal reflector has been shown to be economically and technically practical for antenna aperture size on the order of a few hundred feet. Such a size will satisfy the lower limit of the above mentioned requirements and is exemplified by the characteristics of the JPL 210-foot paraboloid as given in Table A-1. These characteristics afford a convenient reference list for comparison, since they represent the state-of-the-art at 2.3 GHz. However, for aperture sizes on the order of thousand feet it does not require extensive analysis to show that a single steerable paraboloid is not feasible in the next ten or even twenty years. A parabolic dish of this size is relatively impractical, since it must be assumed to have the same surface tolerance and illumination efficiency as the 210 ft. JPL dish and to maintain the same noise temperature but greater pointing accuracy. For a large single reflector spillover, backscattering and aperture blocking contribute to the noise temperature of the antenna since the radiation from the warm earth couples to the back lobes of the antenna pattern. The effect, of course, varies as a function of scan angle which may be as much as $\pm$ 60°. The upper limit in aperture size for a large single steerable paraboloid has probably already been reached and the change of this limit would require the discovery of a new structural material that has a strength to weight ratio several times that of steel.

Paraboloidal antennas are being widely used for deep space communications. The Deep Space Instrumentation Facility is presently equipped at five stations with 85 feet paraboloids having gains of 53 db at 2.5 GHz. A system noise temperature of 55°K is provided at each station. A network of three 210 foot paraboloids is under construction around the world. The first of these antennas has been completed at Goldstone, California. The most recent performance expectations of the 210 ft paraboloid indicate that a noise temperature of 18°K can be achieved with a maser front end and some improvements in the feed design. Since the costs of both the 85 ft. and the 210 ft. are now well established, they shall be used as the basic element in Section IV F, where arrays of dishes are considered. In addition, as indicated by Figure A-1, these structures were designed for optimum performance in the S-band range of frequencies.

Azimuth coverage, deg.	± 300 (from SE at Goldstone)
Elevation coverage, deg.	5 to 88 (tracking sidereal target) 4.5 to 90.5 (final limits)
Pointing accuracy, deg.	0.02 pointing 0.01 tracking
Maximum angular rate azimuth, deg/sec	0.5 (wind ≤ 30mph)
Maximum angular elevation, deg/sec	0.5 (wind ≤ 30mph)
Maximum acceleration azimuth, deg/sec	0.2 (wind ≤ 30mph)
Maximum acceleration elevation, deg/sec	0.2 (wind ≤ 30mph)
Servo bandwidth adjustment, hz.	0.01 to 0.2
Gain at 2300 MHz, db	61
Beamwidth at 2300 MHz, deg.	≈0.13 (2.2×10^{-3} radians)
System temperature, * ^{o}K	18
Antenna temperature, ^{o}K	≈10
Reflector diameter, ft.	210
Reflector f/D ratio	0.4235

* Includes maser amplifier, receiver, transmission line, listening feed, and the antenna pointing at a quiet sky.

Table A-1. Expected performance of 210-foot DSIF altazimuth antenna.

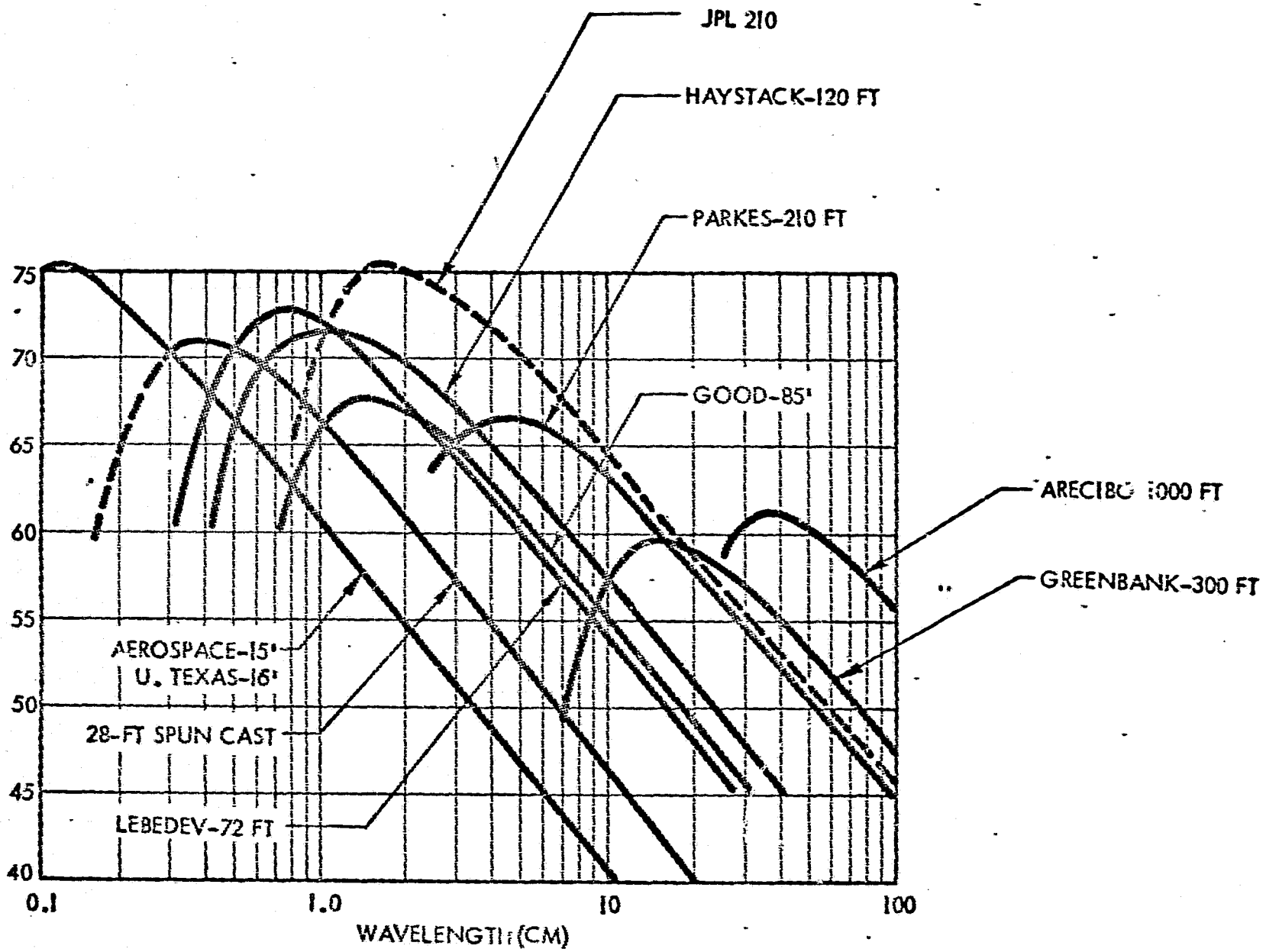

Fig. A-1 GAIN OF LARGE PARABOLOIDS (BASED ON PUBLISHED ESTIMATE).

NOTE: THE 210 FOOT AAS CURVE IS BASED ON UNCORRECTED MEASUREMENTS MADE AT A 45° ELEVATION ANGLE AT A WAVELENGTH OF 3.55 CM WITH NO WINDS IN EXCESS OF 20 MPH.

RUZE - PROC. OF IEEE, 54-4

It has been indicated by JPL (A-1) that apertures which are electrically equivalent, but larger than the 200 ft. in diameter class of paraboloid, are very expensive and are probably not economically warranted for the next ten to fifteen years. Some consideration is being given to a 400 ft. dish for radio astronomy application by the CAMRAC group. Thus, for total apertures less than the aperture of an antenna roughly 250 ft. in diameter, a single paraboloid should be used. For total apertures in excess of this size by an appreciable amount, it will be best realized by arrays paraboloids of optimum size. Several other approaches such as the fixed spherical-reflector approach and multiplate antenna appear to offer a large aperture at low cost. In spite of this apparently attractive feature, they have their respective shortcomings. (A-2, 3, and 4, 5). When used in deep space communications applications, there appears to be little or no economic gain over steerable paraboloids. However, these special forms of optical antennas merit further study in this program.

The requirement of narrow beamwidths, low sidelobe levels and broadband operation for the generation of a pencil-shaped antenna beam has well been achieved by the system of a point source feed and paraboloidal reflector. However, the beam axis coincides with the geometric axis of the paraboloidal surface so that in order to scan the beam, it becomes necessary to move the whole reflector mechanically. A spherical reflector employed in a microwave antenna leads to a system whose beam can be steered without moving the reflector (A-6). The beam axis coincides with the radius of the sphere upon which the feed happens to lie. Scanning is achieved by a single rotation of the feed about the center of the sphere. Due to the spherical aberration, however, a point source feed cannot be used unless the primary illumination of the reflector is confined to a relatively small zone of the spherical surface (A-2). Aperture efficiency is then small and total reflector size becomes enormous relative to an equivalent paraboloid. Several proposals exist, however, for correcting the annoying phenomena of spherical aberration. One approach utilizes a secondary reflector to refocus the aberrant rays to a true point focus (A-7). Another method, analogous to those in present optical use, requires correcting lenses of the Mangan or Maksutov Type. The third approach makes use of the fact that a spherical mirror possesses a line focus. By using a line source, rather than a point

source feed, spherical aberration can be eliminated and primary illumination need not be confined to the paraxial region of the sphere (A-8,9). The gains of the 10-foot spherical reflectors illuminated either by the square-aperture horn at frequency of 11.2 GHz (A-2) or a combined line source (A-9) are in the magnitude of 39 db. This is equivalent to the gain of a uniformly illuminated circular aperture of 31-inch diameter, or a typical paraboloid of 40-inch diameter. The total useful angle of scan of the former 10-foot spherical reflector antenna is about $\pm$ 70° with approximately 1 1/2 db. loss of gain at 70° from the zenith. A 1000-foot spherical dish was completed in 1962 in Arecibo, Puerto Rico, for radio astronomy applications. The specific designed line source feed corrects for the optical aberrations of the sphere and permits off-axis scanning to 20° with less than 3 db. loss of gain (A-3). It seems that by use of a fixed spherical reflector to achieve narrow beam of large aperture antenna, high aperture efficiency and wide-angle scan designs are mutually exclusive.

A multiplate reflector system is another distinct approach to steer antenna beams without moving a huge reflector. A multiplate antenna consists of a large number of independently adjustable reflecting plates with optimum sizes, which could be used with a fixed feed to form a steerable beam. For a feed located above the plates which are distributed over an area, energy radiated from the feed impinges upon the identical plates which are individually tilted and tipped to redirect the energy in the desired direction. However, the gaps between plates, the diffraction around plate edges and the double reflection due to the openings of the gaps are the kind of problems which the antenna system with a continuous reflector surface does not encounter. The multiplate antenna tested by Air Force Cambridge Research Lab. suffers from low efficiency and coverage problems, compounded by high antenna noise temperature (A-4,5).

7. REFERENCES

A-1. Potter, Merrick, Ludwig ,"Large Antenna Apertures and Arrays for Deep Space Communications", JPL Technical Report No. 32-848, Jet Propulsion Laboratory, California Institute of Technology, Pasadena, California, November 1965.

A-2. Li, Tingye, "A Study of Spherical Reflectors as Wide Angle Scanning Antennas," IRE Transactions on Antennas and Propagation, vol. Ap-7, No. 3, pp. 223-226, July 1959.

A-3. Kay, A. F., "Design of Line Feed for World's Largest Aperture Antenna," Electronics vol. 34, pp. 46-47, July, 1961.

A-4. Schell, A. C., "An Analysis of the Effects Caused by Interstices on a Multiplate Plate Antenna; AFCRL Technical Memo CRRD-81, Feb., 1963.

A-5. Schell, A. C. "A Multiplate Radio Astronomy Antenna," Nerem Record, pp. 196-197, 1963.

A-6. Ashmead J. and Pipard A. B., "The Use of Spherical Reflectors as Microwave Scanning Aerials," J. IEE, vol. 93, pt. IIIA, p.627, July, 1946.

A-7. Head, A. K., "A New Form for a Giant Radio Telescope," Nature, vol. 170, pp. 692-693, April, 1957.

A-8. Spencer, R. C., Sleten C. J., and Walsh, J. E., "Correction of Spherical Aberration By a Phase Line Source," PROC. N.E.C., vol. 5, pp. 320-333, 1959.

A-9. Shell, A. C. "The Diffraction Theory of Large-Aperture Spherical Reflector Antenna," IEEE Trans. on Antennas and Propagation, vol. ap-11, pp.428-432, July, 1963.

B. AN ARRAY OF LARGE DISH ANTENNAS

1) Introduction

As has been mentioned before, an array of independently mechanically steerable paraboloids with proper size and separation may be one of several workable approaches capable of achieving the high gain requirement for the DSCS. To provide the requisite scanning angle of $\pm 60^{\circ}$ without interference between adjacent paraboloids, the spacing between reflectors must be kept at a reasonable distance which is larger than the diameter of the paraboloids. Thus, a minimum separation distance must be determined which utilizes a given aperture size most efficiently. As the separation is increased, the formation of grating lobes in a large array of parabolic reflectors constitutes a serious difficulty for which no generally satisfactory solution has yet been developed. The problem can be visualized if the array pattern is considered as the product of an element pattern and an array factor. The element pattern consists of the radiation pattern produced by a parabolic reflector, while the array factor is the pattern of an array of isotropic radiators which is a two-dimensional grating lobe pattern. The array factor can be steered electronically by shifting the phase between elements while the element pattern is directed by the mechanical movement of the individual dishes. In the ideal case, the element pattern and a single lobe of the array factor will both point in the desired direction. Multiple beams appear, however, when more than one grating lobe falls within the main beam of the element factor; this condition occurs when the array spacing is substantially greater than the diameter of the subapertures.

It can be easily shown that the spacing of the grating lobes from the main beam can be increased by a decrease in the separation of the parabolic reflector antenna elements. However, if this spacing is decreased, the diameter of the reflectors must also be decreased so that the effective scan range can be maintained, while at the same time more array elements must be added to meet the gain requirement. The end result will be a broader element pattern which in turn will ensure that the grating lobes will have essentially the same amplitude relative to the main beam. The beamwidth of both the main beam and the grating lobes will, for all practical purposes, remain the same as long as the overall array dimensions remain unaltered.

The fine grain structure around the various lobes will change, however, as more elements are added. Similarly, if the spacing between the elements is increased, and the diameter of the reflectors is increased correspondingly, the grating lobes will be moved in closer to the principal beam. Once again the relative amplitude and beamwidth of all the grating lobes should remain essentially constant.

There are some esoteric techniques available to suppress the size of the grating lobes. A possibility exists that the grating lobes adjacent to the principal beam may be reduced in amplitude by the use of random spacing among the array elements. However, it is anticipated that the selection of such a design will prove to be an extremely difficult problem. Another means of suppressing the grating lobes might involve the use of an auxiliary array that could be steered and phased to cancel out any given lobe. A major difficulty that might be anticipated from such a scheme would be the obtaining of sufficient gain from the auxiliary array.

The juxtaposition of spacing and reflector size discussed above is predicated on little or no interaction between the elements as a function of scan angle. When this interaction effect is taken into account an entirely different solution may be obtained for the competing parameters. Thus, it shall be the purpose of this section to study the problems associated with being able to analytically determine a spacing and antenna size which is optimum between the interference effects at minimum separation, and the grating lobe effects at a maximum distance commensurate with high aperture efficiency. Since the theory and manipulation of the array factor and element pattern is available elsewhere, the effort herein shall be concerned with methods and techniques for analyzing the interaction effects between large parabolic reflectors in a relatively closely spaced array.

2) Theoretical Consideration of the Interaction between Neighboring Paraboloid Antennas

a) Introduction - It has been learned that some mutual coupling measurements on neighboring paraboloid antennas has been done by Andrews (B-1) for Collins Radio Co. and a similar measurement also has been done recently by Reiche (B-2) at the Hughes Aircraft Co. It seems, however, that there is

no literature concerning theoretical analysis available. Therefore, it is desirable to develop the analytical form which governs the fields of a paraboloid antenna as a function of scan angle in the presence of neighboring array elements of an identical kind.

The far field transmitting and receiving patterns of the neighboring paraboloidal antennas with their vertices far apart will be the vector sum of individual contributions at the field point and the vector sum of the receiving fields at individual feeds respectively. In fact, the transmitting and receiving patterns of the paraboloidal antennas system in Fraunhofer region are the same in this case. As the positions of the vertices of the paraboloidal antennas get near enough, the interaction between them can no longer be negligible. The interaction between the paraboloidal antennas for which the system being used for transmitting function and that for which the system being use for receiving function will constitute different problems which merit separate investigations. In this report, however, the following paragraphs are devoted to the interaction between the paraboloidal antennas for transmitting function. The case for receiving function will be included in a future report.

For transmitting function, the interaction may be approximately solved by considering the second paraboloid as a disklike obstacle in the near field of the first paraboloid. The surface current distribution on the disk due to the first paraboloid can be calculated; this current distribution on the disk then sets up a secondary surface current distribution on the surface of the first paraboloid. This secondary current distribution then becomes a modification factor on the primary current distribution due to the feed of the first paraboloid and thus modifies its far-field pattern.

The surface current density $\bar{K}$ on the disk due to the primary current distribution of the first paraboloid and the secondary current density $\bar{K}'$ on the first paraboloid due to the current density $\bar{K}$ on the disk have been formulated in paragraph (b) and paragraph (c) respectively. In paragraph (d), the electric field $\bar{E}'_{P_1}$ due to the secondary current density $\bar{K}'$ on the first paraboloid has been found. Also, the electric field $\bar{E}_{P_1}$ due to the primary current distribution of the first paraboloid and the electric field $\bar{E}_{P_2}$ due to the primary current distribution of the second paraboloid have been found in paragraph (e). The total electric field $\bar{E}_P$ in the far-zone region of these neighboring parab-

oloidal antennas is the vector sum of $\bar{E}_{P_1}$, $\bar{E}'_{P_1}$, and $\bar{E}_{P_2}$.

b) <u>The Surface Current Distribution on the Disk</u> The coordinate of the current distribution on the disk is $P'(U,\alpha,\beta)$ in the spherical coordinate with the origin at the focus, F_1 , of the first paraboloid and also is $P'(R',\theta',\psi')$ in the fixed spherical coordinate with the origin at point O. The source point Q on the surface of the first paraboloid is $Q(\rho,\xi,\psi)$ with the origin at the focus F_1; the axes of the paraboloids are in (θ_1, ϕ_1) direction as shown in Fig. 1 and Fig. 2.

Considering the case where the disk being in the far-zone region of the first paraboloid, the electric field at point P' on the disk is

$$\bar{E}_{P'} = -\frac{j\omega\mu}{4\pi}\frac{e^{-jkU}}{U}\left[8\left(\frac{\epsilon}{\mu}\right)^{1/2}\frac{P_T}{4\pi}\right]^{1/2}$$

$$\cdot\int_{S'}\left[G_f(\xi,\psi)\right]^{1/2}\frac{e^{-jk\rho[1-\bar{a}_U\cdot\bar{a}_\rho]}}{\rho}$$

$$\cdot\left[-\cos\frac{\psi}{2}\,\bar{e}_1 + (\bar{n}\cdot\bar{e}_1)\,\bar{s}_1\right]ds'$$

where

$$\bar{a}_U = \sin\alpha\cos\beta\,\bar{a}_{x'} + \sin\alpha\sin\beta\,\bar{a}_{y'} + \cos\alpha\,\bar{a}_{z'}$$

$$\bar{a}_\rho = \sin\psi\cos\xi\,\bar{a}_{x'} + \sin\psi\sin\beta\,\bar{a}_{y'} - \cos\psi\,\bar{a}_{z'}$$

$$\bar{a}_U\cdot\bar{a}_\rho = -\cos\alpha\cos\psi + \sin\alpha\sin\psi\cos(\beta-\xi)$$

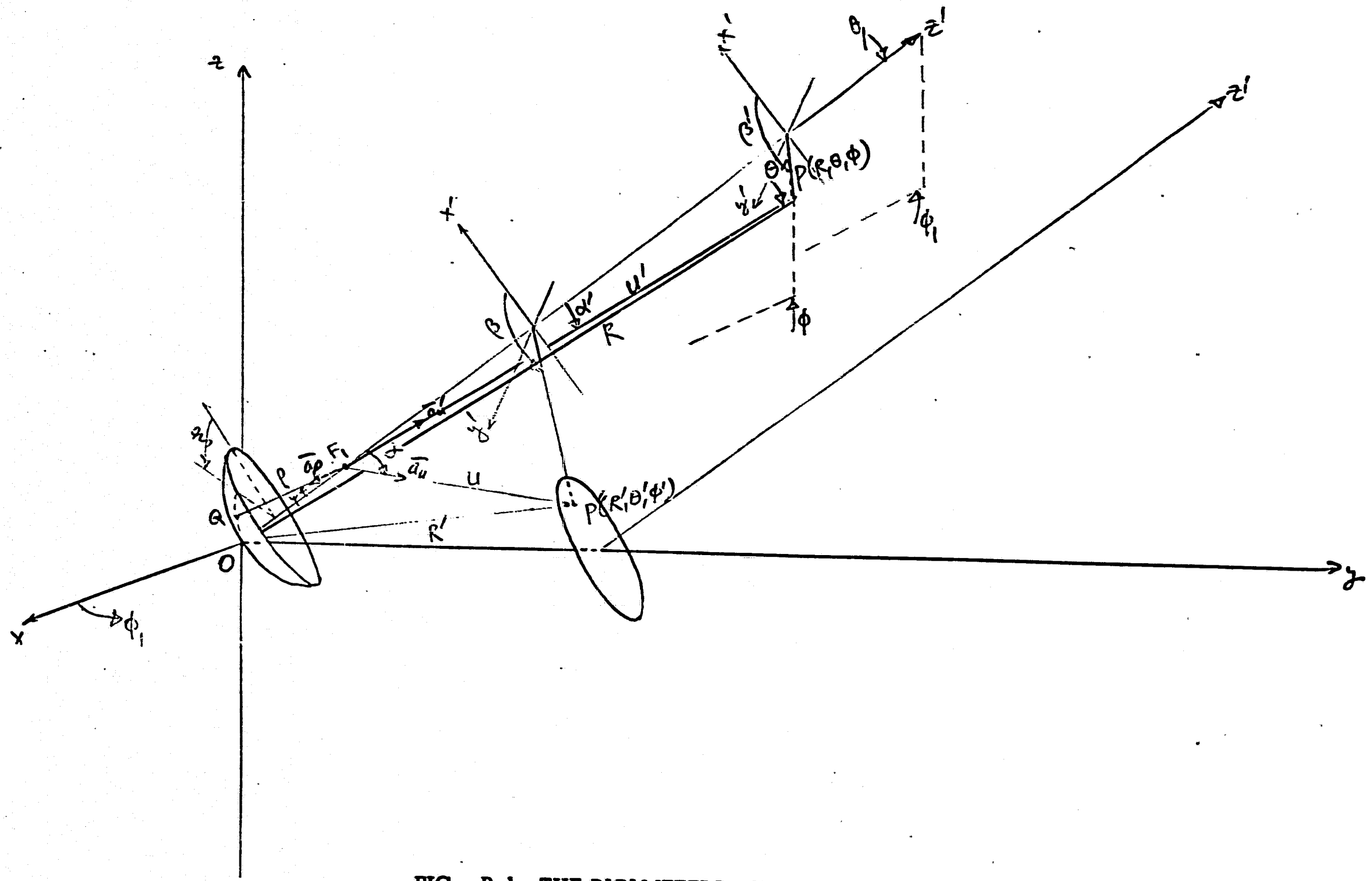

FIG. B-1 THE PARAMETERS FOR CALCULATING THE CURRENT DENSITY AT P (R', θ', φ') ON THE CONDUCTING DISK

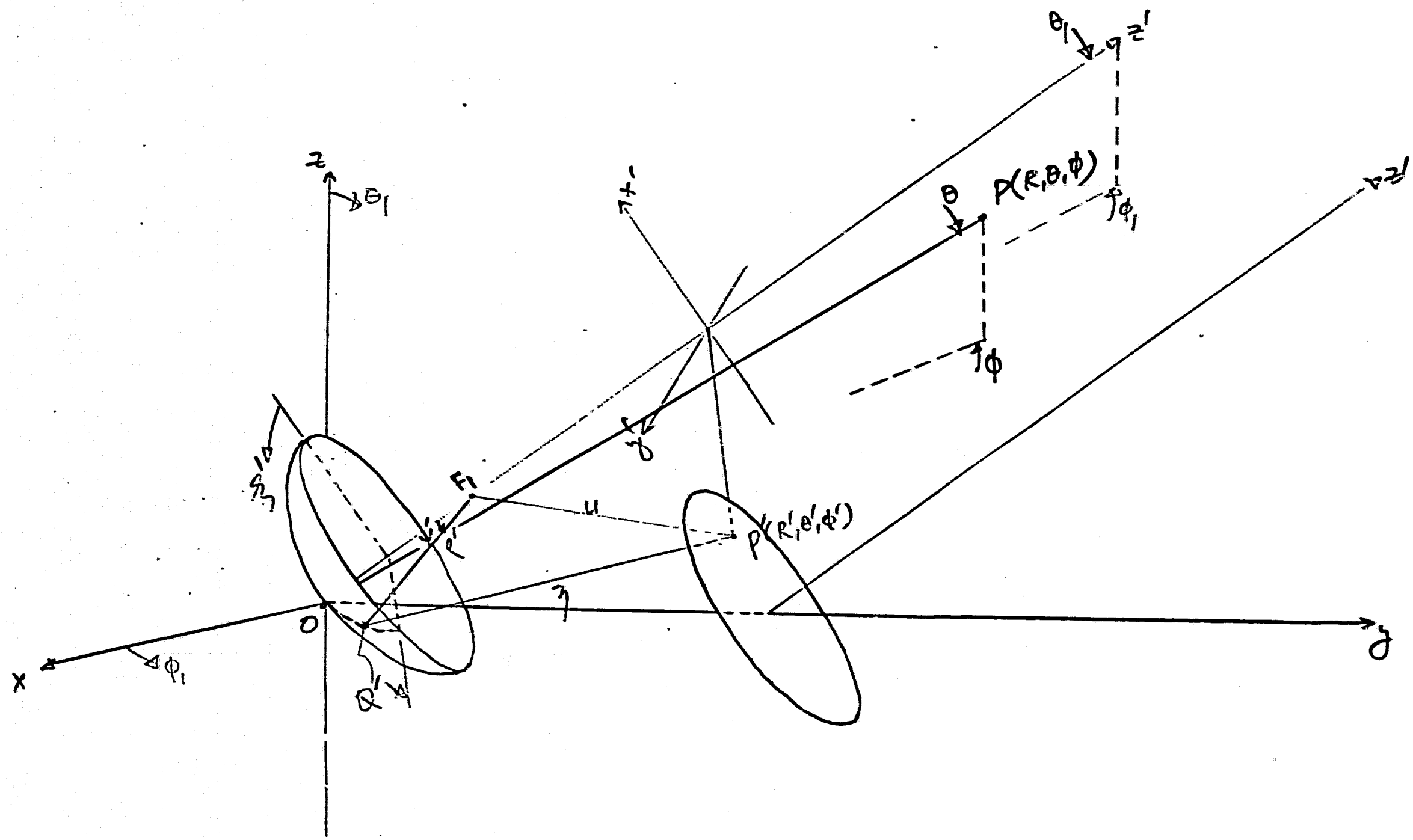

FIG . B-2 THE PARAMETERS FOR CALCULATING THE SECONDARY CURRENT DENSITY AT Q'(P', Ψ', ξ') ON THE FIRST PARABOLOID.

and

ϵ	permitivity of the medium
μ	permeability of the medium
P_T	The total power transmitted by the feeds of the paraboloids
$G_f(\xi,\psi)$	The directivity of the feeds of the paraboloids
$\bar{n}$	The unit normal vector to the surface of the paraboloids, which is $n_x \bar{a}_x + n_y \bar{a}_y + n_z \bar{a}_z$
$\bar{e}_1$	The polarization of the reflected wave from the paraboloids, which is $e_{1x} \bar{a}_x + e_{1y} \bar{a}_y + e_{1z} \bar{a}_z$
$\bar{S}_1$	The propagation direction of the reflected wave, for present case, $\bar{S}_1 = \bar{a}_{z1} = \sin\theta_1 \cos\phi_1 \bar{a}_x + \sin\theta_1 \sin\phi_1 \bar{a}_y + \cos\theta_1 \bar{a}_z$
ds'	The element of the surface of the paraboloids, which is $\rho^2 \sin\psi \sec\frac{\psi}{2} d\psi d\xi$
F	The focal length of the paraboloids

To the first approximation, the electric field at P' on the disk becomes

$$\bar{E}_{P'} = -\frac{j\omega\mu}{4\pi}\left[8\left(\frac{\epsilon}{\mu}\right)^{1/2}\frac{P_T}{4\pi}\right]^{1/2}\frac{e^{-jkR'}}{R'}e^{jkF\cos(\phi_1-\phi')} \cdot\left\{\bar{I}_1+\bar{I}_2\right\}$$

where

$$\bar{I}_1 = \int_{\xi=0}^{2\pi}\int_{\psi=0}^{\bar{\Psi}}\left[G_f(\xi,\psi)\right]^{1/2}\frac{e^{-jk\rho[1-\bar{a}_u\cdot\bar{a}_\rho]}}{\rho}\left[-\cos\frac{\psi}{2}\,\bar{e}_1\right]\cdot\rho^2\sin\psi\sec\frac{\Psi}{2}\,d\psi\,d\xi$$

$$\bar{I}_2 = \int_{\xi=0}^{2\pi}\int_{\psi=0}^{\bar{\Psi}}\left[G_f(\xi,\psi)\right]^{1/2}\frac{e^{-jk\rho[1-\bar{a}_u\cdot\bar{a}_\rho]}}{\rho}\left[(\bar{n}\cdot\bar{e}_1)\,\bar{a}_{z'}\right]\cdot\rho^2\sin\psi\sec\frac{\Psi}{2}\,d\psi\,d\xi$$

Thus, the magnetic field at point P' on the disk becomes

$$\bar{H}_{P'} = -\frac{j\omega\mu}{4\pi}\left(\frac{\epsilon}{\mu}\right)^{1/2}\left[8\left(\frac{\epsilon}{\mu}\right)^{1/2}\frac{P_T}{4\pi}\right]^{1/2}\frac{e^{-jkR'}}{R'}e^{jkF\cos(\phi_1-\phi')} \cdot\int_{\xi=0}^{2\pi}\int_{\psi=0}^{\bar{\Psi}}\left[G_f(\xi,\psi)\right]^{1/2}\frac{e^{-jk\rho[1-\bar{a}_u\cdot\bar{a}_\rho]}}{\rho}\cos\frac{\Psi}{2} \cdot\left[\bar{e}_1\times\bar{a}_{z'}\right] \cdot\rho^2\sin\psi\sec\frac{\Psi}{2}\,d\psi\,d\xi$$

Then, the surface distributed current density $\bar{K}$ on the conducting disk is

$$\bar{K} = (-\hat{z}) \left\{ -\frac{j\omega\mu}{4\pi} \left(\frac{\epsilon}{\mu}\right)^{1/2} \left[8 \left(\frac{\epsilon}{\mu}\right)^{1/2} \frac{P_T}{4\pi} \right]^{1/2} \right\} \frac{e^{-jkR'}}{R'} e^{jkF\cos(\phi_1 - \phi')}$$

$$\cdot \int_{\xi=0}^{2\pi} \int_{\psi=0}^{\Psi_c} \left[G_x(\xi,\psi) \right]^{1/2} \frac{e^{-jk\rho[1-\bar{a}_u \cdot \bar{a}_\rho]}}{\rho} \cos\frac{\psi}{2} \left[\bar{a}_{z'} \times (\bar{e}_1 \times \bar{a}_{z'}) \right]$$

$$\cdot \rho^2 \sin\psi \sec\frac{\psi}{2}\, d\psi\, d\xi$$

Let $$\left[\bar{a}_{z'} \times (\bar{e}_1 \times \bar{a}_{z'}) \right] = A_x \bar{a}_x + A_y \bar{a}_y + A_z \bar{a}_z$$

Where

$$A_x = \sin\theta_1 \sin\phi_1 \left(e_{1x} \sin\theta_1 \sin\phi_1 - e_{1y} \sin\theta_1 \cos\phi_1 \right) - \cos\theta_1 \left(e_{1z} \sin\theta_1 \cos\phi_1 - e_{1x} \cos\theta_1 \right)$$

$$A_y = \cos\theta_1 \left(e_{1y} \cos\theta_1 - e_{1z} \sin\theta_1 \sin\phi_1 \right) - \sin\theta_1 \sin\phi_1 \left(e_{1x} \sin\theta_1 \sin\phi_1 - e_{1y} \sin\theta_1 \cos\phi_1 \right)$$

$$A_z = \sin\theta_1 \cos\phi_1 \left(e_{1z} \sin\theta_1 \cos\phi_1 - e_{1x} \cos\theta_1 \right) - \sin\theta_1 \sin\phi_1 \left(e_{1y} \cos\theta_1 - e_{1z} \sin\theta_1 \sin\phi_1 \right)$$

Finally, the surface current density $\bar{K}$ on the conducting disk becomes

$$\bar{K} = \frac{A e^{-jkR'}}{R'} e^{jkF\cos(\phi_1 - \phi')} \left[I_x \bar{a}_x + I_y \bar{a}_y + I_z \bar{a}_z \right]$$

Where $$A = (-\lambda) \left\{ -\frac{j\omega\mu}{4\pi} \left(\frac{\epsilon}{\mu}\right)^{1/2} \left[8 \left(\frac{\epsilon}{\mu}\right)^{1/2} \frac{P_T}{4\pi} \right]^{1/2} \right\}$$

$$I_x = \int_{\xi=0}^{2\pi} \int_{\psi=0}^{\bar{\Psi}} \left[G_f(\xi,\psi) \right]^{1/2} \frac{e^{-jk\rho[1-\bar{a}_u \cdot \bar{a}_\rho]}}{\rho} A_x \cos\frac{\psi}{\lambda} \cdot \rho^2 \sin\psi \sec\frac{\psi}{2} \, d\psi \, d\xi$$

$$I_y = \int_{\xi=0}^{2\pi} \int_{\psi=0}^{\bar{\Psi}} \left[G_f(\xi,\psi) \right]^{1/2} \frac{e^{-jk\rho[1-\bar{a}_u \cdot \bar{a}_\rho]}}{\rho} A_y \cos\frac{\psi}{\lambda} \cdot \rho^2 \sin\psi \sec\frac{\psi}{2} \, d\psi \, d\xi$$

$$I_z = \int_{\xi=0}^{2\pi} \int_{\psi=0}^{\bar{\Psi}} \left[G_f(\xi,\psi) \right]^{1/2} \frac{e^{-jk\rho[1-\bar{a}_u \cdot \bar{a}_\rho]}}{\rho} A_z \cos\frac{\psi}{\lambda} \cdot \rho^2 \sin\psi \sec\frac{\psi}{2} \, d\psi \, d\xi$$

c) <u>The Secondary Surface Current Distribution on the First Paraboloid</u> The surface distributed current density $\bar{K}$ at point P' on the conducting disk will again set up a secondary current density $\bar{K}'$ on the surface of the first paraboloid. This secondary surface current density will become a modification factor to the far-field pattern of these neighboring paraboloid antennas system.

The magnetic field at Q' on the first paraboloid due to the current density $\bar{K}$ at P' on the disk is

$$\bar{H}_{Q'} = \frac{jkA}{4\pi}\left[L_x \bar{a}_x + L_y \bar{a}_y + L_z \bar{a}_z \right]$$

where

$$L_x = \int_{\xi'=0}^{2\pi} \int_{\psi'=0}^{\Psi} \frac{e^{-j2kR'}}{(R')^2} e^{jkF\cos(\phi_1-\phi')} \cdot \left[\sin\theta'\sin\phi' I_z - \cos\theta' I_y \right] \cdot e^{jkB_1} \cdot e^{jkB_2} \cdot e^{jkB_3} \cdot (\rho')^2 \sin\psi' \sec\frac{\psi'}{2}\, d\psi' d\xi'$$

$$L_y = \int_{\xi'=0}^{2\pi}\int_{\psi'=0}^{\Psi} \frac{e^{-j2kR'}}{(R')^2} e^{jkF\cos(\phi_1-\phi')}\left[\cos\theta' I_x - \sin\theta'\cos\phi' I_z\right] \cdot e^{jkB_1} \cdot e^{jkB_2} \cdot e^{jkB_3} \cdot (\rho')^2 \sin\psi' \sec\frac{\Psi}{2}\, d\psi' d\xi'$$

$$L_z = \int_{\xi'=0}^{2\pi}\int_{\psi'=0}^{\Psi} \frac{e^{-j2kR'}}{(R')^2} e^{jkF\cos(\phi_1-\phi')}\left[\sin\theta'\cos\phi' I_y - \sin\theta'\sin\phi' I_x\right] \cdot e^{jkB_1} \cdot e^{jkB_2} \cdot e^{jkB_3} \cdot (\rho')^2 \sin\psi' \sec\frac{\Psi}{2}\, d\psi' d\xi'$$

with

$$B_1 = \sin\theta'\cos\phi'\left[F\sin\theta_1\cos\phi_1 + \rho'\left(A_1\sin\psi'\cos\xi' + A_2\sin\psi'\sin\xi' - A_3\cos\psi'\right)\right]$$

$$B_2 = \sin\theta'\sin\phi'\left[F\sin\theta_1\sin\phi_1 + \rho'\left(A_4\sin\psi'\cos\xi' + A_5\sin\psi'\sin\xi' - A_6\cos\psi'\right)\right]$$

$$B_3 = \cos\theta'\left[F\cos\theta_1 + \rho'\left(A_7\sin\psi'\cos\xi' + A_8\sin\psi'\sin\xi' - A_9\cos\psi'\right)\right]$$

$$A_1 = \sin\theta_2 \cos\phi_2$$

$$A_2 = \sin\theta_1 \sin\phi_1 \cos\theta_2 - \sin\theta_2 \sin\phi_2 \cos\theta_1$$

$$A_3 = \sin\theta_1 \sin\phi_1$$

$$A_4 = \sin\theta_2 \sin\phi_2$$

$$A_5 = \sin\theta_2 \cos\phi_2 \cos\theta_1 - \sin\theta_1 \cos\phi_1 \cos\theta_2$$

$$A_6 = \sin\theta_1 \sin\phi_1$$

$$A_7 = \cos\theta_2$$

$$A_8 = \sin\theta_1 \sin\theta_2$$

$$A_9 = \cos\theta_1$$

The angles θ_1, ϕ_1 ; θ_2, ϕ_2 are defined as follows:

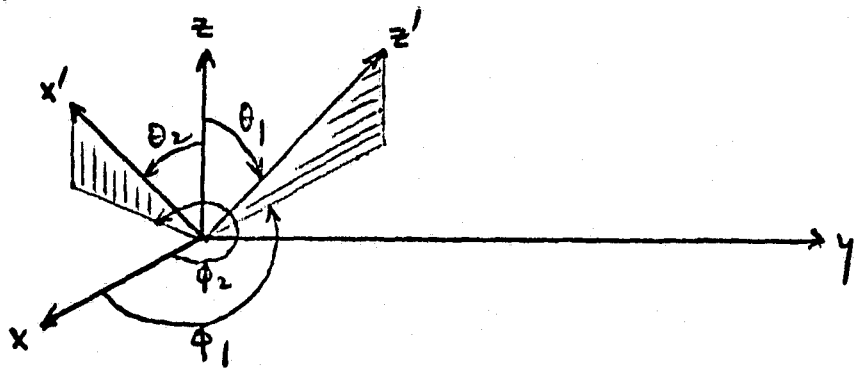

$$\bar{a}_{x'} = \sin\theta_2 \cos\phi_2 \, \bar{a}_x + \sin\theta_2 \sin\phi_2 \, \bar{a}_y + \cos\theta_2 \, \bar{a}_z$$

$$\bar{a}_{z'} = \sin\theta_1 \cos\phi_1 \, \bar{a}_x + \sin\theta_1 \sin\phi_1 \, \bar{a}_y + \cos\theta_1 \, \bar{a}_z$$

$$\bar{a}_{y'} = \bar{a}_{z'} \times \bar{a}_{x'}$$

Thus, the secondary current density $\bar{K}'$ on the first paraboloid due to the current density $\bar{K}$ on the conducting disk becomes

$$\bar{K}' = 2\frac{jkA}{4\pi}\left[\bar{a}_x(n_y L_z - n_z L_y) + \bar{a}_y(n_z L_x - n_x L_z) + \bar{a}_z(n_x L_y - n_y L_x)\right]$$

d) <u>The Electric Field in Fraunhofer Region due to the Secondary Surface Current Distribution</u> The electric field at observation point $P(R,\theta,\phi)$ in the far-field zone due to the secondary current density $\bar{K}'$ on the surface of the first paraboloid is

$$\bar{E}'_{P_1} = -\frac{jk^2}{4\pi\omega\epsilon}\,\frac{j2kA}{4\pi}\,\frac{e^{-jkR}}{R}$$

$$\cdot\Bigg[\bar{a}_x \int_{\xi'=0}^{2\pi}\int_{\psi'=0}^{\bar{\Psi}}\Big[(n_y L_z - n_z L_y) - C\sin\theta\cos\phi\Big]\, e^{jk\bar{OQ}'\cdot\bar{a}_R}$$

$$\cdot(\rho')^2\sin\psi'\sec\tfrac{\Psi'}{2}\,d\psi'd\xi'$$

$$+\bar{a}_y \int_{\xi'=0}^{2\pi}\int_{\psi'=0}^{\bar{\Psi}}\Big[(n_z L_x - n_x L_z) - C\sin\theta\sin\phi\Big]\, e^{jk\bar{OQ}'\cdot\bar{a}_R}$$

$$\cdot(\rho')^2\sin\psi'\sec\tfrac{\Psi'}{2}\,d\psi'd\xi'$$

$$+\bar{a}_z \int_{\xi'=0}^{2\pi}\int_{\psi'=0}^{\bar{\Psi}}\Big[(n_x L_y - n_y L_x) - C\cos\theta\Big]\, e^{jk\bar{OQ}'\cdot\bar{a}_R}$$

$$\cdot(\rho')^2\sin\psi'\sec\tfrac{\Psi'}{2}\,d\psi'd\xi'\Bigg]$$

where

$$C = \sin\theta\cos\phi\,(n_y L_z - n_z L_y) + \sin\theta\sin\phi\,(n_z L_x - n_x L_z) + \cos\theta\,(n_x L_y - n_y L_x)$$

$$\bar{a}_R = \sin\theta\cos\phi\;\bar{a}_x + \sin\theta\sin\phi\;\bar{a}_y + \cos\theta\;\bar{a}_z$$

$$\overline{OQ'} = F\,\bar{a}_{z'} + \rho'\bar{a}_{\rho'}$$

$$= \bar{a}_x\left[F\sin\theta_1\cos\phi_1 + \rho'(A_1\sin\psi'\cos\xi' + A_2\sin\psi'\sin\xi' - A_3\cos\psi')\right]$$

$$+ \bar{a}_y\left[F\sin\theta_1\sin\phi_1 + \rho'(A_4\sin\psi'\cos\xi' + A_5\sin\psi'\sin\xi' - A_6\cos\psi')\right]$$

$$+ \bar{a}_z\left[F\cos\theta_1 + \rho'(A_7\sin\psi'\cos\xi' + A_8\sin\psi'\sin\xi' - A_9\cos\psi')\right]$$

Notice that the equation for $\bar{E}'_{p_1}$ involves three surface integrals.

e) <u>The Electric Field of Neighboring Paraboloid Antennas in Fraunhofer Region</u> The electric field at observation point P due to the primary current density of the first paraboloid is

$$\bar{E}_{p1} = -\frac{j\omega\mu}{4\pi}\left[8\left(\frac{\epsilon}{\mu}\right)^{1/2}\frac{P_T}{4\pi}\right]^{1/2}\frac{e^{-jkR}}{R}\,e^{jkF\cos(\phi_1-\phi)}$$

$$\cdot\int_{\xi=0}^{2\pi}\int_{\psi=0}^{\Psi}\left[G_f(\xi,\psi)\right]^{1/2}\frac{e^{-jk\rho[1-\bar{a}_{u'}\cdot\bar{a}_\rho]}}{\rho}$$

$$\cdot\left[-\cos\frac{\psi}{2}\,\bar{e}_1 + (\bar{n}\cdot\bar{e}_1)\,\bar{a}_{z'}\right]\cdot\rho^2\sin\psi\sec\frac{\psi}{2}\,d\psi\,d\xi$$

where

$$\bar{a}_{u'} = \sin\alpha'\cos\beta'\,\bar{a}_{x'} + \sin\alpha'\sin\beta'\,\bar{a}_{y'} + \cos\alpha'\,\bar{a}_{z'}$$

$$\bar{a}_\rho = \sin\psi\cos\xi\,\bar{a}_{x'} + \sin\psi\sin\xi\,\bar{a}_{y'} - \cos\psi\,\bar{a}_{z'}$$

$$\bar{a}_{u'}\cdot\bar{a}_\rho = -\cos\alpha'\cos\psi + \sin\alpha'\sin\psi\cdot\cos(\beta'-\xi)$$

The electric field, for the first approximation, at observation point P due to the primary current distribution of the second paraboloid is

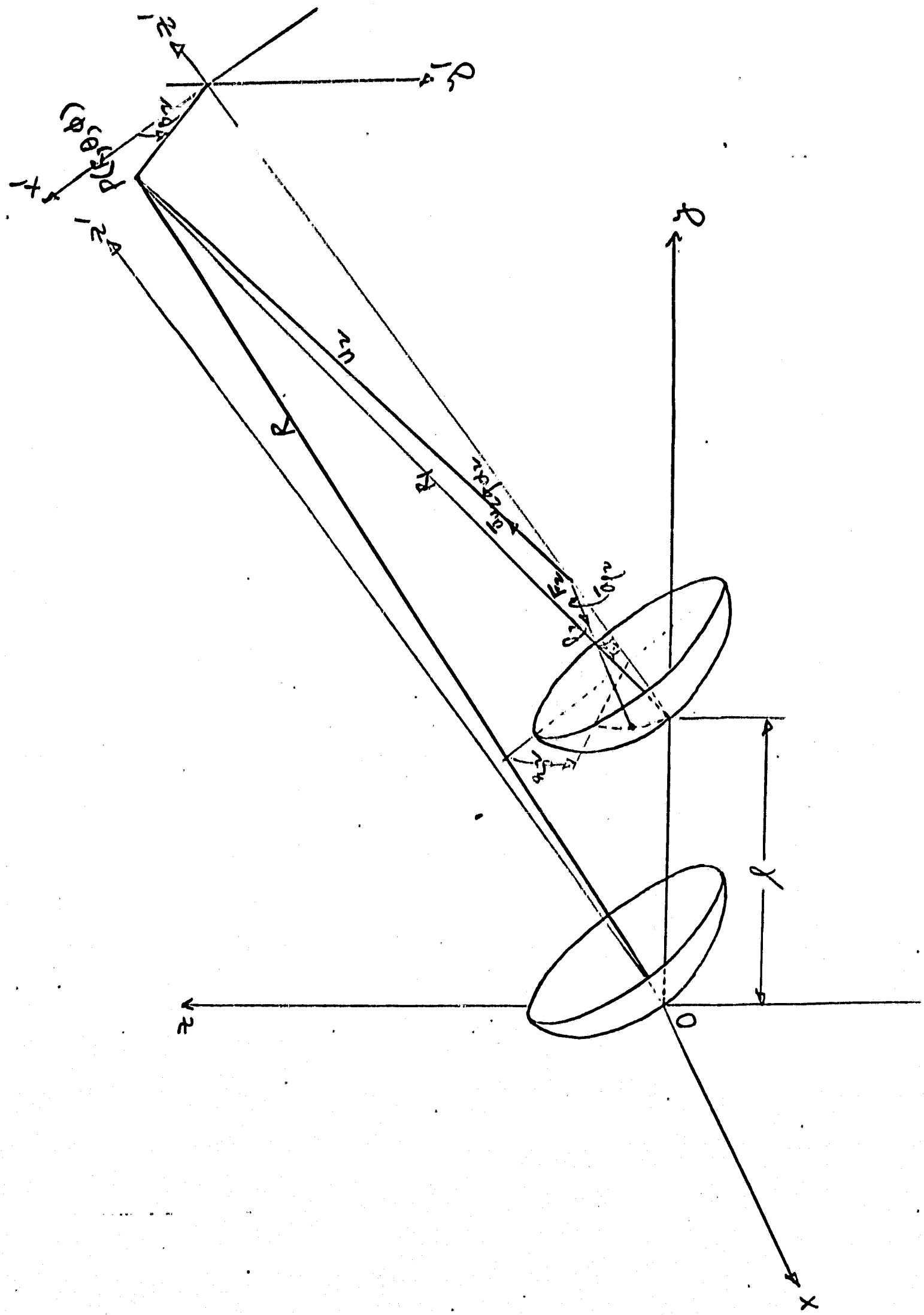

FIG. B-3. THE PARAMETERS FOR CALCULATING THE ELECTRIC FIELD AT P(R,Θ,Φ) DUE TO THE CONTRIBUTION OF SECOND PARABOLOID.

$$\bar{E}_{p_2} = -\frac{j\omega\mu}{4\pi}\left[\delta\left(\frac{\epsilon}{\mu}\right)^{1/2}\frac{P_T}{4\pi}\right]^{1/2}\frac{e^{-jkR}}{R}$$

$$\cdot e^{jkL\sin\theta\sin\phi}$$

$$\cdot e^{jkF[\cos\theta\cos\theta_1 + \sin\theta\sin\theta_1\cos(\phi-\phi_1)]}$$

$$\cdot e^{-jk\frac{LF}{R}\sin\theta_1\sin\phi_1}$$

$$\cdot \int_{\xi_2=0}^{2\pi}\int_{\psi_2=0}^{\overline{\psi}} \left[G_2(\xi_2,\psi_2)\right]^{1/2}\frac{e^{-jk\rho_2[1-\bar{a}_{u_2}\cdot\bar{a}_{\rho_2}]}}{\rho_2}$$

$$\cdot\left[-\cos\frac{\psi_2}{2}\bar{e}_1 + (\bar{n}\cdot\bar{e}_1)\bar{a}_{z_1}\right]\cdot\rho_2^2\sin\psi_2\sec\frac{\psi_2}{2}\,d\psi_2\,d\xi_2$$

where $\bar{a}_{u_2} = \sin\alpha_2\cos\beta_2\,\bar{a}_{x'} + \sin\alpha_2\sin\beta_2\,\bar{a}_{y'} + \cos\alpha_2\,\bar{a}_{z'}$

$$\bar{a}_{\rho_2} = \sin\psi_2\cos\xi_2\,\bar{a}_{x'} + \sin\psi_2\sin\xi_2\,\bar{a}_{y'} - \cos\psi_2\,\bar{a}_{z'}$$

$$\bar{a}_{u_2}\cdot\bar{a}_{\rho_2} = -\cos\alpha_2\cos\psi_2 + \sin\alpha_2\sin\psi_2\cos(\beta_2-\xi_2)$$

The parameters for calculating the electric field at $P(R,\theta,\phi)$ due to the contribution of second paraboloid as shown in Fig. 3. The separation between vertices of the paraboloids is L.

The total electric field at observation point P, $\bar{E}_p$, is the vector sum of the following components which are found in the previous paragraphs:

$\bar{E}_{p1}$ The electric field at P due to the primary current distribution of the first paraboloid.

$\bar{E}'_{p1}$ The electric field at P due to the secondary current distribution of the first paraboloid.

$\bar{E}_{p2}$ The electric field at P due to the primary current distribution of the second paraboloid.

Thus,

$$\bar{E}_p = \bar{E}_{p1} + \bar{E}'_{p1} + \bar{E}_{p2}$$

$$= \bar{a}_x (\bar{E}_p)_x + \bar{a}_y (\bar{E}_p)_y + \bar{a}_z (\bar{E}_p)_z$$

where $(\bar{E}_p)_x$, $(\bar{E}_p)_y$ and $(\bar{E}_p)_z$ are defined in the following pages.

$$(\bar{E}_p)_x = -\frac{j\omega\mu}{4\pi}\left[8\left(\frac{\epsilon}{\mu}\right)^{1/2}\frac{P_T}{4\pi}\right]^{1/2}\frac{e^{-jkR}}{R}\, e^{jkF\cos(\phi_1-\phi)}$$

$$\cdot\int_{\xi=0}^{2\pi}\int_{\psi=0}^{\Psi}\left[G_f(\xi,\psi)\right]^{1/2}\frac{e^{-jk\rho[1+\cos\alpha'\cos\psi-\sin\alpha'\sin\psi\cos(\beta'-\xi)]}}{\rho}$$

$$\cdot\left[-\cos\frac{\Psi}{2}\,e_{1x}+(n_x e_{1x}+n_y e_{1y}+e_z e_{1z})\sin\theta_1\cos\phi_1\right]$$

$$\cdot\rho^2\sin\psi\sec\frac{\Psi}{2}\,d\psi\,d\xi$$

$$-\frac{jk^2}{4\pi\omega\epsilon}\,\frac{j2kA}{4\pi}\,\frac{e^{-jkR}}{R}$$

$$\cdot\int_{\xi'=0}^{2\pi}\int_{\psi'=0}^{\Psi}\left[(n_y L_z-n_z L_y)-c\sin\theta\cos\phi\right]e^{jk\,\overline{OQ'}\cdot\bar{a}_R}$$

$$\cdot(\rho')^2\sin\psi'\sec\frac{\Psi'}{2}\,d\psi'\,d\xi'$$

$$-\frac{j\omega\mu}{4\pi}\left[8\left(\frac{\epsilon}{\mu}\right)^{1/2}\frac{P_T}{4\pi}\right]^{1/2}\frac{e^{-jkR}}{R}$$

$$\cdot e^{jkL\sin\theta\sin\phi}$$

$$\cdot e^{jkF[\cos\theta\cos\theta_1+\sin\theta\sin\theta_1\cos(\phi-\phi_1)]}$$

$$\cdot e^{-jk\frac{LF}{R}\sin\theta_1\sin\phi_1}$$

$$\cdot\int_{\xi_2=0}^{2\pi}\int_{\psi_2=0}^{\Psi}\left[G_f(\xi_2,\psi_2)\right]^{1/2}\frac{e^{-jk\rho_2[1+\cos\alpha_2\cos\psi_2-\sin\alpha_2\sin\psi_2\cos(\beta_2-\xi_2)]}}{\rho_2}$$

$$\cdot\left[-\cos\frac{\Psi_2}{2}\,e_{1x}+(n_x e_{1x}+n_y e_{1y}+n_z e_{1z})\sin\theta_1\cos\phi_1\right]$$

$$\cdot\rho_2^2\sin\psi_2\sec\frac{\Psi_2}{2}\,d\psi_2\,d\xi_2$$

$$(\bar{E}_p)_y = -\frac{j\omega\mu}{4\pi}\left[8\left(\frac{\epsilon}{\mu}\right)^{1/2}\frac{P_T}{4\pi}\right]^{1/2}\frac{e^{-jkR}}{R}\,e^{jkF\cos(\phi_1-\phi)}\cdot$$

$$\cdot\int_{\xi=0}^{2\pi}\int_{\psi=0}^{\Psi}\left[G_f(\xi,\psi)\right]^{1/2}\frac{e^{-jk\rho[1+\cos\alpha'\cos\psi-\sin\alpha'\sin\psi\cos(\beta'-\xi)]}}{\rho}$$

$$\cdot\left[-\cos\tfrac{\Psi}{2}\,e_{1y}+(n_x e_{1x}+n_y e_{1y}+n_z e_{1z})\sin\theta_1\sin\phi_1\right]$$

$$\cdot\rho^2\sin\psi\sec\tfrac{\Psi}{2}\,d\psi\,d\xi$$

$$-\frac{j\eta k^2}{4\pi\omega\epsilon}\,\frac{j2kA}{4\pi}\,\frac{e^{-jkR}}{R}$$

$$\cdot\int_{\xi'=0}^{2\pi}\int_{\psi'=0}^{\Psi}\left[(n_z L_x-n_x L_z)-C\sin\theta\sin\phi\right]e^{jk\overline{OQ'}\cdot\bar{a}_R}$$

$$\cdot(\rho')^2\sin\psi'\sec\tfrac{\Psi'}{2}\,d\psi'\,d\xi'$$

$$-\frac{j\omega\mu}{4\pi}\left[8\left(\frac{\epsilon}{\mu}\right)^{1/2}\frac{P_T}{4\pi}\right]^{1/2}\frac{e^{-jkR}}{R}$$

$$\cdot e^{jkL\sin\theta\cos\phi}$$

$$\cdot e^{jkF[\cos\theta\cos\theta_1+\sin\theta\sin\theta_1\cos(\phi-\phi_1)]}$$

$$\cdot e^{-jk(FL/R)\sin\theta_1\sin\phi_1}$$

$$\cdot\int_{\xi_2=0}^{2\pi}\int_{\psi_2=0}^{\Psi_2}\left[G_f(\xi_2,\psi_2)\right]^{1/2}\frac{e^{-jk\rho_2[1+\cos\alpha_2\cos\psi_2-\sin\alpha_2\sin\psi_2\cos(\beta_2-\xi_2)]}}{\rho_2}$$

$$\cdot\left[-\cos\tfrac{\Psi_2}{2}\,e_{1y}+(n_x e_{1x}+n_y e_{1y}+n_z e_{1z})\sin\theta\sin\phi_1\right]$$

$$\cdot\rho_2^2\sin\psi_2\sec\tfrac{\Psi_2}{2}\,d\psi_2\,d\xi_2$$

$$(\bar{E}_\rho)_z = -\frac{j\omega\mu}{4\pi}\left[8\left(\frac{\epsilon}{\mu}\right)^{1/2}\frac{P_T}{4\pi}\right]^{1/2}\frac{e^{-jkR}}{R}\,e^{jkF\cos(\phi_1-\phi)}$$

$$\cdot\int_{\xi=0}^{2\pi}\int_{\psi=0}^{\bar{\Psi}}\left[g_E(\xi,\psi)\right]^{1/2}\cdot\frac{e^{-jk\rho[1+\cos\alpha'\cos\psi-\sin\alpha'\sin\psi\cos(\beta'-\xi)]}}{\rho}$$

$$\cdot\left[-\cos\tfrac{\Psi}{2}\,e_{1z}+(n_x e_{1x}+n_y e_{1y}+n_z e_{1z})\cos\theta_1\right]$$

$$\cdot\rho^2\sin\psi\sec\tfrac{\Psi}{2}\,d\psi\,d\xi$$

$$-\frac{jk^2}{4\pi\omega\epsilon}\frac{j2kA}{4\pi}\frac{e^{-jkR}}{R}$$

$$\cdot\int_{\xi'=0}^{2\pi}\int_{\psi'=0}^{\bar{\Psi}}\left[(n_x L_y-n_y L_x)-c\cos\theta\right]e^{jk\,\bar{OQ'}\cdot\bar{a}_R}$$

$$\cdot(\rho')^2\sin\psi'\sec\tfrac{\Psi}{2}'\,d\psi'\,d\xi'$$

$$-\frac{j\omega\mu}{4\pi}\left[8\left(\frac{\epsilon}{\mu}\right)^{1/2}\frac{P_T}{4\pi}\right]^{1/2}\frac{e^{-jkR}}{R}$$

$$\cdot e^{jkL\sin\theta\sin\phi}$$

$$\cdot e^{jkF[\cos\theta\cos\theta_1+\sin\theta\sin\theta_1\cos(\phi-\phi_1)]}$$

$$\cdot e^{-jk(FL/R)\sin\theta_1\sin\phi_1}$$

$$\cdot\int_{\xi_2=0}^{2\pi}\int_{\psi_2=0}^{\bar{\Psi}}\left[g_E(\xi_2,\psi_2)\right]^{1/2}\frac{e^{-jk\rho_2[1+\cos\alpha_2\cos\psi_2-\sin\alpha_2\sin\psi_2\cos(\beta_2-\xi_2)]}}{\rho_2}$$

$$\cdot\left[-\cos\tfrac{\Psi_2}{2}\,e_{1z}+(n_x e_{1x}+n_y e_{1y}+n_z e_{1z})\cos\theta_1\right]$$

$$\cdot\rho_2^2\sin\psi_2\sec\tfrac{\Psi_2}{2}\,d\psi_2\,d\xi_2$$

f) Future Work As to the present, no numerical result has been obtained from this formulation; it is helpful to perform the numerical calculation with the aid of computer in order to check the data obtained by Reiche and Andrews. Furthermore, in the course of investigation, the edge effect, the spillover phenomena, the diffraction effect and the feed-to-feed coupling, which will add more complexity to the analysis, have not yet been considered. It is important to look further into these complicated factors in order to gain more accurate result to the analysis.

REFERENCES

B-1 Private Communication of work done by the Andrews Corporation, Chicago, Illinois for the Collins Radio Corporation.

B-2 Private Communication from J. Reiche, Hughes Aircraft Company, Culver City, California as an Interdepartmental Correspondence.

C. A PHASED ARRAY OF SMALL CLOSELY SPACED ELEMENTS ORGANIZED INTO SUBAPERTURES

1) Introduction

Although the present state-of-the-art in extremely large phased arrays, especially at S-band, is behind that for large dishes, there is no fundamental reason that limits the size of an array except the questions of signal to noise ratio, availability of low loss transmission line, and the basic cost of the individual components. At present these questions concerned with the fundamentals of organization versus economics is one of the problems to which this program has been addressed during its entirety. There will be more discussion of this point at a later date after some of the results obtained in the section can be analyzed and compared with the corresponding results from the other types of antenna systems. These problems coupled with the practical problems of distribution and feeding techniques, element type, and scanning techniques require some special consideration when the array is divided into an appropriate number of subapertures. It is the purpose of this report to delineate some of the studies and to present the information that has been uncovered in the area of phase array technology which must be advanced to make such an array feasible for the DSCS program. An additional purpose is to relate the problems areas of various phased array techniques and to establish avenues for the solution in each of the problem areas to have the highest probability of success.

An important consideration in the design of such a large array is how the system should be organized; i.e., how the individual elements should be combined, phase shifted and detected to obtain the required specifications at the minimum cost. In order to quantitatively study this problem and obtain some numerical results, a dense array of dipoles over a ground plane was chosen as a receiving antenna model; this choice of a model was made partly because it could be analyzed rather easily and partly because it represents a practical high gain element which could be economically mass produced by depositing or photoetching techniques. All the calculations reported here were made for uniform distribution broadside condition (equal amplitude and constant phase) and linear polarization. Phase shifters were included in the models, however, so that the results could validly be extended to the beam steering mode of operation and used for problems in adaptive systems.

It was assumed that for large arrays or subarrays with fixed interelement spacing the effective collecting aperture is proportional to the number of elements and, in fact, is equal to the physical array size. This assumption is verified in Appendix I. Thus an interelement spacing was fixed at $\lambda/2$ (center to center) in both directions and elevated $\lambda/4$ over a ground plane; this choice was made because it represents a model commonly used in practice, and because it avoids any spurious or grating lobes.

In order to make some quantitative evaluation of the merits of the different organization schemes some numerical values were established for the communication link. These are

Frequency	2.3 GHz
Transmitted power	50 watts
Transmitter antenna gain (30' parabolic dish with 55% aper. eff.)	44 dB
Data rate	10^6 bits/sec
Maximum bit error probability	10^{-5}
Modulation	Biphase modulation 70°

During this six-month period, an economic analysis was developed for the array of dipoles. A computer program was written that calculates the required system cost as a function component characteristics cost using the component cost subarray size parameters. Several choices and values for each component can be analyzed simultaneously; the program determines how to construct the array with the minimum total cost and also tabulates the cost and size of the remaining possible system configurations. Of course, the results are highly dependent upon component characteristics and costs which require frequent review and update. However, the technique for this economic analysis can be easily applied at any time to new date points since the computer program is listed in its entirety in Appendix A-II.

2) Theoretical SNR Considerations

a) Received Signal Power - The total signal power received at the output of an antenna system is given by the one-way transmission equation:

$$S_R = \frac{G_T P_T}{L} \left(\frac{\lambda}{4\pi R}\right)^2 G_R$$

where

S_R = signal power received G_T = transmitter antenna gain

G_R = receiver antenna gain P_T = transmitter power

λ = signal wavelength R = transmission pathlength

L = transmission losses (greater than unity)

The factor $\left(\frac{\lambda}{4\pi R}\right)^2$ is commonly called the free space loss and has a value of -264 dB at 2.3 GHz for 1 Au. The signal losses, L, included in the transmission equation comprise small losses due to inefficiencies of transmitting and receiving antennas, feeds, etc., and transmission losses due to the fundamental propagation characteristics of the earth's atmosphere. The signal losses due to atmospheric attenuation, as well as those due to plasma effects during atmospheric entry and exit by high velocity vehicle are discussed elsewhere. The effective gains, G_T and G_R, of transmitter and receiver antennas, respectively, may be limited by atmospheric propagation effects as well as by practical limitations on achievable fabrication tolerances. Wavefront distortions due to atmospheric inhomogeneities across the aperture will have an effect similar to that caused by deviations in the antenna surface. The problem of illumination errors across large apertures is discussed by Bailin and Hamren. (C-1)

The division of power between the carrier and the spectrum which carries useful information depends on the particular type of modulation used. For example, the biphase modulation scheme considered here yields about 10% residual carrier when the modulation swing is $\pm 70^{\circ}$; this represents a loss in useful signal power of only 0.5 dB. The residual carrier is used by the phase lock system to coherently combine the subarrays to produce a single array output. There are techniques available in which no carrier is required, for example the squaring loop; (C-2) but since an improvement in SNR would be 0.5 db maximum, it was felt that the more commonly used technique of locking to a carrier could be used without significantly effecting the result.

b) Received Noise Power - The signal power required at the receiver, however, is determined by the required data accuracy and by the total noise

present, due both to external sources and to the receiver itself. Almost all of the noise power is contributed by three general sources; antenna noise, noise produced by lossy components, and excess noise generated in the receiver mostly by the first amplifier. Thus noise presents a fundamental limitation on system performance and can be accounted for in terms of the ideal noise limit (C-3)

$$N_R = hf\left[1 + \left(e^{hf/kt} - 1\right)^{-1}\right] B$$

where

h = Planck's constant
f = c/λ = signal frequency
k = Boltzmann's constant
T = effective absolute temperature of the receiver
B = receiver bandwidth.

In the microwave region where $kT >> hf$, this expression converges to the familiar quantity kTB. For non-ideal systems detection efficiency and the additional noise contribution due both to external and internal noise sources can be included by taking T as the equivalent system noise input temperature of the receiver. This temperature is the sum of various contributions as discussed below.

b1) Antenna Temperature - The antenna noise temperature in the direction Θ_o is given by (C-4)

$$T_{ant}(\Theta_o) = \frac{\sum_{i=1}^{2} \int_o^{2\pi} \int_o^{\pi} T_i(\Theta') f_i(\Theta', \phi') \sin\Theta' d\Theta' d\phi'}{\sum_{i=1}^{2} \int_o^{2\pi} \int_o^{\pi} f_i(\Theta', \phi') \sin\Theta' d\Theta' d\phi'}$$

where $f_1(\Theta', \phi')$ is the normalized antenna power pattern measured with the design polarization and $T_1(\Theta)$ is the temperature of radiation impinging on the antenna with that polarization; $f_2(\Theta', \phi')$ is the antenna pattern

for polarization orthogonal to the design polarization and $T_2(\theta)$ is the incident radiation of the corresponding polarization. For a well designed antenna the cross polarized component contributes only a degree or two. This equation assumes that the pattern does not change significantly over the frequency band of interest; if this assumption is not valid the integration must be carried out over the frequency domain as well as the spatial domain. For an array of elements the above expression is still valid and the appropriate power pattern to be integrated is the product of the element pattern and the subarray factor.

It is interesting to note that the effective array temperature is quite insensitive to array size when the array is looking in the zenith direction with no interference from the sun. This is due to the slowly varying form of the radiometric sky absorption temperature distribution. An expression for this distribution which has been shown to agree quite well with measurements is given by (C-5)

$$T_{sky}(\theta) = (1 - t_o^{\sec\theta})\, T_m$$

where

t_o is the fractional transmission of atmosphere at zenith ($\theta = 0$)

T_m is the mean absorption temperature

At S-band the normal zenith temperature is about 3^oK; at 60^o from zenith it has increased to only 6^oK. Thus, the component of antenna temperature due to this type of noise for a large array is not much different than from a single dipole element. This excludes the contribution from other sources such as the sun.

b2) Noise Produced by Lossy Components - The total output noise contribution from any matched network of reciprocal lossy elements is given by (C-6)

$$T_{eff} = \sum_{i=1}^{N} T_i P_i$$

where

N = number of elements in the network

T_i = temperature in the i-th element

P_i = fraction of power received by the i-th element when unit power is sent back in the system from the output terminals

$$\left(\sum_{i=1}^{N} P_i = 1 \right)$$

Thus the effective output temperature is the sum of the contributions from each of the elements weighted by the amount of power absorbed when unit power is delivered to the network. For a single lossy element this reduces to the well known expression

$$T_{out} = \alpha T_{in} + (1 - \alpha) T_o$$

where $(1 - \alpha)$ is the fraction of power absorbed by the element at T_o and T_{in} is the effective input temperature to the element. The loss factors for several types of transmission lines and their effects on performance are discussed in the subsection on distribution networks.

b3) Excess Noise Produced by Amplifiers - The excess noise produced by several commonly used amplifiers is shown in Table C-1 (see Reference C-7).

TABLE C-1

Ampl. type	Physical temp. T_c	Noise temp. T_e
TWT	290°K	400°K
TDA	290°	380°
Transistor	290°	625°
Paramp	290°	80°
Paramp	20°	20°
Maser	5°	10-15°

The amplifier's noise figure F is related to its excess noise temperature T_e by

$$T_e = (F - 1)\, T_o \qquad \text{where} \qquad T_o = 290^{\circ}K$$

c) Relationship Between SNR and Bit Error Probability - One of the most important considerations for evaluating a communication link is the bit error probability. For a given modulation and detection scheme this parameter can be related to the SNR, which is a more convenient parameter to work with. Figure C-1 shows this relationship for several coherent and non-coherent binary systems. (C-8). It can be seen that for large SNR bit error the probability decreases quite rapidly. For a system utilizing binary phase shift keying (PSK), a SNR of 10 dB is adequate to assure an error probability of approximately 10^{-5}. This SNR is sufficient for both coherent and differentially coherent PSK, but not for either of the frequency shift keying (PSK) systems. Therefore, a nominal value of SNR = 10 dB was chosen for the analysis and comparison of the systems examined below.

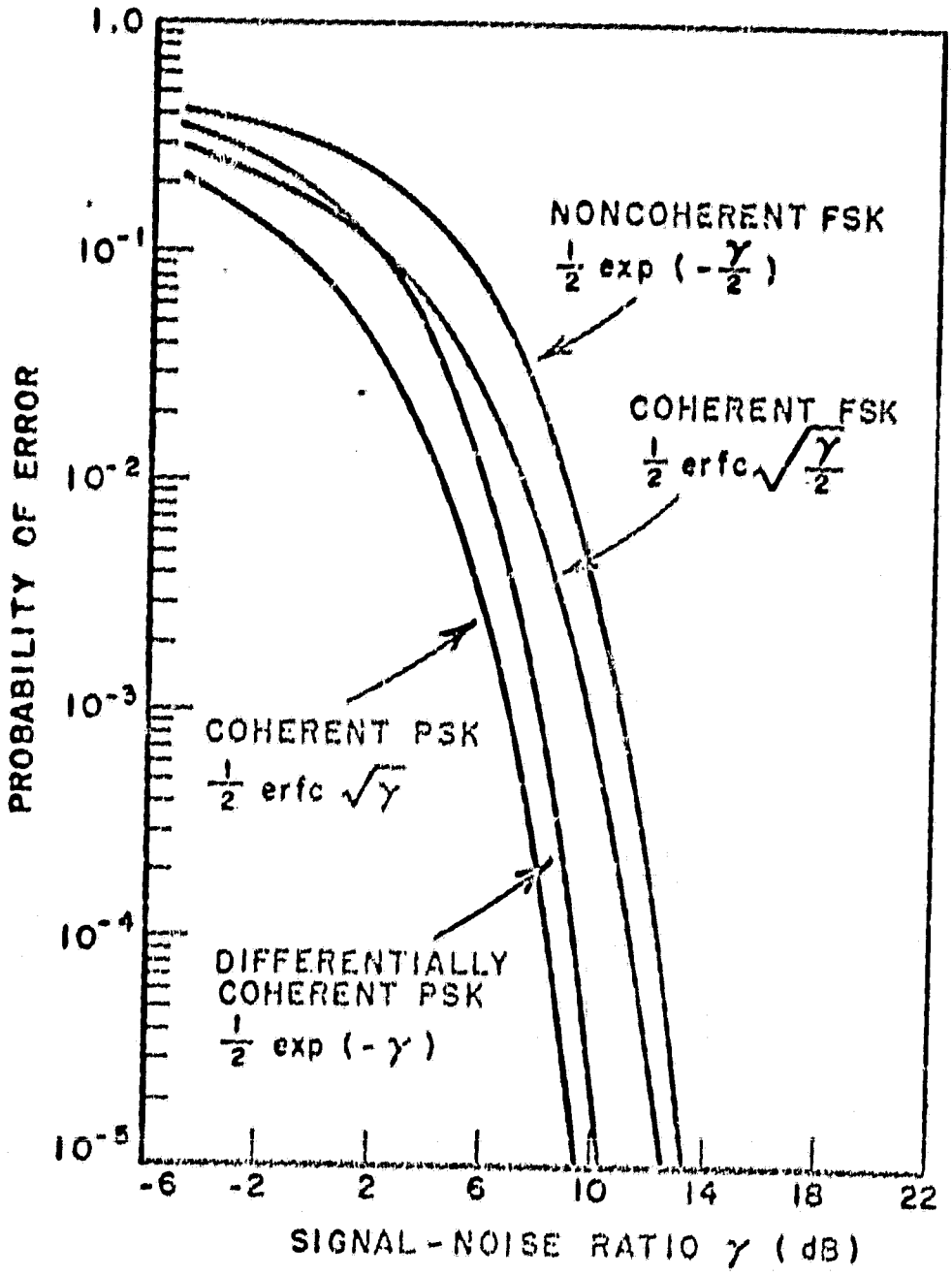

Fig. C-1 Error rates for several binary systems.
(Reference C-8)

3) Predection vs. Postdetection Combining

There are two basic ways in which the detection process can be performed. The first, as shown in Fig. C-2, consists of summing the properly adjusted IF ouputs from each subarray and then detecting the resultant to obtain a series of ones and zeros at the modulation rate. The second scheme, as shown in Fig. C-3, consists of detecting the output of each subarray at the IF level and then using a majority count to make the final decision as to whether a one or a zero occurred. The first, the coherent addition scheme, will obviously be more efficient than the second, but the latter system has several advantages which merit closer consideration; for example, the time delay can be a digital device such as a shift register. The summation is also done digitally at the base band frequency rate, rather than at IF.

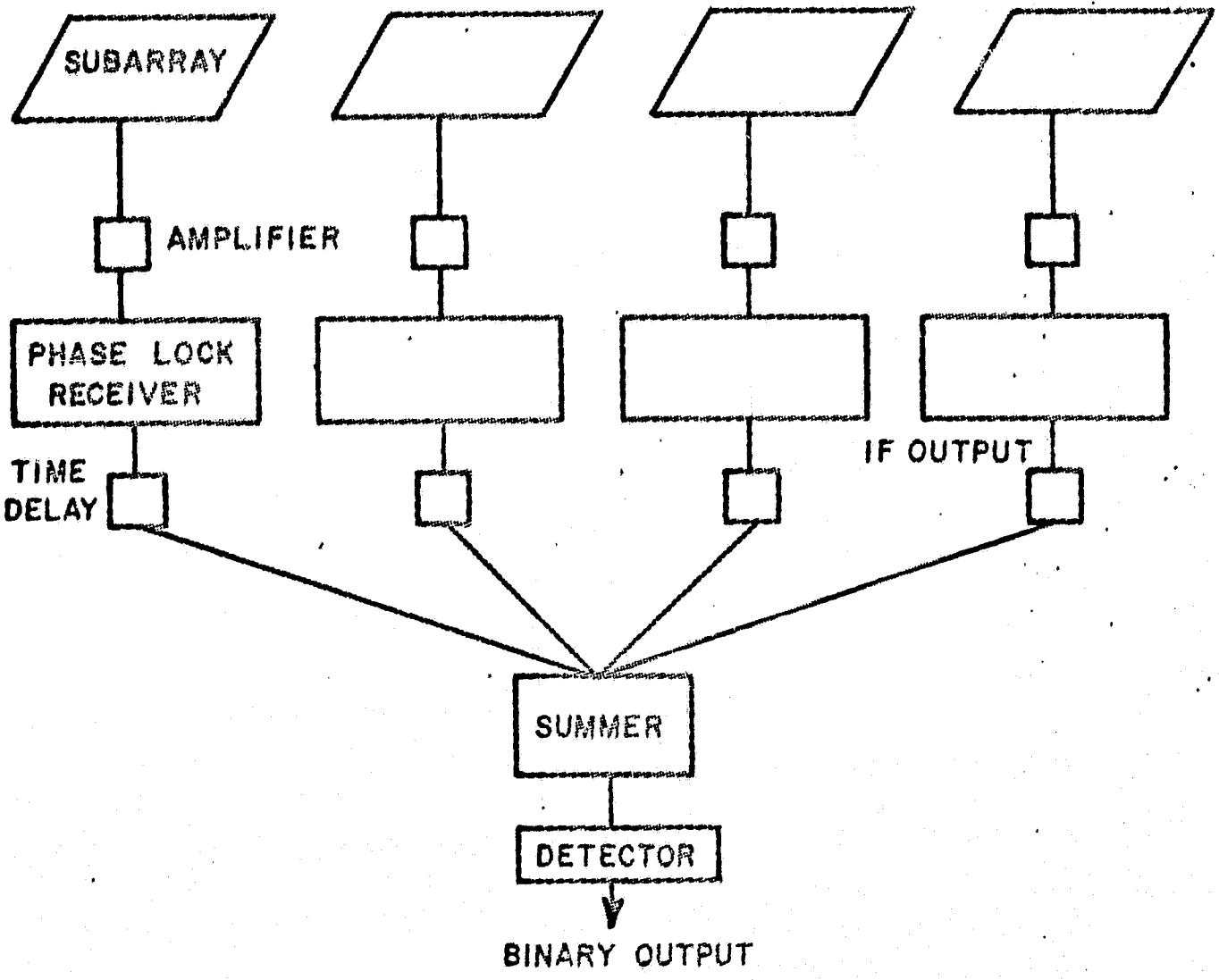

Fig. C-2 Predetection combining program

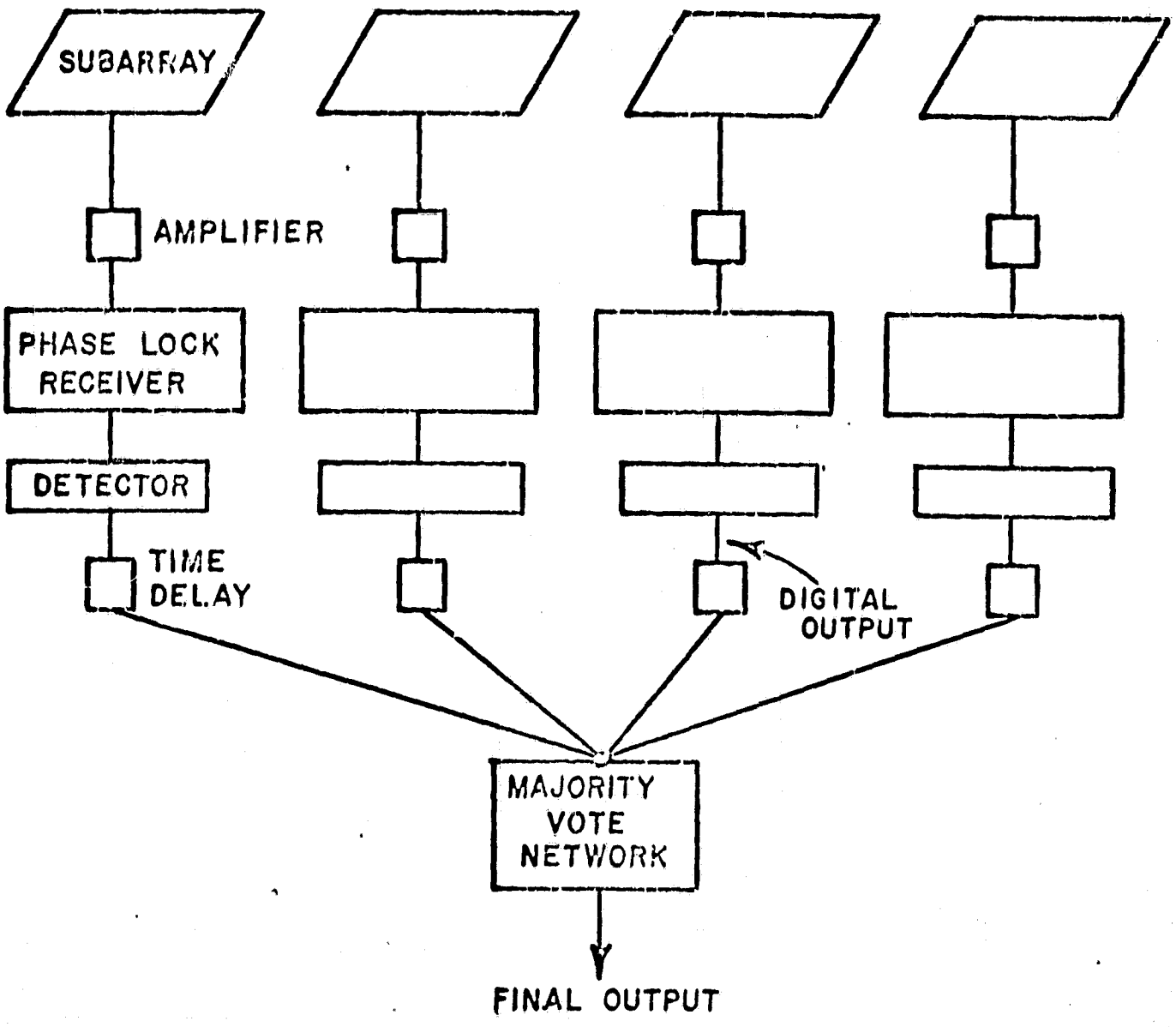

Fig. C-3 Postdetection combining diagram.

An analysis has been done on these two schemes (C-5) which showed that for the limiting case where the SNR of each subarray is very small, but the SNR of the combined subarrays is large, the postdetection summing requires a total SNR $\pi/2$ (2dB) greater than the predetection combining in order to produce the same bit error probability. Since this establishes the relationship between the two processes the remainder of this report will be concerned with coherent predetection combining system.

4) Array-Subarray Organization

The subarray model consists of dipole elements which are phase shifted and combined to form a single output at the RF frequency. Due to the relatively large beamwidth of a single subarray, it is expected that the proper phase adjustment can be performed with a special purpose computer using a priori knowledge of the source location.

The number of elements required to achieve the specified 10 dB SNR will, in general, be a function of the phase shifter loss and temperature, feed line losses, amplifier noise temperature, and subarray size.

a) Maximum Subarray Size If phase control is used for combining, rather than time delay compensation, the total time delay across the subarray must be less than the modulation period in order that each element simultaneously receives the same information bit. For an information rate of 10^6 bits per second this time delay must be much less than 1μ sec, which limits the maximum subarray size to about 30 meters (1μ sec has spatial length of 300 meters) if the system is required to operate at low elevation angles. This does not represent a stringent limitation; for the antenna model considered here a subarray of this size would contain about 200,000 elements.

b) Minimum Subarray Size For any adaptive scheme each subarray must produce a SNR which is sufficient to lock on the signal during the acquisition mode and maintain lock during the information transfer mode. For a typical phase lock system using coherent addition the following equations can be used to obtain a comparison between different organizational parameters:

$$SNR_{TOT} = N \quad SNR_{SA} = 10$$

$$CNR_{PLL} = K \quad SNR_{SA} \quad \frac{B_{IF}}{B_{PLL}}$$

where

SNR_{TOT} = total numeric signal-to-noise power ratio taken to be 10 in order to produce a bit error probability of 10^{-5} .

N = number of subarrays

CNR_{PLL} = carrier to noise ratio in the phase lock loop of each subarray receiver

K = fraction of power transmitted at the carrier frequency

B_{IF} = bandwidth of the IF, taken to be 0.5×10^6 Hz to receive 10^6 bits/sec using matched integrate and dump detection

B_{PLL} = bandwidth of phase lock loop, taken to be 10 Hz.

During the acquisition time all the power can be transmitted at the carrier frequency (K = 1) so that

$$CNR_{PLL} = SNR_{SA} \quad \frac{B_{IF}}{B_{PLL}} = \frac{10^6}{2N}$$

From experience (9),(10) it has been shown that about 6-7 dB CNR_{PLL} is required for acquisition; using this criteria and the above constants yields the minimum SNR_{SA} = -40 dB to obtain lock. However, during normal operation of this subarray, when most of the power is contained in the modulation components, the CNR_{PLL} would drop to -3 dB which is not sufficient to maintain phase lock. Hence the actual minimum SNR_{SA} is not set by the acquisition requirement but rather by having to maintain lock during the signaling. Requiring a 3 dB SNR_{SA} during normal operation constrains the minimum SNR_{SA} to be -34 dB .

c) Feeding Techniques Two types of feed systems were considered; the commonly used modified series-series shown in Fig. C-4 and the equal length corporate feed shown in Fig. C-5. The effective noise temperature and SNR at the subarray output are now calculated for both feeding systems.

Series-series model - Consider an arbitrary unit of power delivered to this subarray (Fig.C-4). The fraction of power delivered to the phase shifters is

$$\Gamma = \frac{\alpha}{N^2} \left(\sum_{n=1}^{N} \alpha^{n-1} \right)^2$$

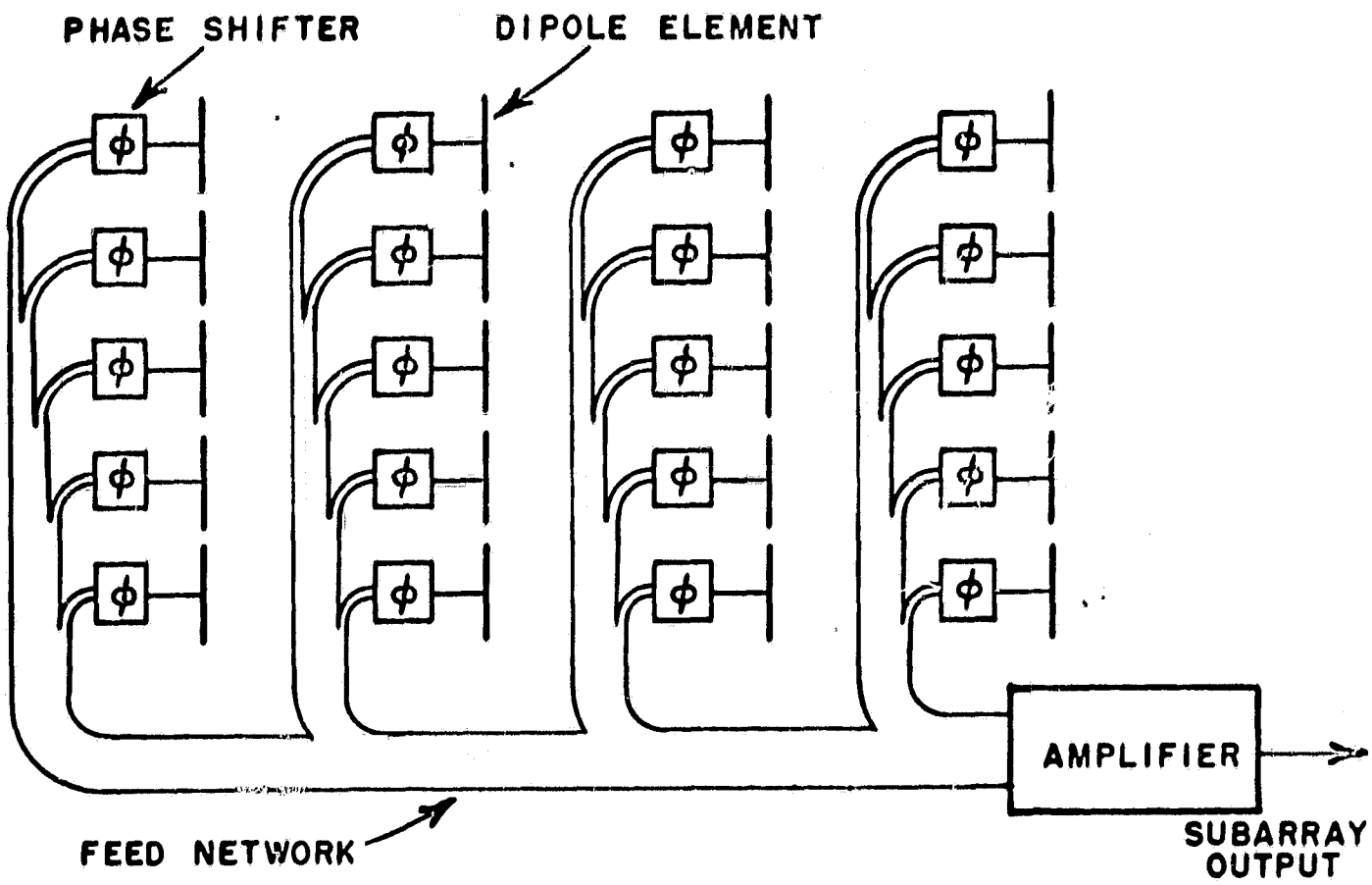

Fig. C-4 Series-series feed system.

where

N^2 = number of elements in the subarray
α = transmission coefficient for a $\lambda/2$ section of the feed line.

Hence the fraction of power absorbed by the feed system is $1 - \Gamma$. The fraction absorbed by the phase shifters is $(1 - \alpha_\phi) \Gamma$, where α_ϕ is the transmission coefficient of the phase shifters, and the fraction of power is delivered to the dipole antennas is $\alpha_\phi \Gamma$.

Finally, the expression for the total effective noise temperature of the subarray is

$$T_{eff} = \left[1 - \Gamma\right] T_o + T_\phi \left[1-\alpha_\phi\right] \Gamma + T_a \alpha_\phi \Gamma + T_{amp}$$

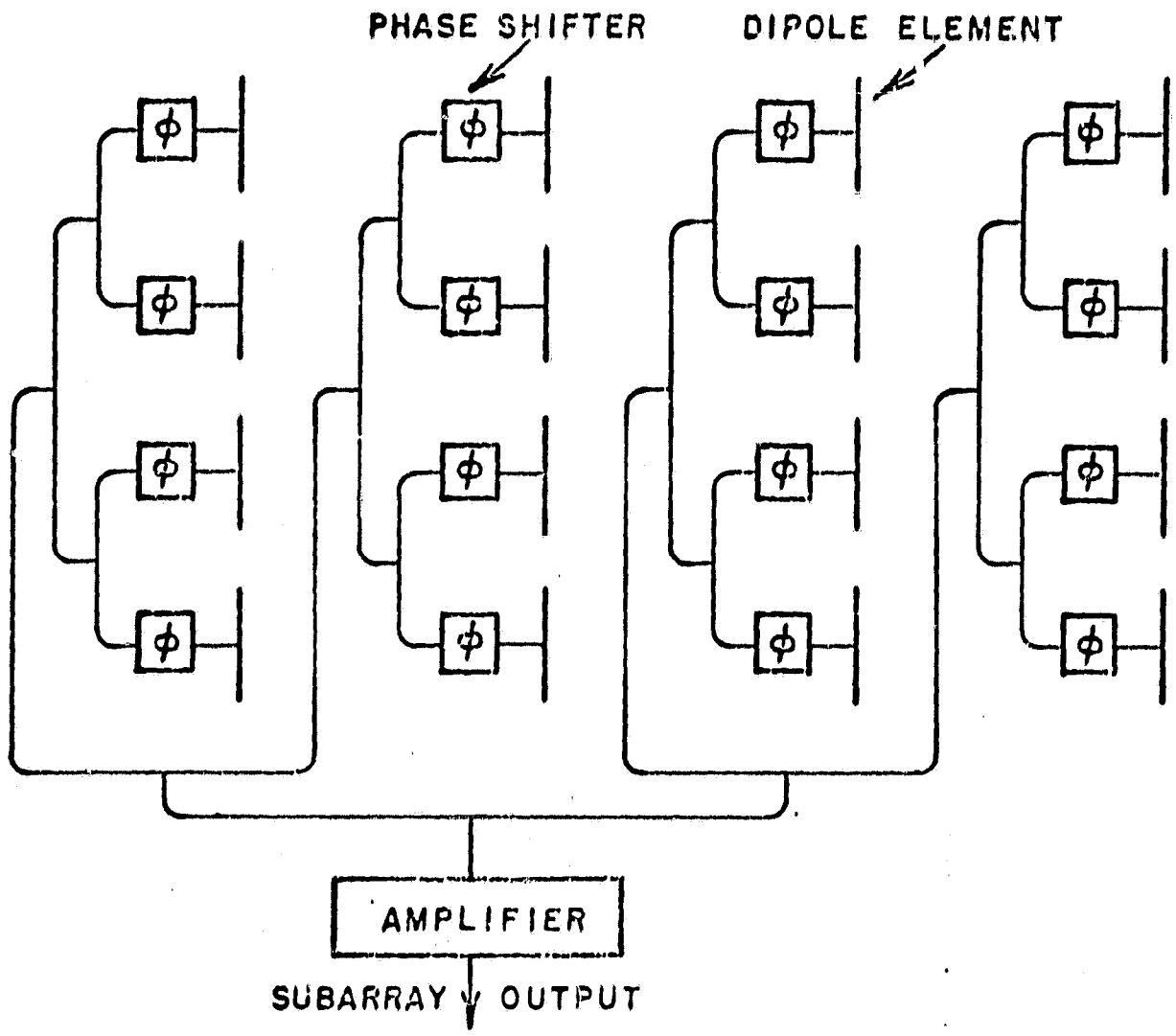

Figure c-5 Equal length corporate feed system

where

T_o = physical temperature of the feed structure assumed constant at 290°K

T_ϕ = physical temperature of the phase shifters

T_a = antenna temperature = 9°K for the dipole model

T_{amp} = effective amplifier noise temperature.

For a transmitted power of 50 watts and a thirty-foot transmit antenna two Au from the array the resulting expression for the subarray SNR in dB is

$$SNR_{SA} = -144 - PSLDB + 10 \log_{10} N^2 - 10 \log_{10}\left(\frac{1}{\Gamma}\right) - 10 \log_{10}(k\ T_{eff}\ B)$$

where

PSLDB = phase shifter loss in db

k = Boltzmann constant

B = bandwidth = 0.5×10^6 Hz

Equal length corporate model A similar analysis yields the effective temperature for this subarray model :

$$T_{eff} = LT_{\phi} + L_{\phi}\left[T_a - T_{\phi}\right] + \left[1-L\right] T_o + T_{amp}$$

where

$$L = \exp\left[-2.3LDB/10\right]$$

$$LDB = LPF\,(\lambda/2)\left[2\log_2 N + \sum_{i=0}^{\log_2(N-1)} 2^i\right]$$

LPF = Attenuation of the feed in db per foot

The resulting SNR in db at the subarray is:

$$SNR = -144 - LDB - PSLDB + 10\log_{10}N^2 - 10\log_{10}\left[k\,T_{eff}B\right].$$

As shown in the numerical results the equal length system is slightly less efficient than the series-series system; it has the advantage of not requiring any phase shifting devices if the subarray panels are to be mechanically pointed.

5) Circuit Components

The optimum antenna system for the ground terminal is one that maximizes the signal-to-noise ratio under the practical constraints imposed by tolerance, reliability, noise environment, and cost. The antenna must have a low equivalent noise temperature and must provide a high-gain pattern which is steerable through a wide angle ($\pm$ 60°). It will be the purpose of this section to consider the circuit components and techniques appropriate to the design of a large phased array and to delineate their characteristics as parameters in determining sub-aperture size and performance characteristics. A phased array consists of radiating elements, a power distribution or collection network, a beam-steering or phasing system, and an optimal number of low noise preamplifiers. Each of these antenna components plays an important and interdependent role in the determination of the overall antenna performance. There exist a variety of beamsteering techniques applicable to a phased-array; these

include the use of a phase shifter at each element, and the use of a mixing scheme that translates a phase shift from the operating frequency to a convenient frequency band. Those areas in phased-array distribution and component technology that must be advanced to make the large arrays practical are to be discussed and delineated in this section.

a) Distribution Networks The distribution network collects the signal from each of the radiating elements and phase shifters of the array and brings them to a common receiving port so that they combine in phase with a minimum of loss. The distribution network largely and sometimes wholly determines the antenna aperture distribution; hence, it determines the antenna pattern, side-lobe level, and directivity. In the present study where the applicability of any particular overall system technique is determined by the various loss factors discussed above, the nature of the distribution network is most critical since it can shift the balance of effectiveness from one type of ground based system to another; a few tenths of db/100' of loss in a transmission line can change the desirability of a particular technique since there are many hundreds of feet involved in the overall signal distribution. Distribution systems to be considered herein will include those which are essentially optical and the several types of transmission lines as shown in Table C-II (See Ref C-11). The various types of distribution networks to be evaluated in this phase scanned system can also apply to multiple-beam system where low-noise is an essential feature. At this stage in this study, it is already obvious that performance figure of merit of a large phased array will be largely determined by the characteristics of the distribution network and that further study and development beyond the present state-of the-art in low loss transmission lines will be needed to satisfy the requirements of this program.

In this section of the report, only transmission line feeding systems have been considered which to date are deemed appropriate for large phased arrays. From a manufacturing viewpoint stripline is by far the most desirable type of transmission line because it is readily adaptable to mass producing techniques. However, its extremely high loss relative to coax and waveguide is due to dielectric losses rather than ohmic conductor loss. One of the most useful low loss high frequency dielectrics is Teflon (polytetrafluoroethylene). Because pure Teflon has such a poor coefficient of thermal expansion it is usually mixed with glass or quartz; it is this additive which seriously degrades its attenuation

properties. It is expected that considerable improvements will be made in dielectric materials and will make stripline devices more desirable.

TABLE C-II

	Attenuation in db/100' at 2 Gc
Brass Waveguide	0.6
Rigid and Semi-rigid coax	1 -2.5
Flexible coax - RG 20	6
Flexible coax - RG 9	12
Flexible coax - RG 58	35
Microstrip	19
Stripline (Triplate)	18

All subsequent calculations will be made using nominal values of feed line loss ranging from a lossless line to that of coax.

b) R-F Phase Shifters Beam steering for a phased array of the conventional type requires some type of phase shifting device at each element. The primary requirements for such a device are that it be capable of 360 degrees of phase shift and that it have an extremely low insertion loss, preferably less than 0.1 db. In addition these devices must be relatively inexpensive since their requisite number is proportional to the total aperture size, be capable of being packaged to fit within the array element spacing, and be temperature insensitive to ambient environments. At present, there is no phase shifting device that will meet all of these requirements. However, as a basis for evaluating the objectives of the present programs, consideration will be given to the performance parameters of the present state-of-the art devices employed at X-band frequencies since these are readily available and similar devices can be obtained to operate at S-band frequencies. The results for X-band phase shifters are given in Table C-III only as a temporary expedient until precise descriptions of the corresponding S-band values can be obtained. As may be seen from the table, many of the devices have relatively high insertion losses for the present communication application. These large loss values are due partly to the universal requirements of fast switching speed and high power handling capacity

Microwave Phase Shifters (May 1968)

Characteristic	Ferrite Longitudinal Field, Digital, Reciprocal	Ferrite Transverse Field, Digital, Nonreciprocal	Ferrite Longitudinal Field, Digital, Reciprocal	P-I-N Diode Transmission Digital (Stripline)	P-I-N Diode Reflection Digital - One Port Device	P-I-N Diode Reflection Digital - with 3-db Coupler
Frequency	X-band	X-band	X-band	X-band	X-band	X-band
Phase Shift (Maximum)	360° continuous	360° 22.5° steps (4-bit)	360° 22.5° steps (4-bit)	360° 22.5° steps (4-bit)	360° 90° steps (2-bit)	360° 90° steps (2-bit)
Figure of Merit	600°/db	500°/db	350°/db	100°/db	100°/db	200°/db
Temperature Sensitivity	5°/°C	1°-3°/°C	5°/°C	Negligible	Negligible	Negligible
Excess Noise Temperature	0° K	0° K	0° K	Negligible	Negligible	Negligible
Control Power	0.1 watt	3 by 10^{-4} watt-sec.	10^{-3} watt-sec	0.1 watt	0.05 watt	0.1 watt
Time Constant	100 μsec.	2-10 μsec.	2-10 μsec.	0.2-10 μsec.	0.2-10 μsec.	0.2-10 μsec.
Size (inches)*	6 by 1 by 1/2	5 by 1 by 1/2	7 by 1 by 1/2	10 by 1 by 1/2	1 by 1 by 0.025	2 by 1 by 0.025
Weight	2-1/2 oz. + waveguide	2-1/2 oz. + waveguide	5 oz. + waveguide	1-1/2 oz.	1/2 oz.	1 oz.
Disadvantages	1. Requires magnetic shielding 2. Requires temperature stabilization 3. Requires continuous holding power	1. Nonreciprocal 2. High current driver	1. High current driver 2. Requires temperature stabilization	1. Requires large numbers of diodes 2. Difficult to package 3. Susceptible to burnout	1. Susceptible to burnout 2. High loss for large number of phase bits	1. Susceptible to burnout 2. High loss for large number of phase bits
Range of frequencies at which practical devices can be built	2 to 50 GHz	2 to 40 GHz	2 to 20 GHz	0.1 to 10 GHz	2 to 18 GHz	2 to 18 GHz

* Assumes device slips into solid-state array.

Table C-III

as dictated by a radar application. Neither high-speed nor high-power capability are necessary for a ground based communication system, and consequently it can be expected that special designs of the above devices may be available with a substantially lower loss than the values of .6 to 3.0 db for 360° of phase shift as shown in Table C-III. However, for the present studies a nominal insertion loss value of .5 db shall be used until anlaysis and the appropriate experimental hardware are available to reduce the insertion loss to the desired value. The devices that are presently available for phased arrays fall into three general groups which require consideration and some critical observation. A preliminary discussion of these groups, their advantages and disadvantages is given below and will be updated as new pertinent information becomes available:

Diode Phase Shifters. Digital diode phase shifters are small, light-weight devices that are insensitive to temperature and can be switched from one phase setting to another in a few nanoseconds. Two types of digital phase shifters are in current use. One uses a transmission line structure in which different susceptances are switched across the line to produce incremental phase shift. The other design configuration is a reflection structure that may be converted to a transmission component by the employment of a 3-db coupler or a circulator. Diode phase shifters, are at present, somewhat costly because of the cost of the diodes and their mounting structure. P-i-n diodes are typically used as the control elements because of their high power handling capability. Since highpower is not of prime concern in a receiving system, other arrangements of solid state materials may be more desirable although to date there has been no stimulus for such analysis and design. The engineers of the Texas Instrumental Corporation who are involved in the MERA module and system design report that they have been able to produce IC phase shifters with 1.2 db insertion loss as the average value of a large group with 1.5 db as a maximum value.

Ferrite Phase Shifters. Ferrite phase shifters (C-12) are typically waveguide size, moderate in weight, somewhat temperature sensitive, can be switched from one phase setting to another in a few microseconds, and require significant drive energy. They are somewhat costly because of the cost of the ferrite material. Two general configurations are available. One uses a transverse magnetizing field; the second uses a longitudinal magnetizing field. The former is reciprocal only for certain configurations while the latter is intrinsically reciprocal, a property desirable in arrays to be used for both transmission and

reception. Phase shifters that use longitudinal magnetization also produce greater phase shifts at lower levels of applied magnetic field than do those that use transverse magnetization. General characteristics of ferrite phase shifters that affect spacecraft scanning applications are reciprocity impedance matching, frequency dependence of phase shifts, temperature sensitivity, and hysteresis effects. Weight can also be a great problem with ferrite phase shifters for a spaceborne array with large numbers of elements. However, weight is only a secondary problem in a ground array compared to the temperature effects.

Novel Devices. There are several new devices which are now being developed whose progress bears some observation. Ferroelectric phase shifters are quite small and lightweight. They are, at present, extremely temperature sensitive, due to the sensitivity of the ferroelectric crystal, and they have very high insertion loss characteristics. Since they are still in the experimental stages, production costs are unknown. At present, it appears that a major improvement will be required in the basic crystal before these devices can be considered for use in an array. As in the case of the ferroelectric phase shifter, the plasma phase shifter is still in the experimental state. It is moderate in size and weight with a negligible temperature sensitivity. The insertion loss is comparable to that of the ferrite and diode phase shifters, but a significant reduction may be possible. At the present time, it is not a low cost device and requires significant drive energy; both factors are due to the need for the generating and sustaining of a plasma.

The high loss associated with the electronic phase shifting device can be eliminated or reduced by either mechanically scanning the subarrays, by using mechanical phase shifting devices such as a line stretcher, or by some form of simple air filled guide which may employ a multi-moding technique to properly gather the signals from numerous input ports. Each of these schemes needs further study and experimentation to develop the low loss feed system required by a high data rate communication link.

From the preceding equations it can be shown that one of the most important components which influence the required aperture size is the phase shifters. Electronic phase shifters such as ferrite and diode devices typically have insertion losses in the order of 0.5 db instead of the more desirable 0.1db. While this loss does not greatly reduce the incoming signal it does

contribute considerable noise and consequently seriously degrades the SNR. As shown in Fig. C-6 for a typical set of parameters, considerable movement in SNR is possible by cooling; this seems particularly feasible for the diode type phase shifters where a Peltier cooling device could be an integral part of the semiconductor chip. The Peltier cooling effect is a thermo-electric phenomenon in which heat is absorbed or generated by current passing through a semiconductor junction. Several companies (C-12) are presently developing and manufacturing Peltier cooling devices for inclusion in the diode case and for direct attachment to the semiconductor chip. These problems will require further study and work is now in progress to examine the results using parameters that are more closely related to values which are possibilities for the future.

c) I-F Phase Shifting Techniques. Because of the modular nature of the electronically steered systems being considered for this study, it will be possible to employ I-F phase shifting techniques. These techniques (C-1) offer several advantages as compared with R-F phase shifting techniques. First, requirements on the phase-shifting components may be relaxed as compared with requirements on corresponding R-F components. In addition, since the phase shifting for reception is performed after frequency translation and I-F amplification, losses in the phase shifters do not degrade system noise figure nor do they contribute to reduced system gain as would R-F phase shifters without individual R-F preamplifiers. The phase shifting for transmission can be done at low power levels with I-F phase shifters so that the power handling capabilities and losses of the phase shifters do not present problems. Typically, each complete module includes an antenna element, an R-F diplexer, a mixer, an I-F amplifier, and a phase shifter for reception; for transmission a similar set of components is required with the addition of a high-power R-F source. A number of configurations are possible to accomplish the desired performance characteristics but each requires I-F phase shifting devices. These devices are discussed in the following paragraphs.

Delay Line Phase Shifter. The simplest type of I-F digital phase shifter is that composed of discrete sections of delay lines that can be switched in and out with electronically controlled single-pole, double-throw switches. Such a device is illustrated in Figure C-7. The various delay lines could be distributed or lumped parametric types depending on the particular frequency ranges

being used. The 180-degree phase step is obtained merely by reversing the polarity of the line connections at that point.

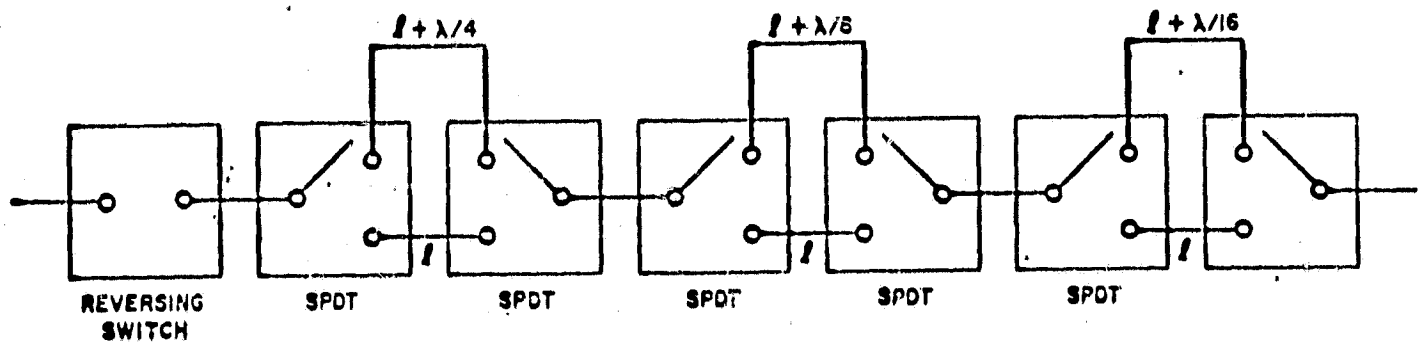

(SPDT = SINGLE-POLE, DOUBLE-THROW SWITCH)

Figure C-7 Digital i-f Phase Shifter Using Switched Delay Lines

d) Solid-State Components. During the past years, technical literature has reported significant improvement in solid-state devices and circuitry for electronically steered arrays. Typically, improvements have been effected in phase shifters, I-F amplifiers, microwave power sources, mixers, filters, and circulators.

Filters. Excellent filters are commercially available in the frequency range up through X-band and beyond. These include filters employed in communication systems; for example, bandpass (nominally flat), band rejection, diplexers, and high Q stabilizing cavities. In these higher frequency ranges the structures may be waveguide, strip transmission line, coaxial, or microstrip; but for space applications, the small, lightweight strip transmission line coaxial devices, or microstrip, are most attractive. The performance of the latter, in terms of loss, needs improvement to be competitive with waveguide filters.

Preamplifiers. There are two possibilities for the preamplifier that lend themselves to microstrip application: Tunnel diode amplifiers (TDA's) and transistor amplifiers. With the present state-of-the-art at 2 to 10 GHz and above, the TDA is slightly lower in noise figure than available transistors. Since a TDA must use a circulator, a 0.5-db insertion loss must be added to the noise figure to give a value of 4.5 db and perhaps 30 db of gain. In comparison,

present-day transistors can give a noise figure of 5.2 db and 20 db of gain.* At present, at 1 GHz, transistors have 3.5-db noise figures, but manufacturers (KMC Corporation and NEC) anticipate that devices with better noise figures will be available within a year. Such devices would give a receiver noise figure of 4.4 db at S-band. A transistor amplifier can be fabricated into a smaller package than the TDA due to the use of microcircuit lumped elements. The TDA uses at least one circulator which, with present technology, has a minimum size of about 1 inch square. Thus, on a size and weight and future performance comparison, the transistor amplifier is the preferred device.

At X-band a tunnel diode amplifier will give the best noise figure. However, because a mixer is simpler, lighter in weight, and lower in cost and has a competitive noise figure, it is anticipated that it will remain the preferred component at the higher frequencies for several years.

Mixer. The element that most determines the design of the receiver is the mixer. Present conventional balanced mixers have produced single sideband noise figures of less than 5 db. at S-band. However, this value represents carefully matched low loss conditions which may be hard to achieve in mass production in microstrip.

An alternative design for the conventional mixer with a low-noise pre-amplifier is the image enhancement mixer. Recently at MIT** an S-Band image enhancement mixer was measured with less than a 3-db single sideband noise figure and 0-dbm saturation level. The local oscillator power and complexity of this device is greater than that of the conventional mixer. A local oscillator drive of 50 mw was reported; this figure compares with 1 or 2 mw for normal operation. This type of mixer will need further development before its merits can be fully evaluated.

* Nippon Electric Co., SM153 Gallium Asenide Schottky Barrier Diode. I-F amplifier noise figure assumed to be 1.5 db.

** R. P. Rafuse and D. Steinbrecher as reported in Sprint, MIT Quarterly Progress Report and by private communication.

6) Numerical Results

This section contains some typical results obtained from a system analysis computer program.

Figures C-8 and C-9 present the subarray perforamance for the two feeding models utilizing stripline and waveguide and lossless feeds. The important range of subarray SNR loss is between -20 and -30 dB which corresponds to 10^3 and 10^4 subarrays in order to satisfy the 10 dB SNR for the communication link. It can be noted in Figure C-8 presenting the performance for 4 Au, that an increase in the number of elements will not improve SNR beyond a certain point if stripline is used. In contrast the waveguide fed subarray improved its SNR proportionally to the number of elements almost as well as a lossless feeding system.

Figures C-10 and C-11 describe the effect of phase shifter loss for various feed loss parameters. Note that the use of phase shifters incurring 0.5 dB of loss may require twice as many elements as would be needed for lossless phase shifters. For the case of stripline feeds that are quite lossy the increase in required number of elements is not as sensitive to phase shifter loss.

Figures C-12 and C-13 present the array performances as a function of amplifier temperature. Note the linear variation of SNR with the number of elements. This linearity is due to the lack of build up with increased number of elements which occurs with feed lines. For large values of amplifier temperature where its effect is dominant, as expected, the SNR declined, linearly with amplifier temperature.

Figure C-14 presents the functional relationship between the number of subarrays and subarray SNR required to satisfy a 10^{-5} bit error probability for the communication system.

Some of the graphical results in this section have been condensed in Table C-III. This shows some of the tradeoffs involved in selecting the system parameters. For example it is not possible to use a stripline feed system at 4 Au for 0.25 dB phase shifter loss using 1,000 subarrays, even with the best maser amplifiers; however this system will be possible if 10,000 subarrays are permitted, in fact the maser may be replaced by an amplifier which has 4 times more noise. Using the larger number of subarrays

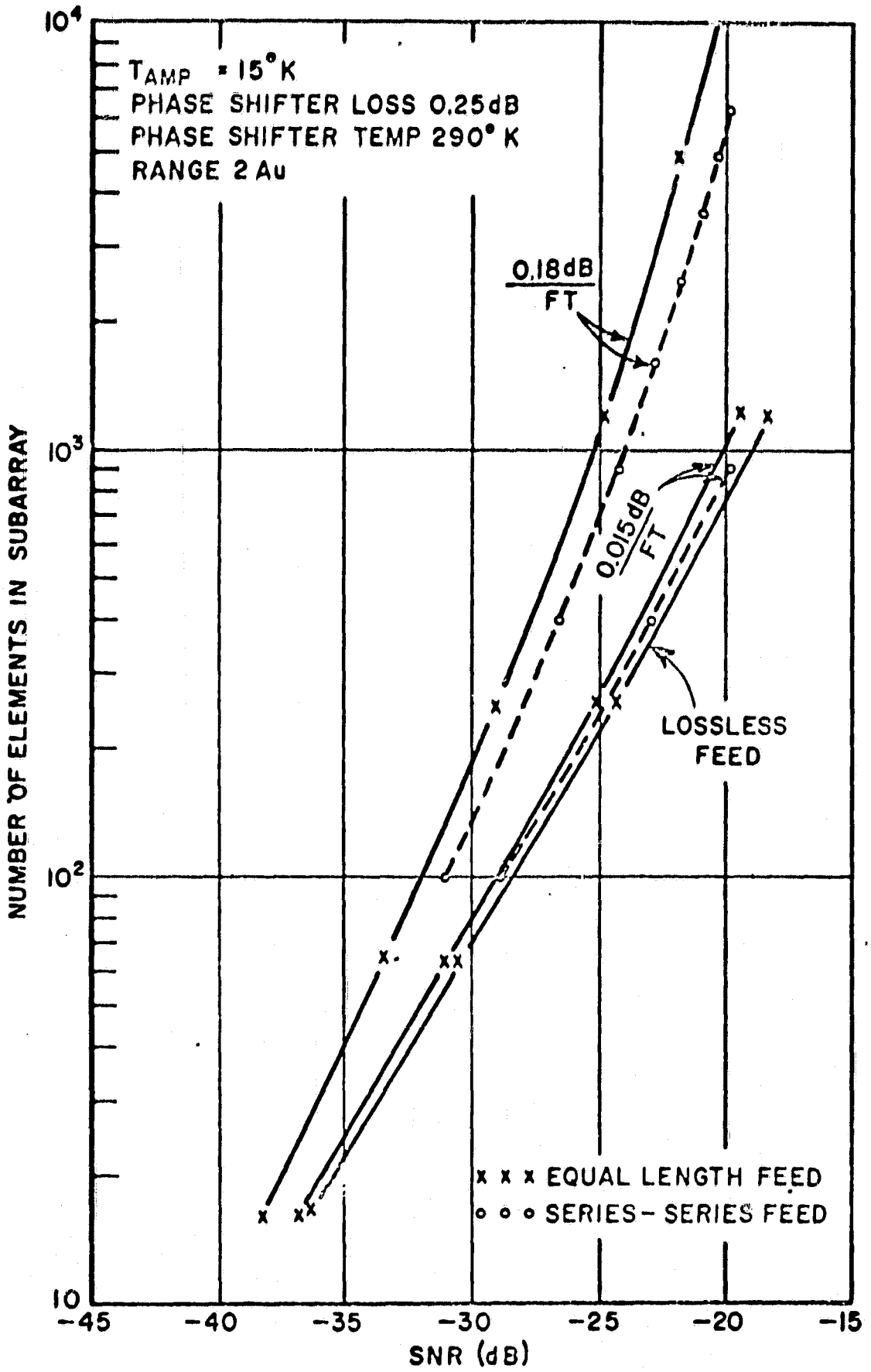

Fig. C-8 Subarray size vs. SNR as a function of feeding model and loss.

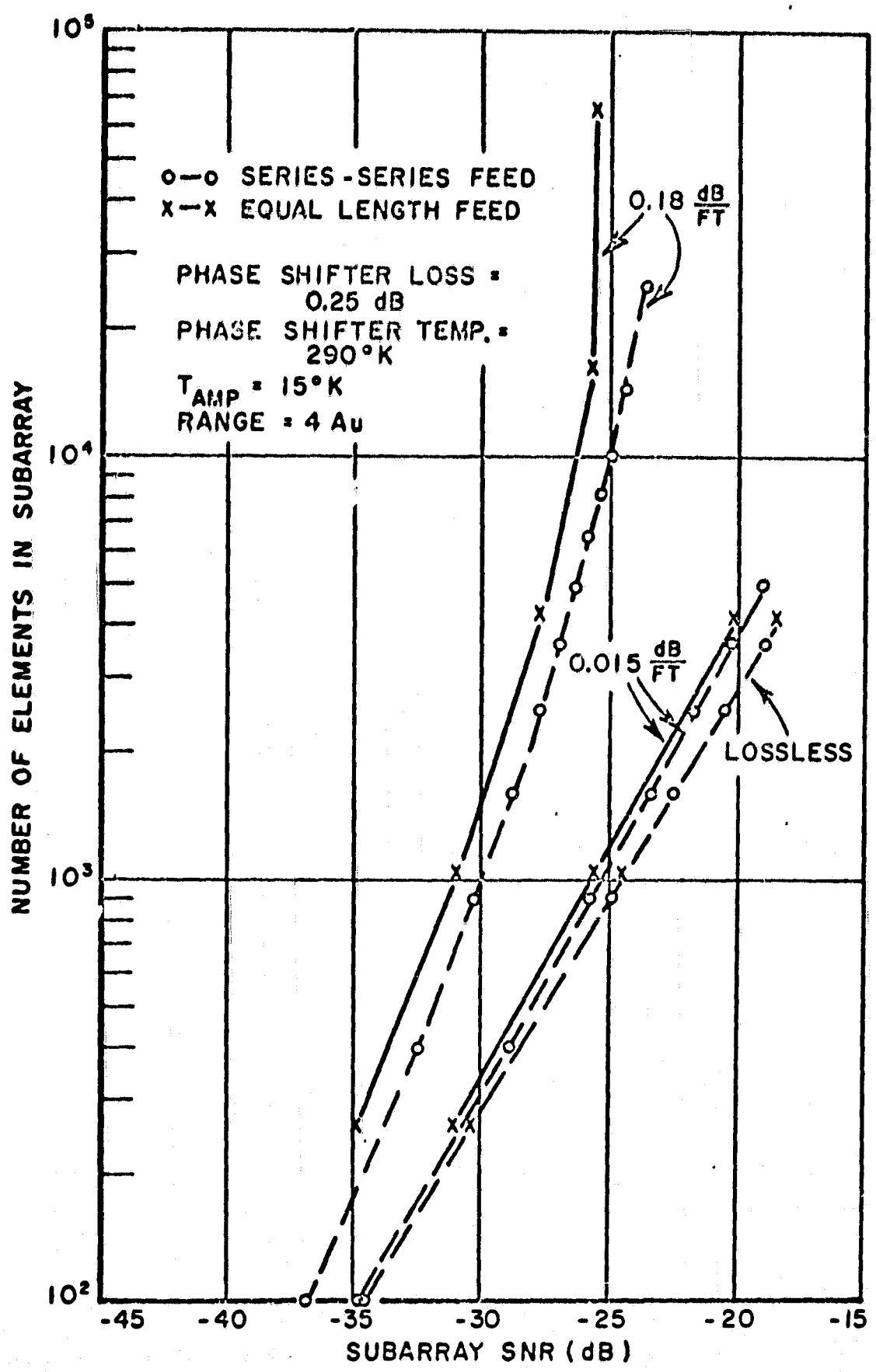

Fig.C-9 Subarray size vs. SNR as a function of feeding model and loss.

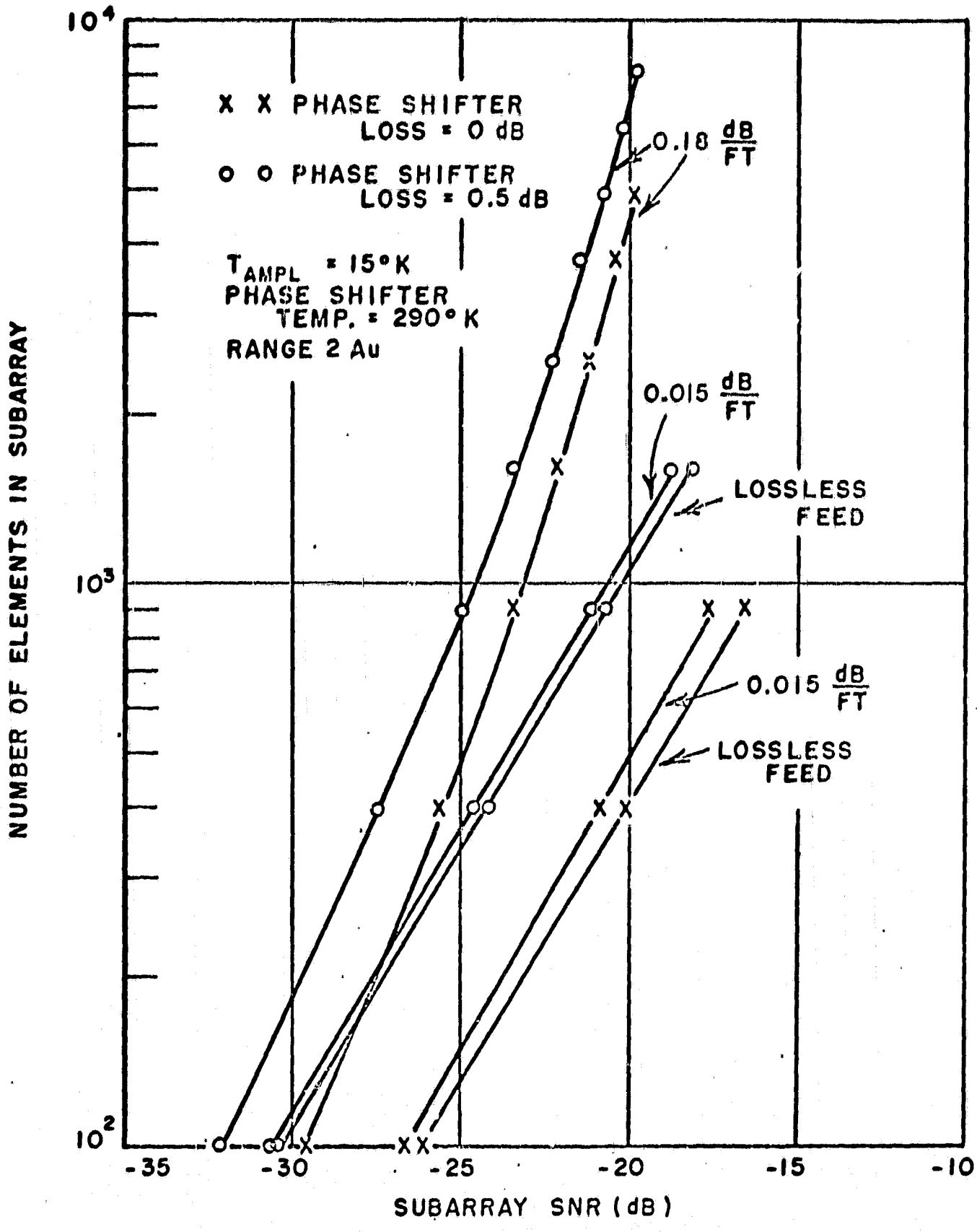

Fig.C-10 Subarray size vs. SNR as a function of phase shifter loss.

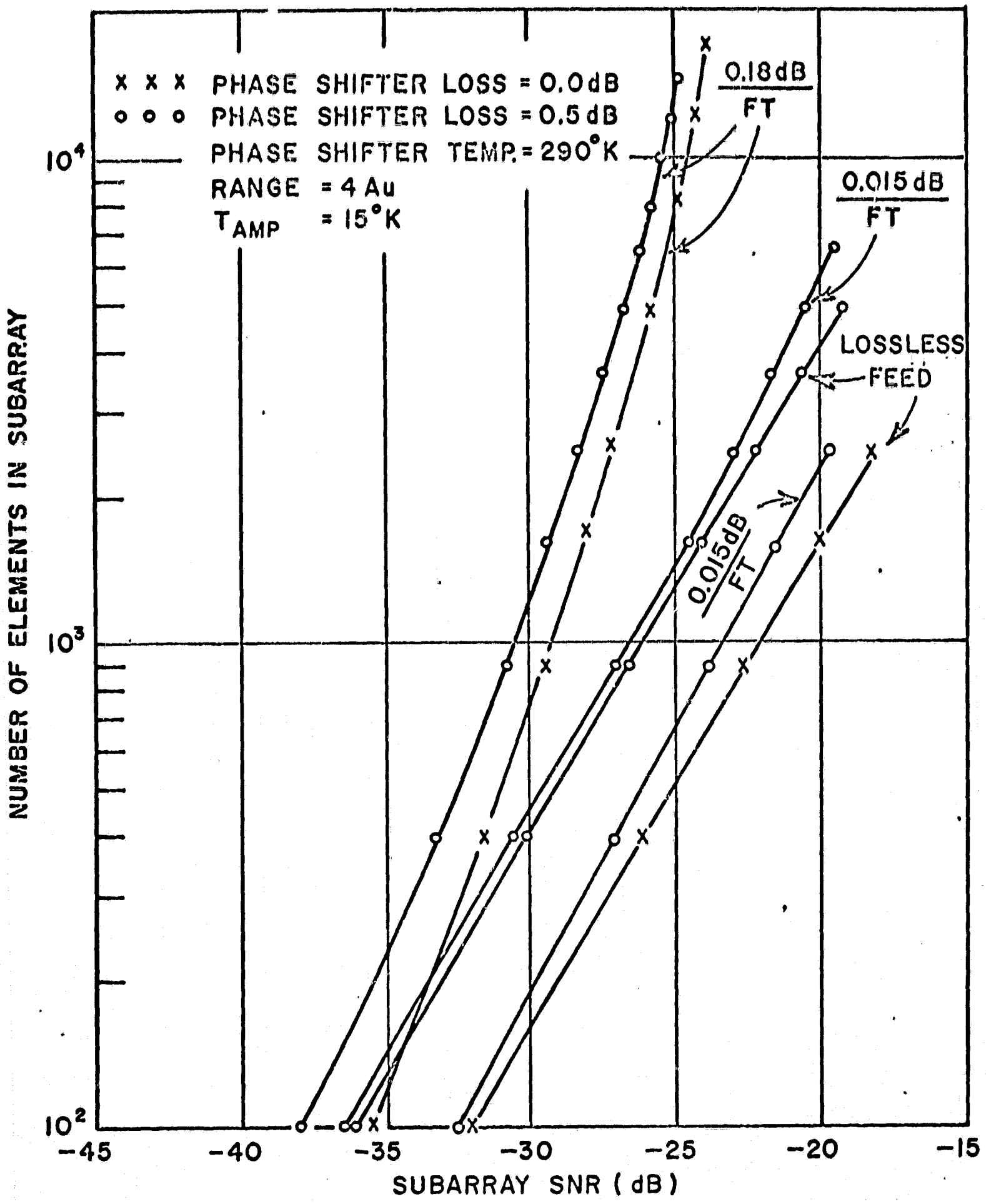

Fig. C-11 Subarray size vs. SNR as a function of phase shifter loss.

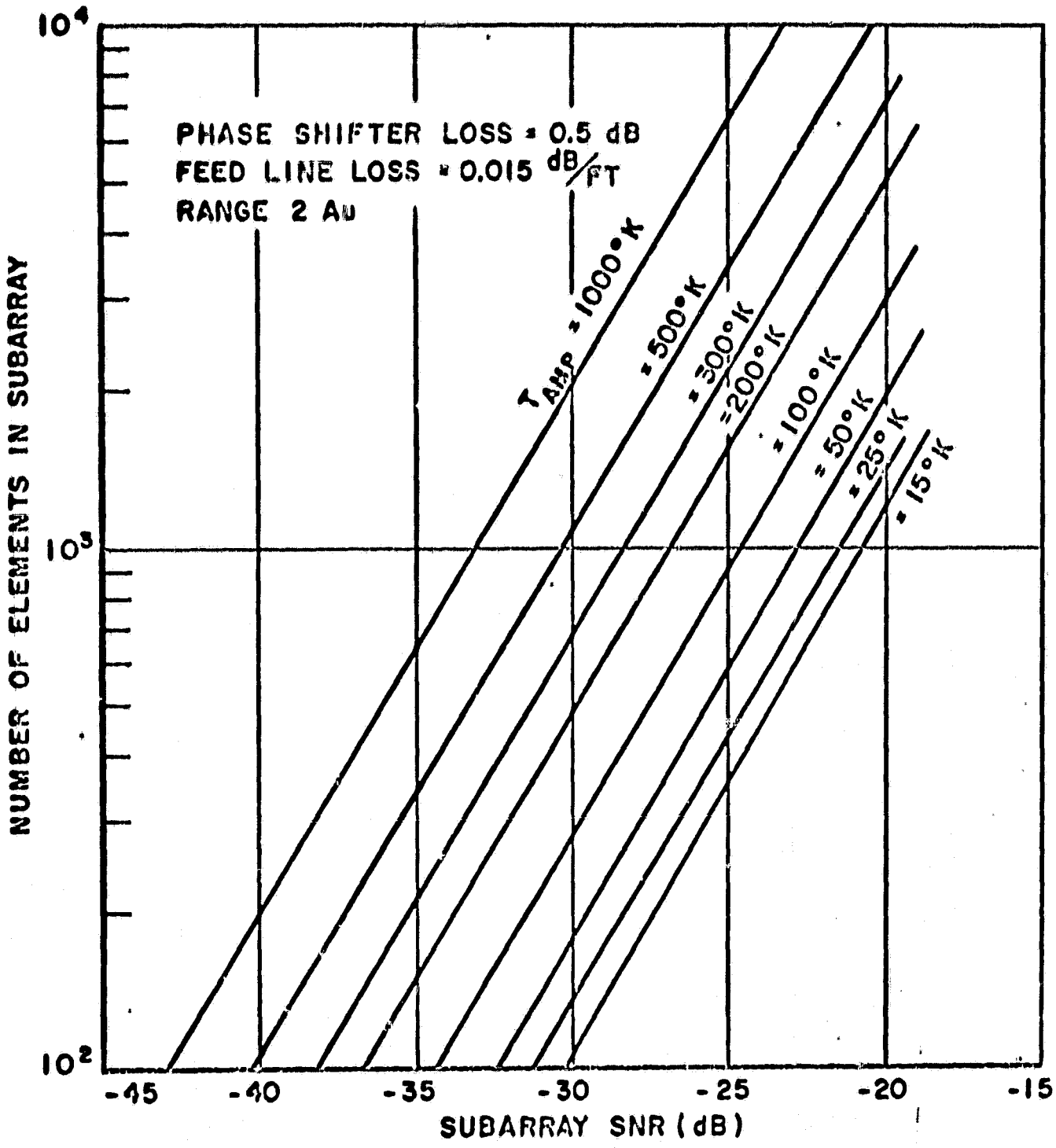

Fig.C-12 Subarray size vs. SNR for various values of amplifier noise temperature.

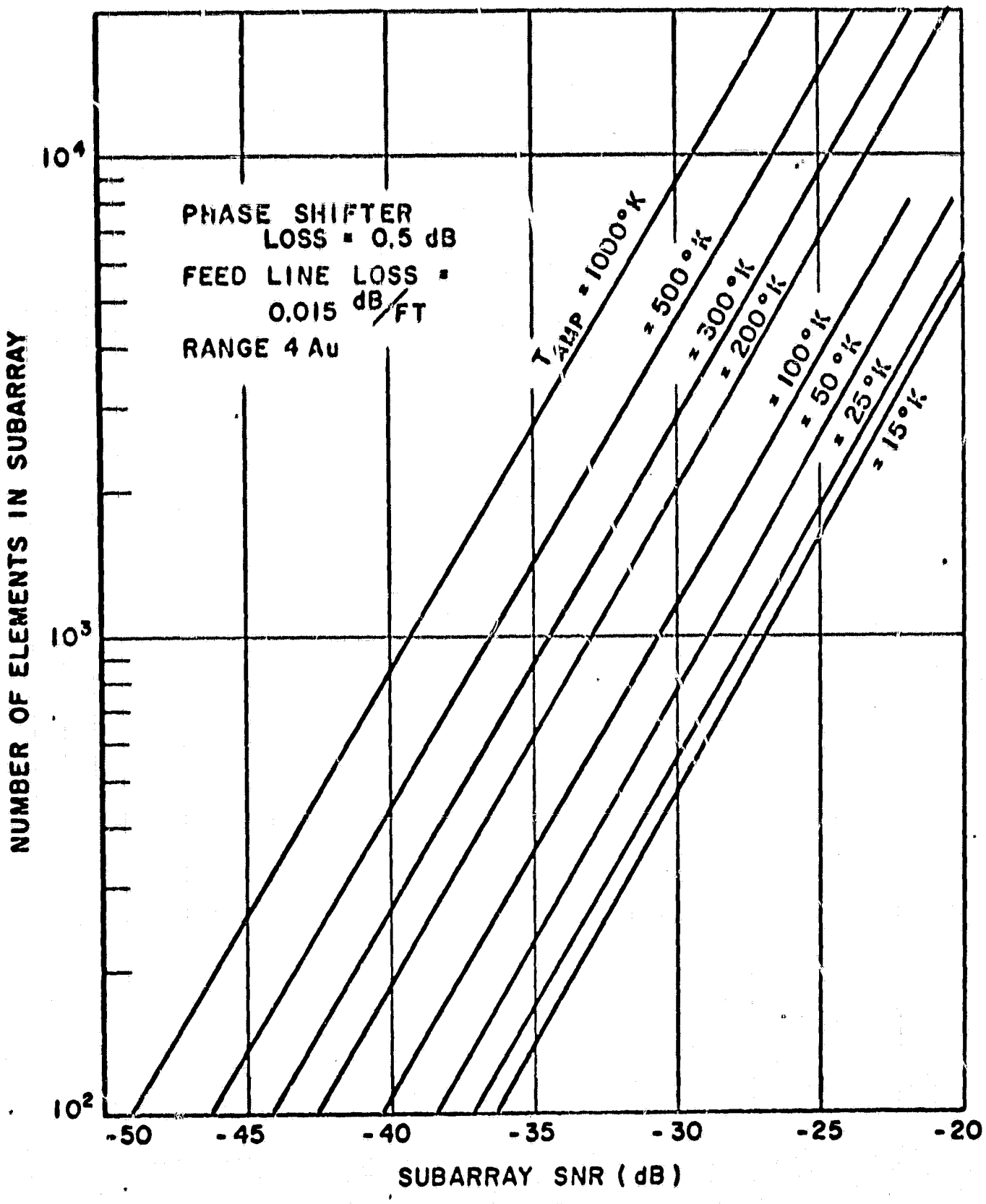

Fig.C-13 Subarray size vs. SNR for various values of amplifier noise temperature.

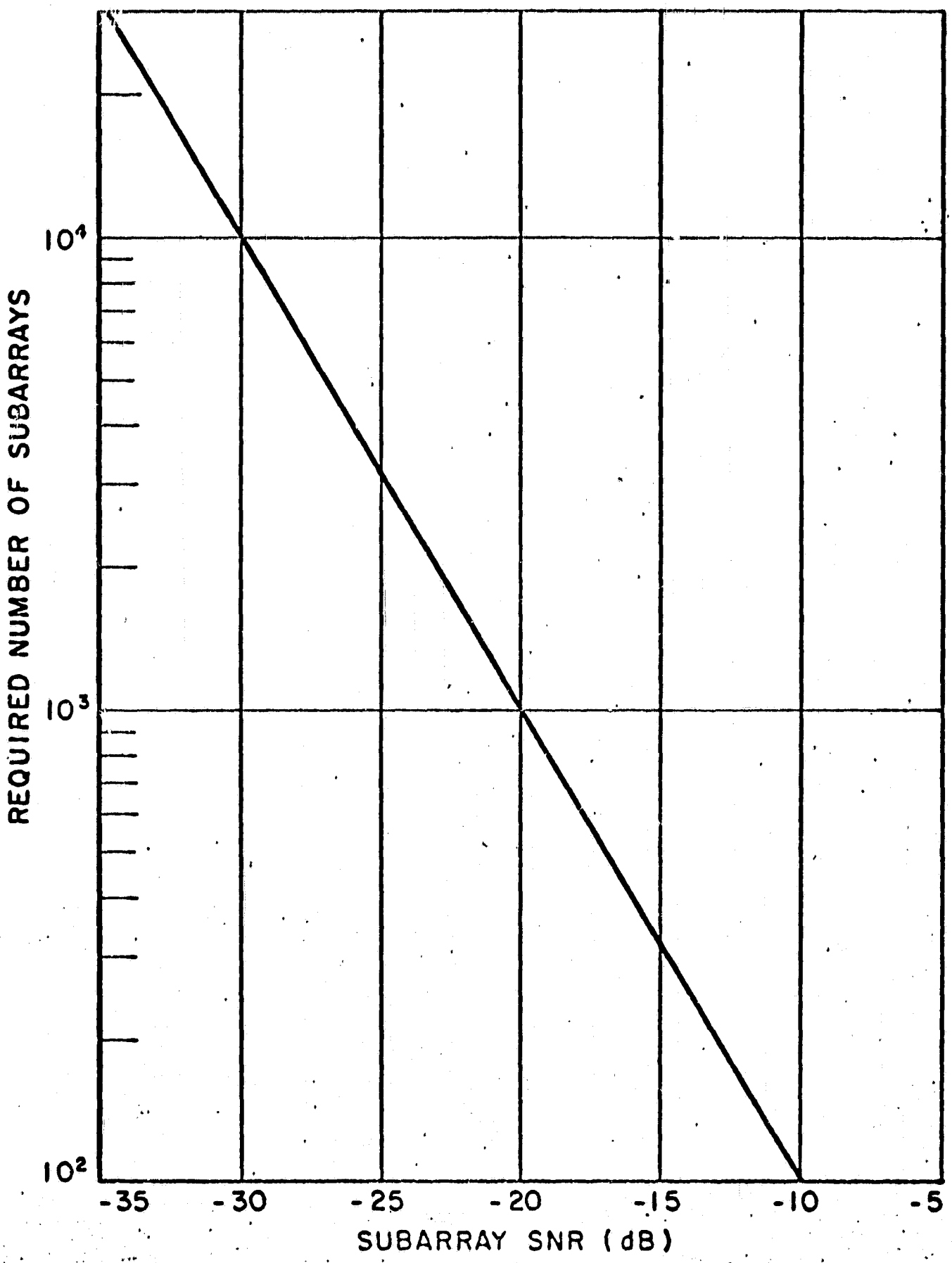

Fig. C-14 Required number of subarrays vs. subarray SNR.

TABLE C-III

REQUIRED APERTURE SIZE TO PRODUCE 10 dB SNR

	Feed line loss	Phase shifter loss	Amplifier noise temperature	Number of subarrays	Required aperture - meters^2 For 2 Au	Required aperture - meters^2 For 4 Au
A. Parabolic dish (70% aperture efficiency) using 15°K maser					2,560 (190 ft. diameter)	10,240 (380 ft. diameter)
B. Dense array of dipoles over a ground plane						
loss-less	0 dB/ft	0 dB	15°	------	1,800	7,200
waveguide	0.015	0	15	1,000	2,100	10,000
waveguide	0.015	0.25	15	10,000	3,380	13,300
waveguide	0.015	0.25	15	1,000	3,800	16,500
waveguide	0.015	0.50	15	1,000	5,000	23,200
waveguide	0.015	0.50	50	1,000	7,600	32,000
waveguide	0.015	0.50	100	1,000	11,800	48,500
waveguide	0.015	0.50	500	1,000	47,000	185,000
stripline	0.18	0	15	1,000	20,000	~∞
stripline	0.18	0.25	15	1,000	25,400	~∞
stripline	0.18	0.25	50	10,000	10,500	67,500
stripline	0.18	0.50	15	1,000	32,000	~∞
stripline	0.18	0.50	50	10,000	12,500	84,500

means the size of a single subarray can be smaller and the cumulative effect of feed loss is not as great as with a larger subarray. Item A lists the characteristics of a conventional parabolic dish antenna as a comparison for the various organizations of phased array of dipoles which are given in item B.

7) Cost Analysis

The cost analysis of this receiving array model is quite difficult due to the large number of parameters involved; moreover these parameters interact in a non-linear manner. For example as the aperture size is doubled the SNR does not double due to an increase in the feed line attenuation and the related thermal noise contribution.

Once the theoretical analysis has been performed it is not difficult to generate a large number of graphs comparing the system performance and cost as the different parameters are varied; for example see Figs. C-15 - C-18. This type of study is hard to interpret simply due to the large number of curves necessary. A more desirable approach used here was to arrange this multiparameter problem into a format in which a computer could be utilized to compare and analyze a large number of cases and present the reduced results in a manner which could be readily used.

The computer program is listed in Appendix II. It requires input data for the following parameters:

1. Range in Au
2. Data Rate
3. Phase shifter loss and cost
4. Feed line loss and cost
5. Amplifier temperature and cost
6. Number of subarrays desired
7. Element cost

The first two input data remain fixed during a given computer run. The last five component and system characteristics represent the parameters to be varied; several values of each may be entered to determine the variation of the total array size and cost with that parameter.

To illustrate how the program might be used, consider the following example. Figure C-19 shows the input data selected; the fixed value of 2 Au and 10^6 bits per second were chosen. Two choices for phase shifters were entered, a ferrite device with .25 dB insertion loss at a cost of $20 and a diode type with .75 dB loss but costing $5. The choices for the feed

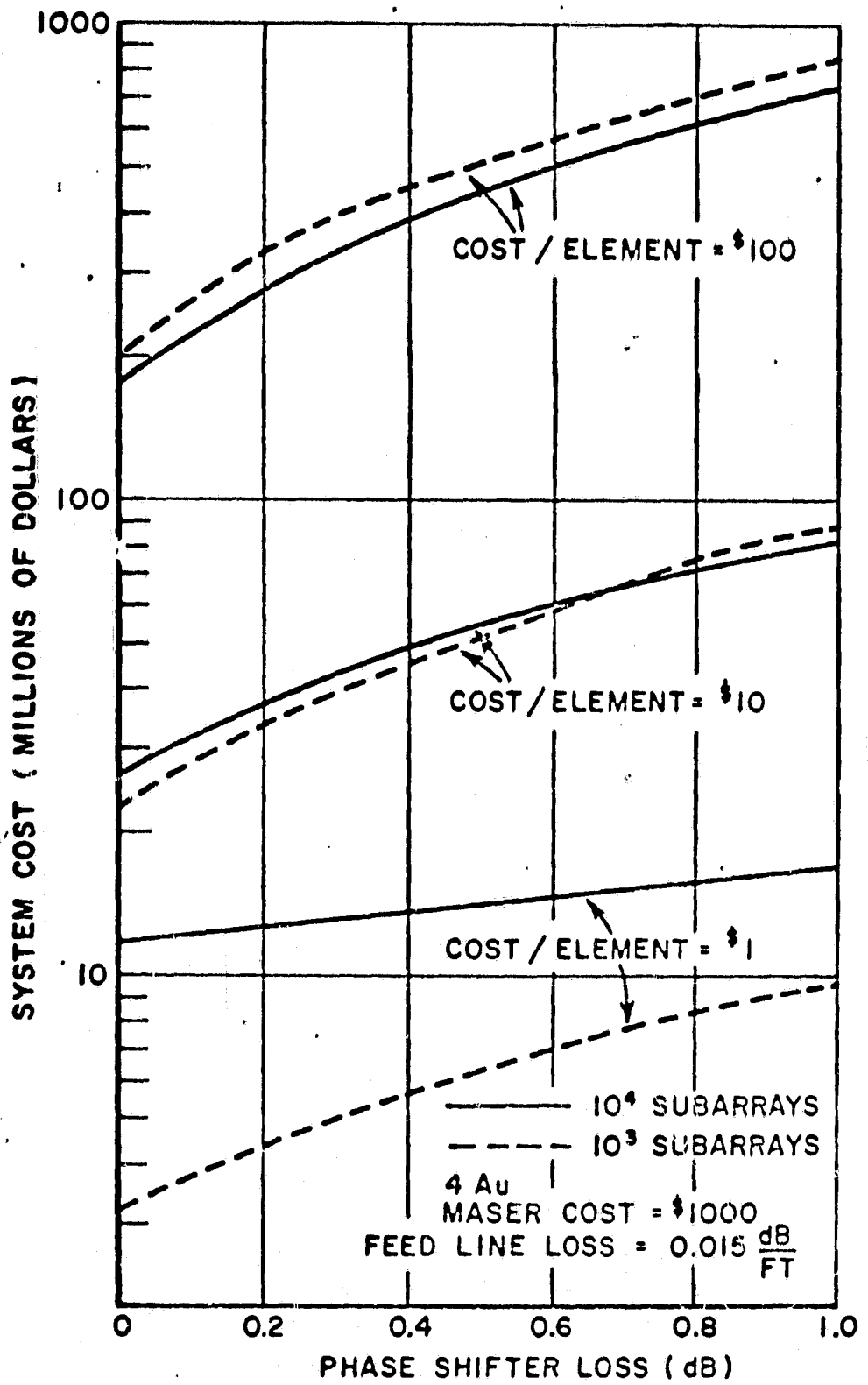

Fig. C-15 System cost vs. phase shifter loss.

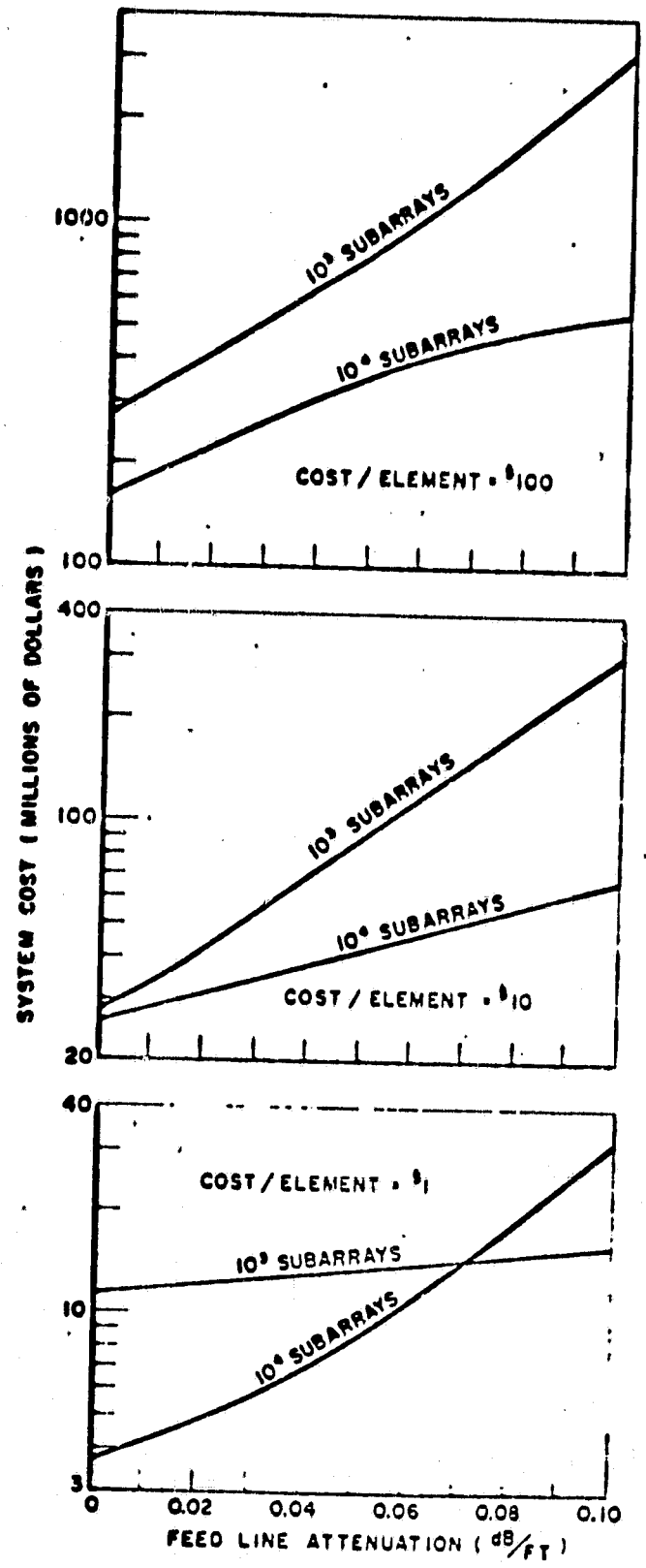

Fig. C-16 System cost vs. attenuation of feed line. Computed for 4Au, Maser cost = $1000, 0.25 dB phase shifter loss.

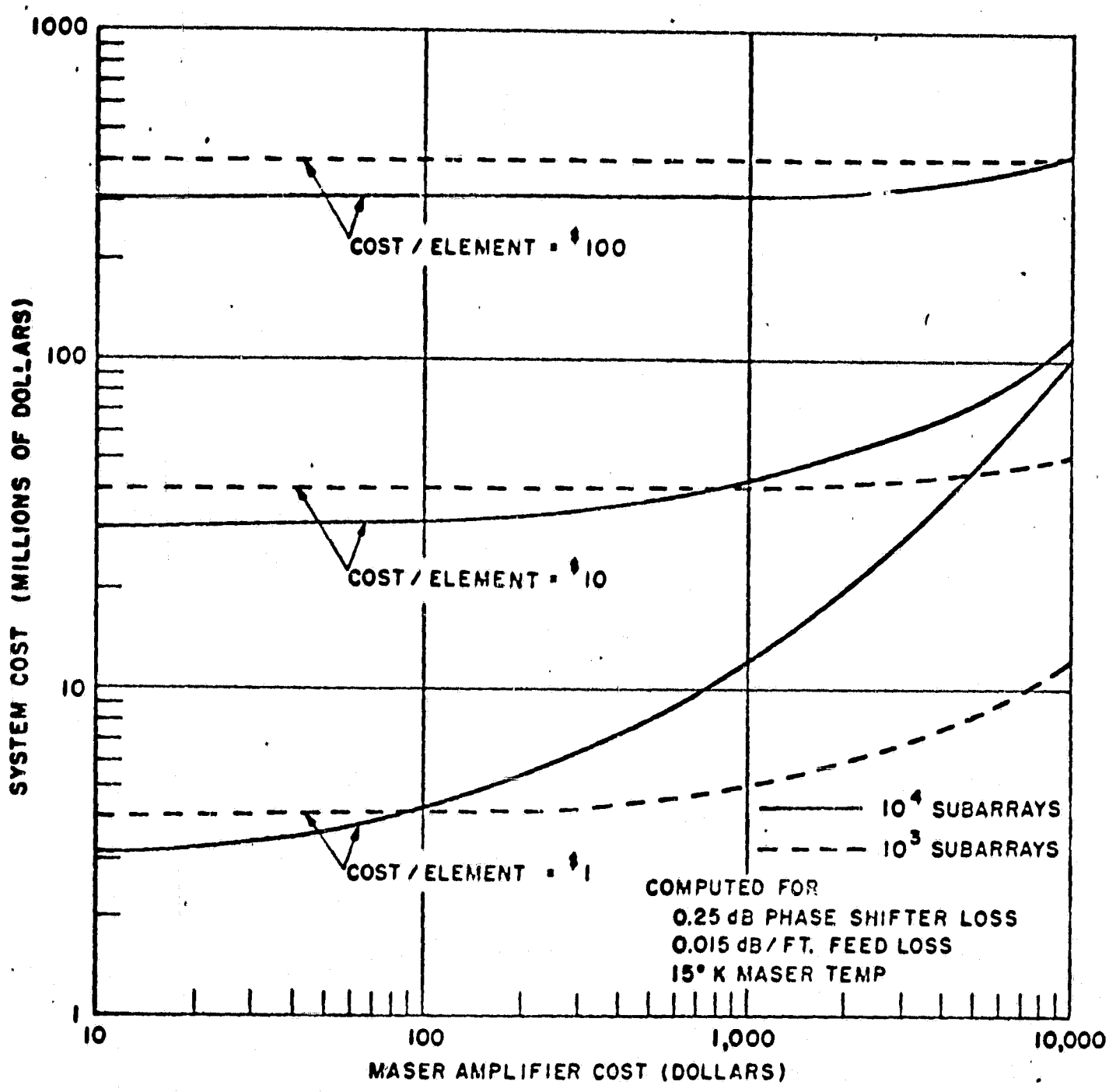

Fig. C-17 System cost vs. maser amplifier cost.

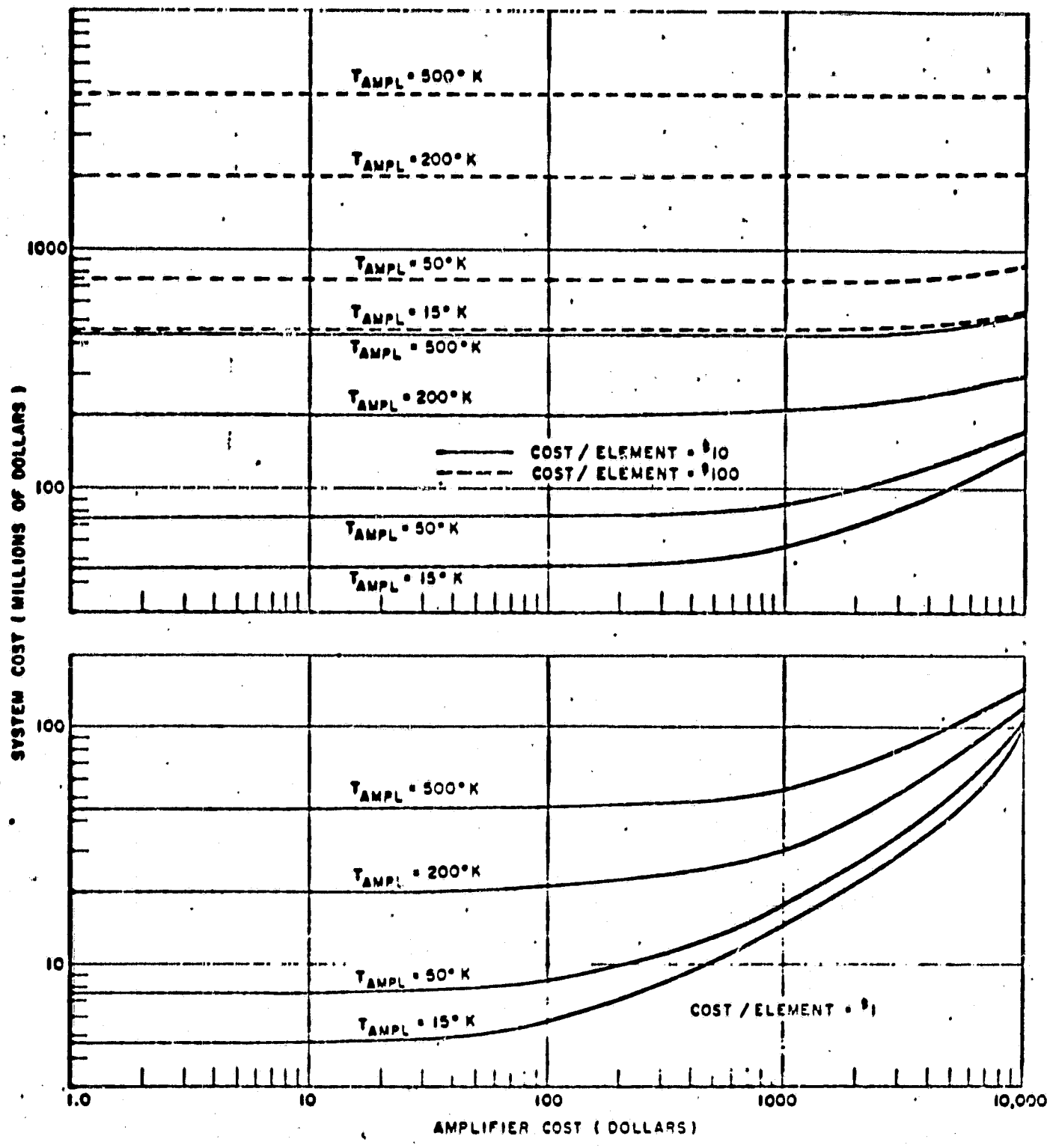

Fig. C-18 System cost vs. subarray amplifier cost for various amplifier noise temperatures. Computed for 4Au, 0.5 dB phase shifter loss, .015 dB/ft feed loss, 10^4 subarrays.

```
COST ANALYSIS FOR S BAND PHASED ARRAY OF DIPOLE ELEMENTS

ENTER DISTANCE IN AU
2
ENTER DATA RATE IN MEGABITS PER SECOND
1
ENTER NUMBER OF CHOICES FOR EACH COMPONENT
2
ENTER PHASE SHIFTER LOSS(DB) AND COST(S)
  CHOICE   1
.25,20
  CHOICE   2
.75,5
ENTER FEED LINE LOSS(DB/FT) AND COST/ELEMENT
  CHOICE   1
.05,5
  CHOICE   2
.15,.5
ENTER AMPLIFIER TEMP AND COST
  CHOICE   1
15,10000
  CHOICE   2
50,1000
ENTER NUMBER OF SUBARRAYS DESIRED
  CHOICE   1
1000
  CHOICE   2
5000
ENTER FIXED COST PER ELEMENT
  CHOICE   1
5
  CHOICE   2
50
   FOR THE ABOVE PARAMETERS THE POSSIBLE SYSTEM CONFIGURATIONS AND THEIR
 COST ARE:
```

PHASE SHIFTER LOSS (DB)	$	AMPLIFIER TEMP	$	FEED LINE DB /FT	$	ELEMENT COST	NUMB S.A.	REQUIRED NO.ELEM	TOT COST MILL $
0.75	5	15	10000	0.05	5.0	5	1000	2252000	43.78
0.75	5	50	1000	0.05	5.0	5	5000	2760000	46.40
0.75	5	50	1000	0.15	0.5	5	5000	3945000	46.42
0.25	20	15	10000	0.05	5.0	5	1000	1310000	49.30
0.75	5	50	1000	0.05	5.0	5	1000	3262000	49.93
0.25	20	50	1000	0.05	5.0	5	5000	1810000	59.30
0.25	20	50	1000	0.05	5.0	5	1000	2201000	67.03
0.25	20	50	1000	0.15	0.5	5	5000	2750000	75.12
0.75	5	15	10000	0.15	0.5	5	1000	6341000	76.56
0.75	5	15	10000	0.05	5.0	5	5000	1840000	77.60
0.75	5	15	10000	0.15	0.5	5	5000	2825000	79.66
0.25	20	15	10000	0.05	5.0	5	5000	1180000	85.40
0.25	20	15	10000	0.15	0.5	5	5000	1720000	93.86
0.75	5	50	1000	0.15	0.5	5	1000	9039000	95.90
0.25	20	15	10000	0.05	5.0	50	1000	1310000	108.25
0.25	20	15	10000	0.15	0.5	5	1000	4138000	115.51
0.25	20	15	10000	0.05	5.0	50	5000	1180000	138.50
0.25	20	50	1000	0.05	5.0	50	5000	1813000	140.75
0.75	5	15	10000	0.05	5.0	50	1000	2252000	145.12
0.25	20	50	1000	0.15	0.5	5	1000	6220000	159.61
0.75	5	15	10000	0.05	5.0	50	5000	1840000	160.40
0.25	20	50	1000	0.05	5.0	50	1000	2201000	166.37
0.75	5	50	1000	0.05	5.0	50	5000	2760000	170.60
0.25	20	15	10000	0.15	0.5	50	5000	1720000	171.26
0.75	5	50	1000	0.05	5.0	50	1000	3262000	196.72
0.25	20	50	1000	0.15	0.5	50	5000	2750000	198.87
0.75	5	15	10000	0.15	0.5	50	5000	2825000	206.78
0.75	5	50	1000	0.15	0.5	50	5000	3945000	223.94
0.25	20	15	10000	0.15	0.5	50	1000	4138000	331.72
0.75	5	15	10000	0.15	0.5	50	1000	6341000	361.92
0.25	20	50	1000	0.15	0.5	50	1000	6221000	439.51
0.75	5	50	1000	0.15	0.5	50	1000	9339000	532.66

Fig. C-19 Typical example using computer analysis.

system were a waveguide network (.05 dB/ft) costing $5/element and a stripline one (.15 dB/ft) costing only $0.5/element. Two amplifiers were considered, a 15°K maser at a cost of $10,000 and a 50°K paramp at $1,000. To determine how sensitive the cost was to subarray size, arrays composed of 1,000 and 5,000 subarrays were considered. The maximum number of subarrays permitted is bounded, as discussed previously, by requiring sufficient SNR at each subarray to maintain phase lock. For the model discussed here the maximum is about 20,000. The fixed element cost was set at $5/element and $50/element. This includes the cost of all the components not considered above, such as IF amplifiers, control circuitry, etc. Obviously the choice of lowest element cost will result in the lowest overall cost; the purpose of selecting several choices is to study some intangible factors. For example, the first choice might be the minimum possible element cost, the second might be for a system with automatic error detection circuitry to detect and locate system malfunctions such as component failures. For the 5 parameters listed above (3-7), each having two possible choices, there are $32 = 2^5$ distinct ways of constructing the array to obtain the specified error rate or output signal to noise ratio. The computer then calculates the required number of elements and the total cost for each of these systems and displays the output in the increasing cost format shown in Figure C-19. Referring to this figure it can be seen that for the selected input data the most economical array would be obtained by using the .75 dB phase shifter, a waveguide feed, a maser amplifier, the $5 element cost, and 1,000 subarrays. It is interesting to observe that using these same values except increasing the number of subarrays to 5,000 would have produced a more efficient system which contained 20% less elements but cost almost twice as much. The size reduction is due to the individual subarray being smaller so that the cumulative effect of feed line loss is less; the increase in cost is due to the increase in required number of expensive masers. Another perhaps surprising observation is that the economically best three systems all utilized the .75 dB phase shifter rather than the higher performance .25 dB one. This is due of course to the difference in cost ($5 vs. $20).

Initially it was believed that the use of stripline would not be possible due to its large attenuation factor (.15 dB/ft.). It can be seen,

however, that the third best system utilizes a stripline feed network. Even though this system requires considerably more elements (nearly twice as many) the total cost is only slightly more than optimum.

It should be emphasized that the comments on system cost in this example are dependent on the particular component values and element cost selected; these values were considered reasonable at this time but by no means exact. The significant contribution of the analysis and computer program is that given updated values of these components and desired data rate at any time in the future, the optimum way can be obtained to combine these components so as to minimize the total cost.

8) Summary

An analysis of a large receiving array of dipoles has been presented. A computer program was written which calculates the required number of elements and total cost as a function of the desired data rate, distance, and component cost and characteristics. An arbitrary number of values for each component can be entered and the computer then calculates the size and cost for each of the array configurations and lists these results in order of increasing cost. The useful feature of this technique is that the usual intermediate process of plotting performance curves for many different parameters and interpreting these results is performed by the computer. This program could be used, for example, to determine how many subarray modules the total array should be divided into, which type of amplifier and phase shifter should be used, or how cheaply a stripline feed must be to make it competitive with a waveguide system.

REFERENCES

C-1 Bailin, L. L. and Hamren, S. D. "Some Fundamental Limitations Large Antennas," in preparation.

C-2 Lindsey, W. C., "Phase Shift Keyed Signal Detection With Noisy Reference Signals," IEEE Trans. Aerospace and Electronic Systems, p. 393 July, 1966.

C-3 Oliver, B. M., "Thermal and Quantum Noise," Proc: IEEE 53, 5 pp 436-454, 1965.

C-4 Riegler, R. L., "Microwave Radiometric Temperatures of Terrain," Report 1903-2, ElectroScience Laboratory, The Ohio State University Research Foundation; prepared under Contract NSR-36-008-027, National Aeronautics and Space Administration, Washington, D. C., June 31, 1966.

C-5 Wulfsberg, Karl N., "Apparent Sky Temperatures at Millimeter Wave Frequencies," Physical Sciences Research Papers No. 38, Air Force Cambridge Research Laboratories, July, 1964.

C-6 Siegman, E. A., "Thermal Noise in Microwave Systems," Microwave Journal, March, 1961.

C-7 Final Report, Advanced Deep Space Communication Study, Report No. P67-15, Hughes Aircraft Company, January, 1967.

C-8 Schwartz, Bennet, and Stein, Communication Systems and Techniques, McGraw-Hill Book Co., Inc. 1966.

C-9 Gardner, F. M., Phase Lock Techniques, John Wiley and Sons, Inc., 1966.

C-10 Martin, B. D., "The Pioneer IV Lunar Probe: A Minimum Power FM/PM Systems Design" Report 32-215, Jet Propulsion Laboratory, March, 1962.

C-11 Reference Data for Radio Engineers, ITT, p. 615, 1963.

C-12 Kummer, W. H., Feeding and Phase Scanning, Microwave Scanning Antennas, Vol. III, Chap. 1., R. C. Hansen, ed., Academic Press, 1966.

C-13 "Semiconductors Keep Coll Via Peltier," EDN Magazine, p. 56, a Cahners Publication, December, 1967.

D. A SELF-STEERING ARRAY

This portion of the report is concerned with the problems associated with self-phased and adaptive arrays which can be employed to follow the relatively weak signal from a distant spacecraft. These arrays are also called self-focusing antennas since they use the incident RF energy to phase the elements so that a beam is formed in the direction from which the energy is received. The arrays may be contrasted with the usual electronically steerable arrays that require external sensors and information to do the steering. Here, no external commands are necessary to adjust the illumination across the aperture, since, in principle, the self-steering array automatically steers the beam in the desired direction. By the inclusion of appropriate signal processing circuitry, an adaptative array can perform filtering in both the space and the frequency domains thus reducing the sensitivity of the receiving system to interfering directional noise sources. Thus the problems associated with pointing a narrow beam in a specified direction or with atmospheric scintillation effects may be handled in a self-phasing mode and those associated with period interference effects may be handled with adaptive array techniques as an alternative mode of operation. This section will consider the feasibility of switching from a system where the steering is accomplished by externally controlling the phase between elements to a self-steering or adaptive array whenever a high external noise or interference level is present in the angular region subtended by the receiving beam.

During this report period, an investigation was initiated on adaptive arrays. The objective of this study is to develop techniques that will permit an antenna to receive signals from a desired source in the presence of an interfering one, either man made or natural, such as the sun. The work to date in this area has concerned the adaptive array with a basic element as shown in Fig. D-1 and is on an algorithm for minimization of mean square error (D-1). Utilizing this method, the weighting coefficient for each element of the array is continuously adjusted (in a feedback loop) in a way that forces the output from the antenna to be equal to a "desired response", in at least mean square error sense. The desired output is specified by either the expected angle or arrival or/and the spectrum of the communication signal. This type of array seems promising for the problem of the satellite near the sun, because the array pattern will adjust itself continuously, as the satel-

lite and sun move, to hold the noise output due to the sun to a minimum.

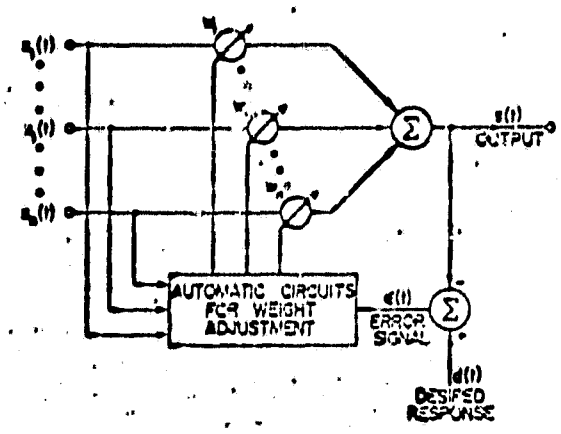

Figure D-1 Basic Adaptive Element

At present, the behavior of a two-element adaptive array and a four-element adaptive array has been studied on the digital computer using the basic algorithm. A number of computer programs were written and used to simulate the operation of these arrays under a variety of conditions (namely, as a function of the feedback loop parameters, the power levels of the signal, the interfering signal, and the noise, and the arrival angles of the signal and interfering signal.) In all cases (once the computer programs were properly debugged) the arrays performed admirably. The weighting coefficients converged, and the resulting antenna patterns were such as to reduce the noise from the interfering signal to the minimum possible, given the number of elements in the array. An experimental adaptive array (at S-Band) based on this principle is presently under construction. It is planned to use this array to learn what limitations are placed on the adaptation process by the idiosyncracies of the actual electronics.

In the future, it is planned to continue the study of the adaptive array based on the LMS algorithm, both experimentally and using the computer model. It is also intended in this portion of the program to study adaptation schemes based on other models (e.g., systems which seek maximum SNR, systems with nulls which track interfering noise signals, etc.). Although adaptive antennas have often been discussed by antenna people, they have not been thoroughly examined for particular applications. It is hoped to find out what the possibilities are, and to learn what limitations arise in practice when adaptive antennas are applied to the particular problems presented by this large high data rate communication system.

REFERENCES

D-1 B. Widrow, P. E. Mantey, L. J. Griffiths and B. B. Goode, "Adaptive Antenna Systems", Proc IEEE, Vol. 55, No. 12, pp. 2143-2159, December, 1967.

APPENDIX I
RELATIONSHIP BETWEEN GAIN AND SIZE FOR THE DIPOLE ANTENNA MODEL

To calculate the gain of the two dimensional array shown in Fig. A1 it is convenient to use the concept of array multiplication, that is the total pattern can be calculated as

$$F_T = F_E F_X F_Y F_Z$$

where F_E = element pattern of a single dipole
F_X, F_Y = array factor for an array of isotropic elements along the X, Y axis
F_Z = array factor for two isotropic elements along the Z direction.

For $D_x = D_y = \lambda/2$ and $D_z = \lambda/4$ the resulting expressions are:

$$F_E = \frac{\cos(\pi/2 \sin\theta \cos\phi)}{\sqrt{1 - \sin^2\theta \cos^2\phi}}$$

$$F_Z = \sin(\pi/2 \cos\theta)$$

$$F_X = 1 + 2\sum_{K=1}^{(N_o-1)/2} \cos(K\pi \sin\theta \cos\phi)$$

$$F_Y = 1 + 2\sum_{K=1}^{(N_o-1)/2} \cos(K\pi \sin\theta \sin\phi)$$

where N_o = number of elements on a side (assumed odd)

The power density $S = F_T^2$ and the directivity is

$$D = \frac{S(\theta = 0)}{\frac{1}{4\pi}\int_0^{2\pi}\int_0^{\pi/2} S(\theta,\phi) \sin\theta \, d\theta \, d\phi}$$

The effective aperture $A_e = \frac{\lambda^2 D}{4\pi}$.

Defining the physical aperture is somewhat arbitrary, for example, a single dipole has zero physical area. However for large arrays each element occupies on the average $\lambda^2/4$ area, hence the total physical aperture is defined as $A_p = N_o^2 \lambda^2/4$. Figure A2 shows the relationship between A_e and A_p. Note that the effective collecting aperture rapidly approaches the physical size.

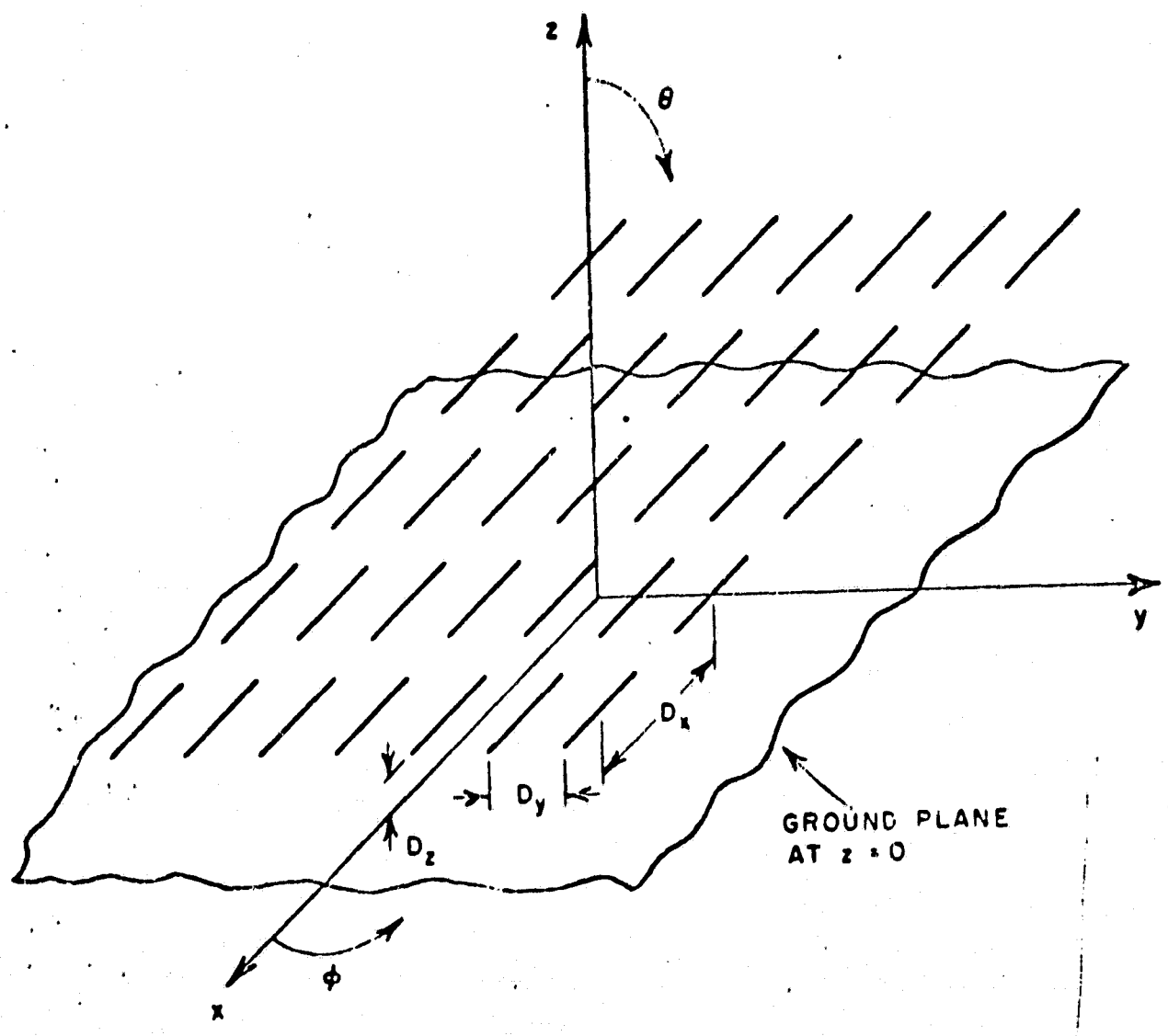

Fig. A1. Dipole array model.

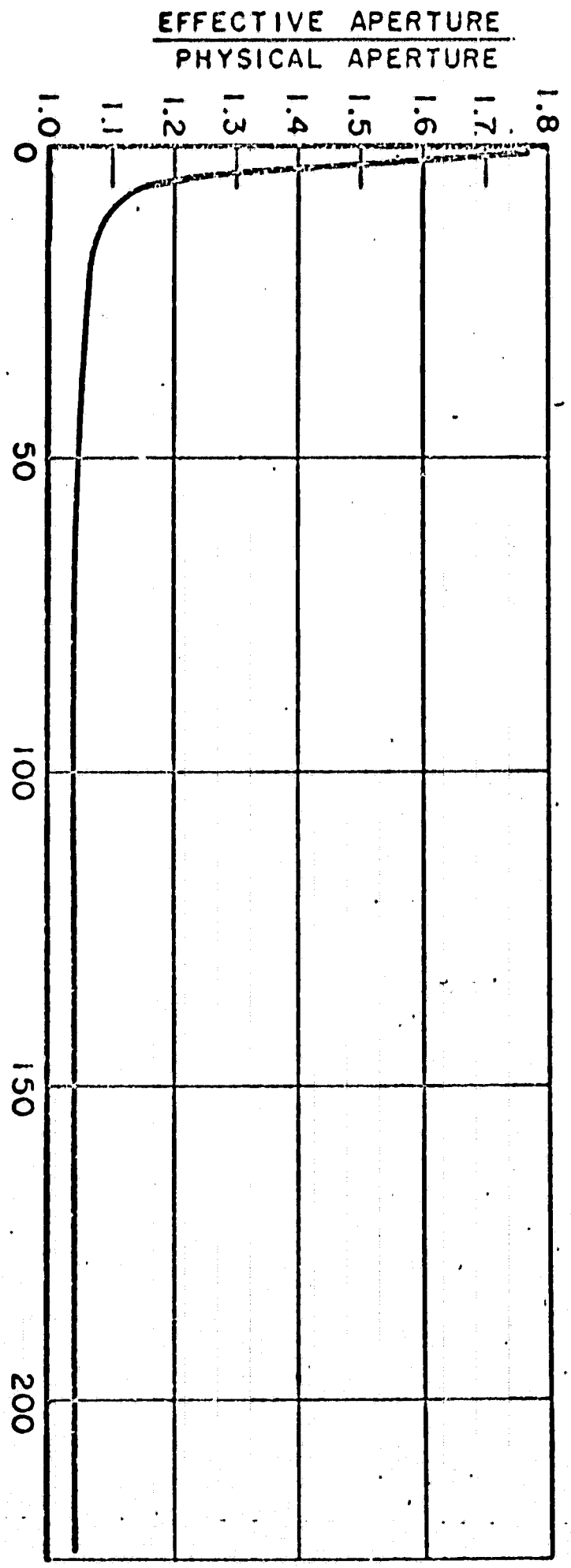

Fig. A2. Relationship between physical aperture and electrical aperture.

APPENDIX II
COMPUTER PROGRAM

This appendix includes a listing of the computer program discussed in the report. A simplified flow diagram is included to show the order in which the data is entered, calculation are performed, and reduced data is displayed.

No particular attempt was made to minimize the computer execution time; casual programming was used throughout for simplicity. The example discussed in the report with 32 possible system configurations required two minutes (about $5) using a commercial time sharing computer.

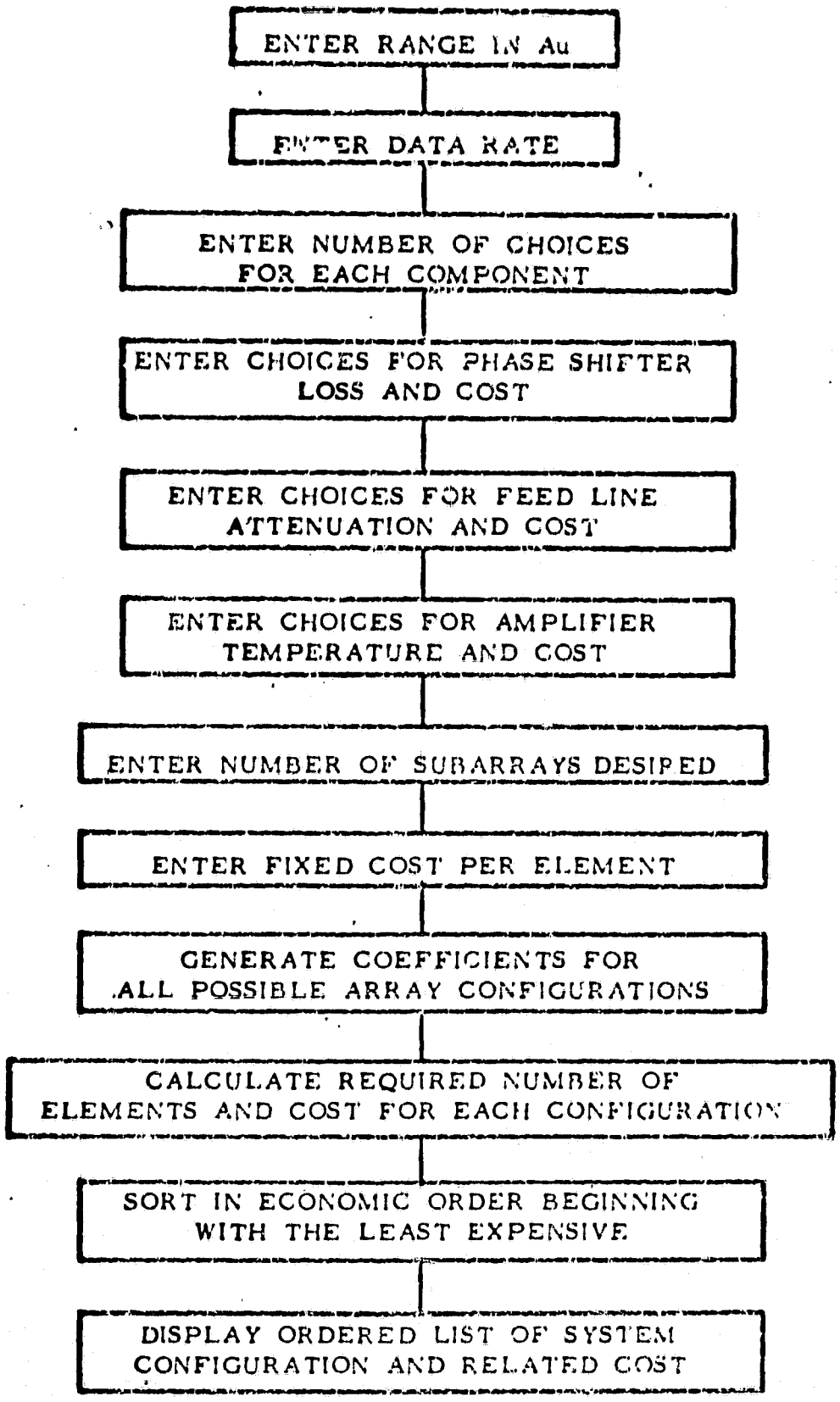

Fig. A3. Simplified flow diagram of computer listing.

```
1.      C:COST OF PLANAR RECEIVING ARRAY OF DIPOLES FOR VARIOUS PARAM.
2.      C: COMPUTED FOR 50 WATTS TRANSMITTER, 30 FOOT DISH
3.      C: MAX BIT ERROR PROB=10**-5 (10 DB SNR)
4.      DISPLAY['COST ANALYSIS FOR S BAND PHASED ARRAY OF DIPOLE ELEMEN
        TS"]
5.      DISPLAY['    "]
6.      DIMENSION PSLDB(5),CPS(5),DBPF(5),TAMP(5),CAMP(5),NSA(5)
7.      DIMENSION LL(5),IFC(5),FEC(5),SNR(99),COST(99),CFL(5)
8.      DIMENSION IC(99),NELEM(99)
9.      99 FORMAT(F5.2,2I4,I9,F5.2,F4.1,I7,I10,I12,F9.2)
10.     DISPLAY['ENTER DISTANCE IN AU"]-
11.     ACCEPT[AU]
12.     DISPLAY['ENTER DATA RATE IN MEGABITS PER SECOND"]
13.     ACCEPT[DR]
14.     DISPLAY['ENTER NUMBER OF CHOICES FOR EACH COMPONENT"]
15.     ACCEPT[NC]
16.     TANT=9
17.     DISPLAY['ENTER PHASE SHIFTER LOSS(DB) AND COST($)"]
18.     DO 10 I=1,NC
19.     DISPLAY['  CHOICE",I]-
20.     10 ACCEPT[PSLDB(I),CPS(I)]
21.     DISPLAY['ENTER FEED LINE LOSS(DB/FT) AND COST/ELEMENT"]
22.     DO 15 J=1,NC
23.     DISPLAY['  CHOICE",J]-
24.     15 ACCEPT[DBPF(J),CFL(J)]
25.     DISPLAY['ENTER AMPLIFIER TEMP AND COST"]
26.     DO 20 K=1,NC
27.     DISPLAY['  CHOICE",K]
28.     20 ACCEPT[TAMP(K),CAMP(K)]
29.     DISPLAY['ENTER NUMBER OF SUBARRAYS DESIRED"]
30.     DO 25,L=1,NC
31.     DISPLAY['  CHOICE",L]
32.     25 ACCEPT[NSA(L)]
33.     DISPLAY['ENTER FIXED COST PER ELEMENT"]
34.     DO 26 M=1,NC
35.     DISPLAY['  CHOICE",M]
36.     26 ACCEPT[FEC(M)]
37.     DISPLAY['   FOR THE ABOVE PARAMETERS THE POSSIBLE SYSTEM CONFIG
        URATIONS AND THEIR COST ARE:"]
38.     DISPLAY['    "]
39.     DISPLAY['  PHASE     AMPLIFIER    FEED     ELEMENT     NUMB     RE
        QUIRED    TOT"]
40.     DISPLAY[' SHIFTER                  LINE      COST      S.A.     NO
        .ELEM    COST"]
41.     DISPLAY['-----------------------------------------------------
        -------------"]
42.     DISPLAY['LOSS   $    TEMP   $   DB   $   "]
43.     DISPLAY['(DB)                    /FT
                MILL $"]
44.     NV=1
45.     DO 5 MM=1,5
46.     5 LL(MM)=1
47.     6 I=LL(1)
```

```
      J=LL(2)
      K=LL(3)
      L=LL(4)
      M=LL(5)
      DSNR=10.*ALOG10(10./NSA(L))
      FLL=1.-DBPF(J)*.23*.22
      TO=290
      PST=290
      A=-168-20*ALOG10(AU)-PSLDB(I)
      BK=(1.38*10**-23)*(.5*DR*10**6)
      PSL=EXP(-2.3*PSLDB(I)/10)
      N=10
   30 SUM=0
      II=N/10
      DO 35 NK=1,N-
   35 SUM=SUM+FLL**(NK-1)-
      Z=(FLL/(N*N))*SUM*SUM
      SIG=A+10*ALOG10(N*N)-10*ALOG10(1/Z)-
      TNOS=10*ALOG10(BK*(TO*(1-Z)+PST*(1-PSL)*Z+TANT*PSL*Z+TAMP(K)))+
      30
      SNR(II)=SIG-TNOS
      IF(SNR(II)-DSNR) 40,42,45
   40 N=N+10
      GO TO 30
   45 SLOPE=((10*II)**2-(10*(II-1))**2)/(SNR(II)-SNR(II-1))
      YINTERCEPT=(10*II)**2-SLOPE*SNR(II)
      NELEM(NV)=SLOPE*DSNR+YINTERCEPT
      GO TO 50
   42 NELEM(NV)=N*N
   50 COST(NV)=(NELEM(NV)*(CPS(I)+CFL(J)+FEC(M))+CAMP(K))*NSA(L)
      IC(NV)=NV
      NV=NV+1
      IF(NV.GT.NC**5) GO TO 90
      CALL COMB(LL,NC,5)
      GO TO 6
   90 CONTINUE
      CALL TPLSORT(1,COST,IC,NELEM,1,NC**5)
      CONTINUE
      DO 91 NV=1,NC**5-
      DO 92 MM=1,5
   92 LL(MM)=1
      IZ=1
   95 I=LL(1)
      J=LL(2)
      K=LL(3)
      L=LL(4)
      M=LL(5)
      IF(IZ.EQ.IC(NV)) GO TO 94-
      CONTINUE
      CALL COMB(LL,NC,5)
      IZ=IZ+1
      GO TO 95
   94 CONTINUE
```

```
100.      91 WRITE(1,99) PSLDB(I),CPS(I),TAMP(K),CAMP(K),DBPF(J),CFL(J),F
          EC(M),NSA(L),NELEM(NV)*NSA(L),COST(NV)/10**6
101.      CONTINUE
102.      END
103.      SUBROUTINE COMB(LL,I,J)
104.      IJ=1
105.      9 LL(IJ)=LL(IJ)+1
106.      IF(LL(IJ).LE.I) RETURN
107.      LL(IJ)=1
108.      IJ=IJ+1
109.      IF(IJ.GT.J) RETURN
110.      GO TO 9
111.      END
112.         SUBROUTINE TPLSORT(KODE,SEEDS,FOLLO,TAKE,JAX,LAX)
113.      C:    IF KODE=1,ASCENDING SORT.  IF KODE=2,DESCENDING SORT.
114.      C:   SEEDS IS THE ARRAY TO BE SORTED.-
115.      C:   FOLLO AND TAKE ARE TWO ARRAYS WHICH ARE TO BE REARRANGED
116.      C:   ACCORDING TO THE NEW ORDER OF SEEDS, SO THAT THE PROPER ITE
          MS
117.      C: WILL STILL BE CORRECTLY ASSOCIATED WITH SEEDS.
118.      C:   JAX IS BEGINNING LOCATION TO SORT FROM.
119.      C:   LAX IS END LOCATION TO SORT TO.
120.      IF(LAX.EQ.1) RETURN
121.         IF(JAX.GT.0)GOTO7
122.          JAX=1
123.        7   IF(KODE.LT.1.OR.KODE.GT.2)GOTO6
124.          DO 1 JO=JAX,LAX-1
125.          DO2 KI=JO+1,LAX
126.          GOTO(3,4)KODE
127.         3    IF(SEEDS(JO).LE.SEEDS(KI))GOTO2
128.          5       SAVE=SEEDS(JO)-
129.           SEEDS(JO)=SEEDS(KI)-
130.         SEEDS(KI)=SAVE
131.           TEMP=FOLLO(JO)
132.           FOLLO(JO)=FOLLO(KI)
133.           FOLLO(KI)=TEMP
134.        HOLD=TAKE(JO)-
135.        TAKE(JO)=TAKE(KI)
136.         TAKE(KI)=HOLD-
137.         GOTO2
138.         4    IF(SEEDS(JO).LE.SEEDS(KI))GOTO5
139.         2 CONTINUE
140.         1   CONTINUE
141.         RETURN
142.        6    DISPLAY['ILLEGAL CODE IN CALLING SEQUENCE."]
143.             DISPLAY['                    KODE=",KODE]-
144.          STOP
145.         END-
```